



National Library  
of Canada

Bibliothèque nationale  
du Canada

Canadian Theses Service

Service des thèses canadiennes

Ottawa, Canada  
K1A 0N4

## NOTICE

The quality of this microform is heavily dependent upon the quality of the original thesis submitted for microfilming. Every effort has been made to ensure the highest quality of reproduction possible.

If pages are missing, contact the university which granted the degree.

Some pages may have indistinct print especially if the original pages were typed with a poor typewriter ribbon or if the university sent us an inferior photocopy.

Previously copyrighted materials (journal articles, published tests, etc.) are not filmed.

Reproduction in full or in part of this microform is governed by the Canadian Copyright Act, R.S.C. 1970, c. C-30.

## AVIS

La qualité de cette microforme dépend grandement de la qualité de la thèse soumise au microfilmage. Nous avons tout fait pour assurer une qualité supérieure de reproduction.

S'il manque des pages, veuillez communiquer avec l'université qui a conféré le grade.

La qualité d'impression de certaines pages peut laisser à désirer, surtout si les pages originales ont été dactylographiées à l'aide d'un ruban usé ou si l'université nous a fait parvenir une photocopie de qualité inférieure.

Les documents qui font déjà l'objet d'un droit d'auteur (articles de revue, tests publiés, etc.) ne sont pas microfilmés.

La reproduction, même partielle, de cette microforme est soumise à la Loi canadienne sur le droit d'auteur, SRC 1970, c. C-30.

THE UNIVERSITY OF ALBERTA

MICROPROCESSOR-BASED SYSTEM FOR MEASUREMENT OF STRAW WALKER  
GRAIN LOSS

by

(C) RONALD G. LARSON

A THESIS

SUBMITTED TO THE FACULTY OF GRADUATE STUDIES AND RESEARCH  
IN PARTIAL FULFILMENT OF THE REQUIREMENTS FOR THE DEGREE  
OF MASTER OF SCIENCE

DEPARTMENT OF AGRICULTURAL ENGINEERING

EDMONTON, ALBERTA

FALL 1987

Permission has been granted to the National Library of Canada to microfilm this thesis and to lend or sell copies of the film.

The author (copyright owner) has reserved other publication rights, and neither the thesis nor extensive extracts from it may be printed or otherwise reproduced without his/her written permission.

L'autorisation a été accordée à la Bibliothèque nationale du Canada de microfilmer cette thèse et de prêter ou de vendre des exemplaires du film.

L'auteur (titulaire du droit d'auteur) se réserve les autres droits de publication; ni la thèse ni de longs extraits de celle-ci ne doivent être imprimés ou autrement reproduits sans son autorisation écrite.

ISBN 0-315-41187-2

THE UNIVERSITY OF ALBERTA

RELEASE FORM

NAME OF AUTHOR

RONALD G. LARSON

TITLE OF THESIS

MICROPROCESSOR-BASED SYSTEM FOR  
MEASUREMENT OF STRAW WALKER GRAIN  
LOSS

DEGREE FOR WHICH THESIS WAS PRESENTED MASTER OF SCIENCE

YEAR THIS DEGREE GRANTED FALL 1987

Permission is hereby granted to THE UNIVERSITY OF ALBERTA LIBRARY to reproduce single copies of this thesis and to lend or sell such copies for private, scholarly or scientific research purposes only.

The author reserves other publication rights, and neither the thesis nor extensive extracts from it may be printed or otherwise reproduced without the author's written permission.

(SIGNED) *Ronald G. Larson*

PERMANENT ADDRESS:

*P.R. #1*  
*BOYLE, ALBERTA*  
*TOA OMO*

DATED *AUGUST 4* ..... 1987



THE UNIVERSITY OF ALBERTA  
FACULTY OF GRADUATE STUDIES AND RESEARCH

The undersigned certify that they have read, and recommend to the Faculty of Graduate Studies and Research, for acceptance, a thesis entitled MICROPROCESSOR-BASED SYSTEM FOR MEASUREMENT OF STRAW WALKER GRAIN LOSS submitted by RONALD G. LARSON in partial fulfillment of the requirements for the degree of MASTER OF SCIENCE.

*David*  
.....

Supervisor  
*[Signature]*  
.....

*Keith C. Stevenson*  
.....

Date... *August 4, 1987* .....

## ABSTRACT

This thesis describes the development of a microprocessor-based system for the measurement of grain loss from the straw walkers of a conventional type grain harvester. The straw walker component of total loss has been shown to be the most significant component of total loss in the harvesting process.

A brief introduction to conventional and axial-flow harvester operation and loss is presented. Current methods of measuring grain loss, along with accuracy and applicability is discussed. A single grain detection sensor at the terminal end of the harvester does not fully indicate true separation loss. The development and testing of a system using four sensors beneath the walkers' length is described.

System test results are discussed at three stages; the fundamental signal, laboratory, and field stages of development. The sensor signal was examined by analog and digital techniques with a microprocessor system. The former technique was chosen as the method for subsequent laboratory and field tests.

Laboratory tests on a stationary straw walker apparatus showed that the sensor system accurately measures separation curve data in a mechanized environment. Field test data displayed accurate measurement of straw walker grain loss. Recommendations are discussed to improve the measurement system and testing procedures.

## ACKNOWLEDGEMENTS

I wish to acknowledge Dr. Jeremy J. Leonard, Department of Agricultural Engineering, University of Alberta, for his advice, encouragement and support throughout the course of this thesis.

I wish to extend my gratitude towards my father, Mr. Ernest T. Larson of Boyle, Alberta, for the supply of the facilities, land and material resources during the field tests herein described. I also wish to thank my brother, Mr. Alvin R. Larson, also of Boyle, for the sacrifice of machinery, operating time and resources, as well as technical assistance that made the field tests possible.

I wish to express appreciation to my wife, Andrea, for her technical assistance, patience, encouragement, and love in the completion of this thesis.

This project was funded by a grant from Agriculture Canada.

## Table of Contents

Chapter	Page
ABSTRACT .....	iv
ACKNOWLEDGEMENTS .....	v
List of Figures .....	ix
List of Tables .....	xii
List of Plates .....	xiii
List of Symbols .....	xiv
1. INTRODUCTION .....	1
1.1 Harvester Operation .....	1
1.2 Harvester Losses .....	4
1.3 Harvester Loss Monitoring .....	7
2. STRAW WALKER GRAIN LOSS .....	10
2.1 Governing Phenomenon .....	10
2.2 Factors Affecting Walker Loss and Separation Curves .....	14
2.3 Measurement of Walker Loss .....	16
2.3.1 Measurement of walker loss with end-placed sensors .....	19
2.3.2 Measurement of the separation curve .....	21
2.4 Objectives .....	22
3. AVAILABLE METHODS FOR MONITORING GRAIN LOSS .....	24
3.1 Sensors .....	24
3.2 Monitor Operation .....	27
3.3 Limitations of Monitor Accuracy .....	28
4. FUNDAMENTAL SENSOR SIGNAL PROCESSING .....	31
4.1 Advantages of a Microprocessor Base .....	31
4.1.1 Description of chosen microprocessor system .....	32

4.2,	Digital Signal Processing .....	34
4.3	Analog Signal Processing .....	35
4.4	Analog Signal Processing Tests .....	41
4.4.1	Single sensor tests .....	41
4.4.2	Multiple sensor tests .....	53
5.	LABORATORY TESTING OF MULTIPLE SENSOR SYSTEM .....	55
5.1	Description of Testing Apparatus. ....	56
5.2	Description of Measuring System. ....	58
5.3	Description of Materials. ....	65
5.4	Experimental Design. ....	66
5.5	Experimental Procedure. ....	67
6.	LABORATORY TEST RESULTS AND DISCUSSION .....	69
6.1	Impact Counting Accuracy .....	69
6.2	Separation Curve Analysis .....	72
6.3	Loss Calculations .....	73
7.	FIELD TESTING OF MULTIPLE SENSOR SYSTEM .....	77
7.1	Description of Equipment. ....	77
7.2	Description of Measurement System. ....	80
7.3	Material Description. ....	84
7.4	Experimental Design. ....	84
7.5	Experimental Procedure. ....	86
8.	FIELD TESTING RESULTS AND DISCUSSION .....	88
8.1	Separation Curves and Loss. ....	88
9.	CONCLUSIONS .....	93
10.	RECOMMENDATIONS .....	95
10.1	Improvements to Sensing System .....	95
10.2	Improvements to Procedure .....	96

11.	REFERENCES. ....	97
12.	APPENDIX I CIRCUIT DIAGRAMS .....	100
13.	APPENDIX II PROGRAM LISTINGS .....	103
	13.1 Microprocessor Data Transfer Programs .....	103
	13.1.1 Mainframe to microprocessor .....	103
	13.1.2 Microprocessor program for IBM personal computer communication .....	106
	13.1.3 IBM personal computer program for microprocessor communication .....	108
	13.2 Digitization of Impact Program .....	110
	13.3 Impact Counting Program for Single Sensor ....	112
	13.4 Impact Counting Program for Multiple Sensors .	113
	13.5 Field Test Program .....	116
14.	APPENDIX III DATA .....	119
15.	APPENDIX IV LABORATORY AND FIELD SEPARATION CURVES	125
16.	APPENDIX V DIGITIZATION OF FUNDAMENTAL SENSOR SIGNAL .....	136

## List of Figures

Figure		Page
1.1	Conventional-Type Combine. A, cylinder; B, concave; C, beater; D, beater grate; E, straw walkers; F, shoe; G, first curtain. (adapted from PAMI, 1980) .....	3
1.2	Axial-Flow Combine. A, rotor; B, threshing grate; C, separating grate; D, rear beater; E, shoe; F, tailings return. (adapted from PAMI, 1979) .....	3
1.3	Axial-Flow and Conventional Type Performance Curves in Barley. (adapted from PAMI, 1979, 1980) .....	8
2.1	Separation Curve. (adapted from Boyce et al. 1974) .....	12
2.2	Grain Remaining Curve. (adapted from Boyce et al. 1974) .....	12
2.3	Differing Losses with the Same End Separation. (adapted from Huisman, 1983) .....	20
3.1	Fundamental Sensor Signal. (adapted from Gullacher and Smith, 1979) .....	25
3.2	Sensor Saturation Effects. (adapted from Gullacher and Smith, 1979) .....	30
3.3	Monitor Inaccuracy. (adapted from Gullacher and Smith, 1979) .....	30
4.1	Analog Signal Processing Block Diagram. ....	37
4.2	System Response to Two Overlapping Impacts. ....	40
4.3	Vibratory Conveyor. ....	43
4.4	Impact Orientations. ....	44
4.5	Single Sensor Impact Counting. (45M) .....	48
4.6	Single Sensor Impact Counting. (45BMT, 10M, 80BMT) .....	48
4.7	Phenomena Causing Double Counts. ....	49
4.8	Single Sensor Impact Counting. (45BMT, 45GSCW) .....	52

Figure	Page
4.9 Multiple Sensor Impact Counting. (45BMT, MULT) .....	52
5.1 Side View of Laboratory Apparatus. (adapted from Luntz, 1986) .....	57
5.2 Gravity Flow Hopper. (adapted from Luntz, 1986) .....	59
5.3 Gravity Flow Hopper Calibration .....	60
5.4 Sensor Placement. (adapted from Luntz, 1986) .....	62
5.5 Laboratory Sensor Housing. (All dimensions in millimetres) .....	63
6.1 Impacts Counted versus Kernels Collected. ....	70
6.2 Typical Laboratory Separation Curve. (Run #5) .....	70
6.3 Calculated Versus Measured Losses. ....	75
7.1 Field Test Sensor Housing. (all dimensions in mm) .....	81
8.1 Sensor-Calculated Loss versus Collected Loss. ....	89
12.1 MEK6802-D5 Evaluation Board Additions. ....	100
12.2 Digital Signal Processing Circuit. IC1, AD7574 analog-to-digital converter; IC2, 1458 dual operational amplifier; IC3, 74LS00, quad-NAND; IC4, MC6802 microprocessor; SIN, sensor input. ....	101
12.3 One Half of Analog Signal Processing Circuit. IC1, IC2 LM324 quad operational amplifiers; IC3, 556 dual timing circuit; IC4, 74LS04 hex-inverter; IC5, MC6821 peripheral interface adapter; S1, S2, sensor inputs. ....	102
15.1 Laboratory Separation Curves. Run #1 .....	125
15.2 Laboratory Separation Curves. Run #2 .....	125
15.3 Laboratory Separation Curves. Run #3 .....	126
15.4 Laboratory Separation Curves. Run #4 .....	126



Figure		Page
15.5	Laboratory Separation Curves. Run #5 .....	127
15.6	Laboratory Separation Curves. Run #6 .....	127
15.7	Laboratory Separation Curves. Run #7 .....	128
15.8	Laboratory Separation Curves. Run #8 .....	128
15.9	Laboratory Separation Curves. Run #9 .....	129
15.10	Laboratory Separation Curves. Run #10 .....	129
15.11	Laboratory Separation Curves. Run #11 .....	130
15.12	Laboratory Separation Curves. Run #12 .....	130
15.13	Field Separation Curve. Run #2 .....	131
15.14	Field Separation Curve. Run #3 .....	131
15.15	Field Separation Curve. Run #4 .....	132
15.16	Field Separation Curve. Run #5 .....	132
15.17	Field Separation Curve. Run #6 .....	133
15.18	Field Separation Curve. Run #7 .....	133
15.19	Field Separation Curve. Run #8 .....	134
15.20	Field Separation Curve. Run #9 .....	134
15.21	Field Separation Curve. Run #10 .....	135
16.1	Digital Signal Processing Block Diagram. ....	137
16.2	Digitized Barley Impact Signal. ....	140

## List of Tables

Table		Page
4.1	Sensor Orientation Test Data Regessions. ....	46
6.1	Laboratory Collection Bag Data. ....	71
8.1	Field Test Separation Data Equations and Losses. ....	90
14.1	Separation Data (Boyce <i>et al.</i> 1974). ....	119
14.2	Sensor Orientation Test Data. ....	120
14.3	Desired Laboratory Test Throughput Data. ....	121
14.4	Laboratory Separation Data. ....	122
14.5	Laboratory Separation Curve Equations and Losses. ....	123
14.6	Field Test Data. ....	124

## List of Plates

Plate		Page
5.1	Front Section Walker Perforations .....	64
5.2	Rear Section Walker Perforations .....	64
7.1	Field Test Machinery. ....	78
7.2	Microprocessor System. ....	78
7.3	Location of Sensors. ....	82
16.1	Amplified Barley Impact Signal (Amplitude=4.5V, Time base=1ms/div) .....	141

## List of Symbols

Symbol	Description	Units
$a_5, a_6$	constants	
A	constant	
b	constant	
B	constant	
$B_{dmog}$	bulk density of M.O.G.	kg/m <sup>3</sup>
$G_f$	final mass of grain on walker	kg
$G_i$	initial mass of grain on walker	kg
$G_o$	grain applied to walker	kg
$G_r$	grain remaining on walker	kg
$H_A$	alternate hypothesis	
$H_o$	null hypothesis	
KE	kinetic energy	J
L	length of walker	m
$L_d$	length of diffusion	m
$L_s$	average length of open space	m
$L_v$	walker loss	%
M	rate of flow of M.O.G.	kg/s
	mass of particle	kg
	sample mean	
MOG	feedrate of M.O.G.	t/h
M.O.G.	material other than grain	
n	sample size	
R	weight ratio of grain to straw	
s	sample standard deviation	
S	operating speed	km/h

$S_0$	rated combine speed	km/h
$S_v$	separation rate on walker	%/m
$t$	t statistic	
$v_1$	initial particle velocity	m/s
$v_2$	final particle velocity	m/s
$V_a$	average velocity of particle	m/s
$X$	distance along walker	m
$X_1$	days past 30% moisture content	
$X_2$	days past technological maturity	
$Y$	constant yield	t/ha
$Y_0$	arbitrarily defined standard yield	t/ha
$\alpha$	level of significance	
$\mu$	population mean	

## 1. INTRODUCTION

The annual ritual of grain harvest has developed into a highly mechanized operation involving far fewer workers than were needed in the labor-intensive community threshing crews of less than fifty years ago. The current harvest is centered around the modern grain harvester, or combine, a complex, efficient and expensive component of a typical grain farming operation.

Utilizing the harvester's full potential is necessary to maximize overall profitability (Huisman, 1983). The suggestion that an optimum rate of threshing efficiency will yield maximum gain has been well documented (McGechan and Glasby, 1982; Huisman, 1983; Leflufy and Stone, 1983; Palmer, 1984). A maximum rate of loss acceptable has been suggested as three percent of the total by the Prairie Agricultural Machinery Institute (PAMI, 1979), while McGechan and Glasby (1982) suggest two percent as an optimum level. The farmer considers many factors, such as time of year, quality and value of crop, operating expenses and even weather uncertainties when accepting a particular level of loss. Regardless of the accepted optimum loss, the continuous measurement thereof has been widely attempted.

### 1.1 Harvester Operation

The objective of the grain harvest is to extract the valuable seeds from the crop stand with little damage and loss, high cost-efficiency and as quickly as possible. Two

major harvester designs have evolved to meet the harvest challenge, the conventional type and the axial-flow combine. The most common type of combine is the conventional, employing a transverse-mounted horizontal threshing cylinder and a number of straw walkers which, together, thresh and separate the crop material (Figure 1.1). The axial-flow combines, which have gained popularity, utilize large horizontal or sloping rotors to both thresh and separate the crop material (Figure 1.2). The straw walkers are not required in the axial-flow combine design. The conventional combine was the only major type available until the axial-flow combine established a market niche with claims of increased performance with less crop damage.

The harvest procedure remains similar regardless of combine type. A standing crop must be cut and fed into the harvester superstructure. The cutting and feeding may be done at the same time by the harvester but often, on the Prairies, the crop is first cut and laid in windrows by a swather. The crop may then be gathered by a pick-up mechanism on the harvester and fed into the threshing components.

The threshing mechanism attempts to dislodge the kernels of grain from the stalk by impact with the rasp bars of the cylinder or rotor. In the conventional combine, the threshing takes place in about one third of a revolution of the threshing cylinder. About 65% of grain is also separated from the straw during the threshing process and falls

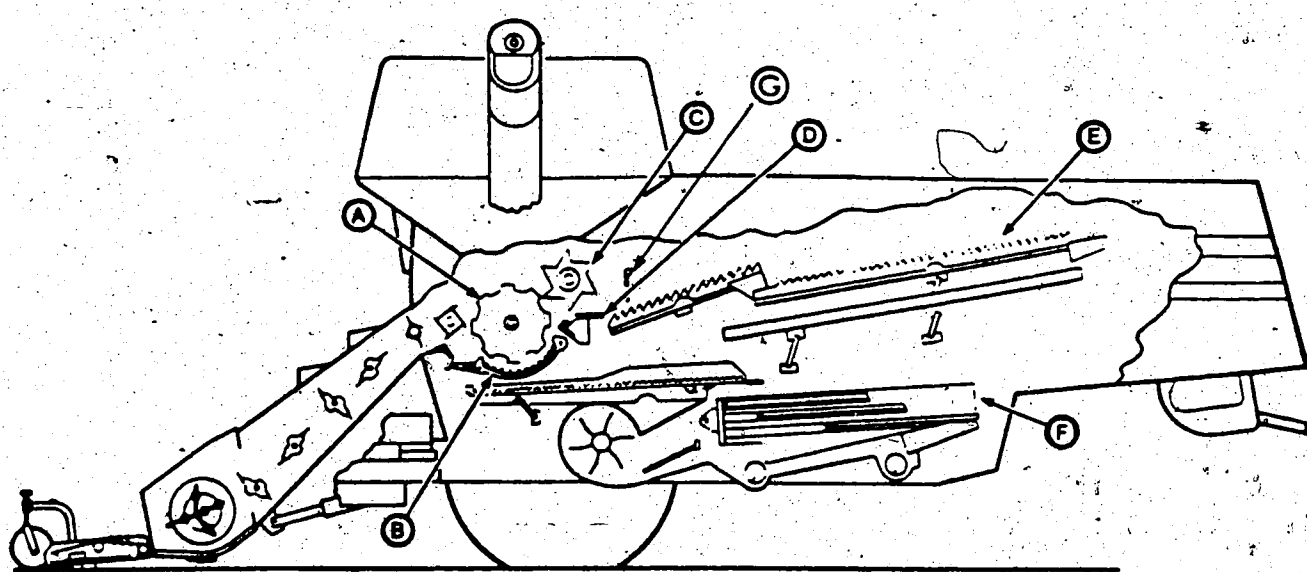


Figure 1.1 Conventional-Type Combine. A, cylinder; B, concave; C, beater; D, beater grate; E, straw walkers; F, shoe; G, first curtain. (adapted from PAMI, 1980)

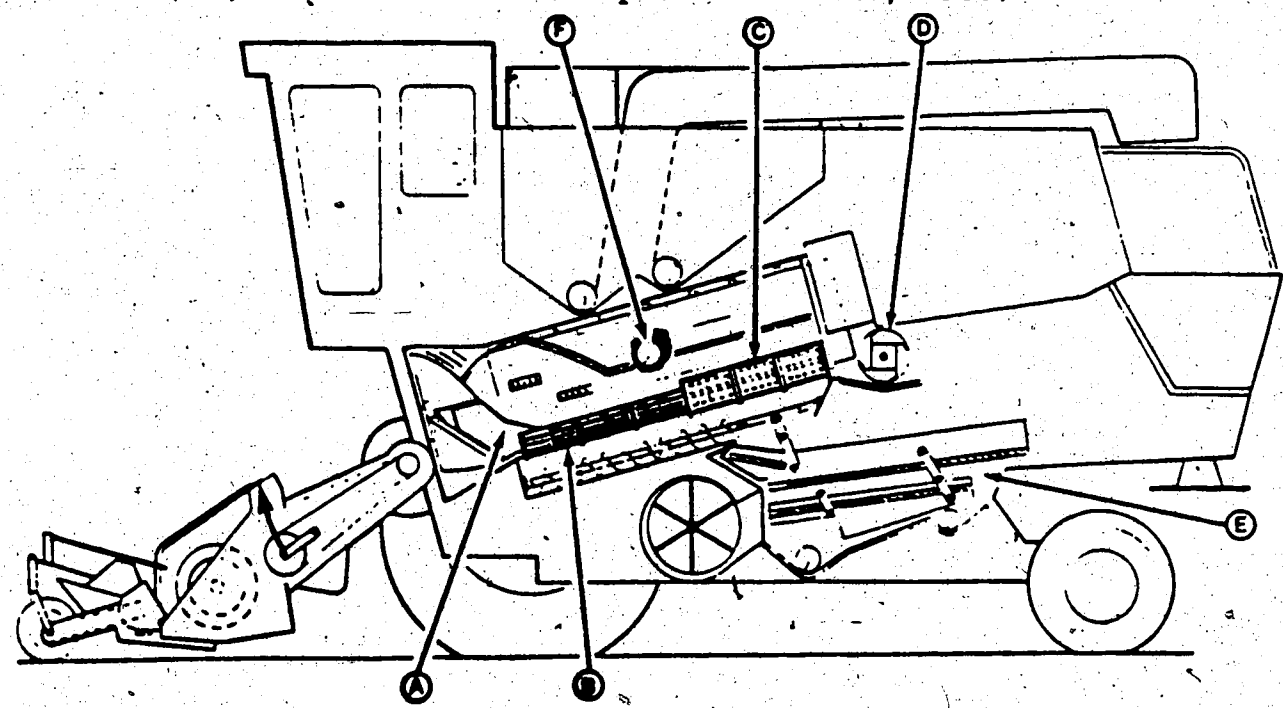



Figure 1.2 Axial-Flow Combine. A, rotor; B, threshing grate; C, separating grate; D, rear beater; E, shoe; F, tailings return. (adapted from PAMI, 1979)





through the threshing grate below the cylinder (Boyce et al. 1974). The axial-flow combine commonly accepts the flow of crop axially at one end of the rotor. The crop is initially threshed by the threshing section of the rotor and concave. The crop continues in a spiral around the rotor concaves towards the discharge end of the harvester.

After threshing, separation of grain from the straw is performed by the straw walkers in the conventional combine and by the latter portion of rotor and separation concaves in the axial-flow. The straw walkers oscillate rapidly, shaking the grain loose and causing the grain to fall through the perforated surface, while moving the straw rearward to be discharged. The axial-flow's rotor spirals the straw and grain rearward, extracting the grain by centrifugal force.

All the grain separated from the straw is cleaned by the shoe, or cleaning sieves. A blast of air from the cleaning fan, as well as the reciprocation of the sieves, keep only the kernels of grain, while blowing the chaff, straw pieces and other contaminants out of the harvester. The clean grain is collected and deposited in a hopper tank for storage until the combine is emptied.

**1.2 Harvester Losses**

There are several types of crop losses which occur prior to and during harvest that reduce the net return from the crop as a whole. Front-end losses occur before the crop

enters the harvester's threshing mechanism. Cutting and shedding losses, which are affected by crop maturity and method of handling and gathering the crop, are considered front-end losses (McGechan and Glasby, 1982). Audsley and Boyce (1974) used two second order polynomial equations to predict front-end loss as a function of days past maturity.

$$\text{Shedding loss} = 0.001(0.6746X_1 - 0.0062X_1^2)Y, \text{ t/ha} \quad 1.1$$

$$\text{Cutting loss} = 0.001(15.3364 + 0.8819X_1 - 0.0065X_1^2)Y, \text{ t/ha} \quad 1.2$$

where:  $X_1$  = days past 30% moisture content (wet basis), and  
 $Y$  = constant yield (t/ha).

Phillips and O'Callaghan (1974) chose a linear relationship for shedding loss and an exponential function for cutting loss as functions of days past technological maturity.

Maturity was defined as the date on which harvesting could commence.

$$\text{Shedding loss} = 0.003X_2Y, \text{ t/ha} \quad 1.3$$

$$\text{Cutting loss} = 0.0011208(15 + (1 + 0.025(X_2 - 40)) * \exp(0.521462 + 0.101165X_2^2)), \text{ t/ha} \quad 1.4$$

where:  $X_2$  = days past technological maturity.

Threshing loss describes the loss of seeds which are damaged by the threshing process or those which have not been adequately loosened from the stalk (Wrubleski and Nyborg, 1978; McGechan and Glasby, 1982).

Audsley and Boyce (1974) used a relationship for threshing loss as a function of available yield and feedrate of material other than grain (MOG):

$$\text{Threshing loss} = 0.02(Y_S / (Y_0 R S_0))^2 Y, \text{ t/ha} \quad 1.5$$

where:  $S$  = operating speed (km/h),  
 $Y$  = constant yield for crop on farm (t/ha),  
 $Y_0$  = an arbitrarily defined standard yield (t/ha),  
 $R$  = weight ratio of grain to straw, and  
 $S_0$  = rated combine speed (km/h).

Phillips and O'Callaghan (1974) also developed a relationship for threshing loss:

$$\text{Threshing loss} = \exp(a_5 + a_6(\text{MOG})), \text{ t/ha} \quad 1.6$$

where:  $a_5$  and  $a_6$  = constants depending on combine size, and  
 $\text{MOG}$  = feedrate of material other than grain (t/h).

Shoe loss, or cleaning loss, occurs over the sieve of the harvester and is usually small unless the sieves and fan are maladjusted severely (Wrubleski and Nyborg, 1978). Shoe loss becomes excessive if the shoe is overloaded, the air blast from the cleaning fan is too powerful or misdirected, or the sieve openings are incorrect. A compromise is established between sieve capacity and cleanliness of harvested grain when adjusting the shoe.

Separation losses occur in both axial-flow and conventional type combines and account for the greatest portion of total losses at an optimum operating level of loss. Axial-flow separation loss is commonly referred to as rotor loss. Separation loss for a conventional combine is the straw walker loss and is the most significant loss in most cases of prairie grain harvesting (Nyborg *et al.* 1969;

Reed *et al.* 1970). Separation losses result from inadequate removal of loose grain from the straw in the separation zone of the harvester. The separation loss increases exponentially with the M.O.G. feedrate, thus influencing the total loss curve to be of similar exponential shape. Figures 1.3(a) and 1.3(b) show the typical relative proportions of loss types for a conventional and an axial-flow combine in barley. Straw walker loss is dealt with, in depth, in chapter 2 of this thesis.

### 1.3 Harvester Loss Monitoring

Current grain loss monitoring has been developed to inform the harvester operator of the machine's functional efficiency. The farmer had the need, or the need was impressed upon him, of knowing the loss of grain occurring at the discharge end of his combine. The monitoring of grain loss focusses on the cleaning and separating losses since they are the most significant and easy to control. Reed *et al.* (1968) developed an acoustic method of detecting grain kernels in the combine effluent by means of impacts on a sensor. Separation or shoe loss could be indicated or monitored by placing a single acoustic sensor pad immediately behind the apparatus concerned. This type of monitoring has been found to be inaccurate, unreliable and widely unused, even by the farmers who own a system (Huisman, 1983). In order to accurately measure the loss occurring while harvesting, an improved method is required.

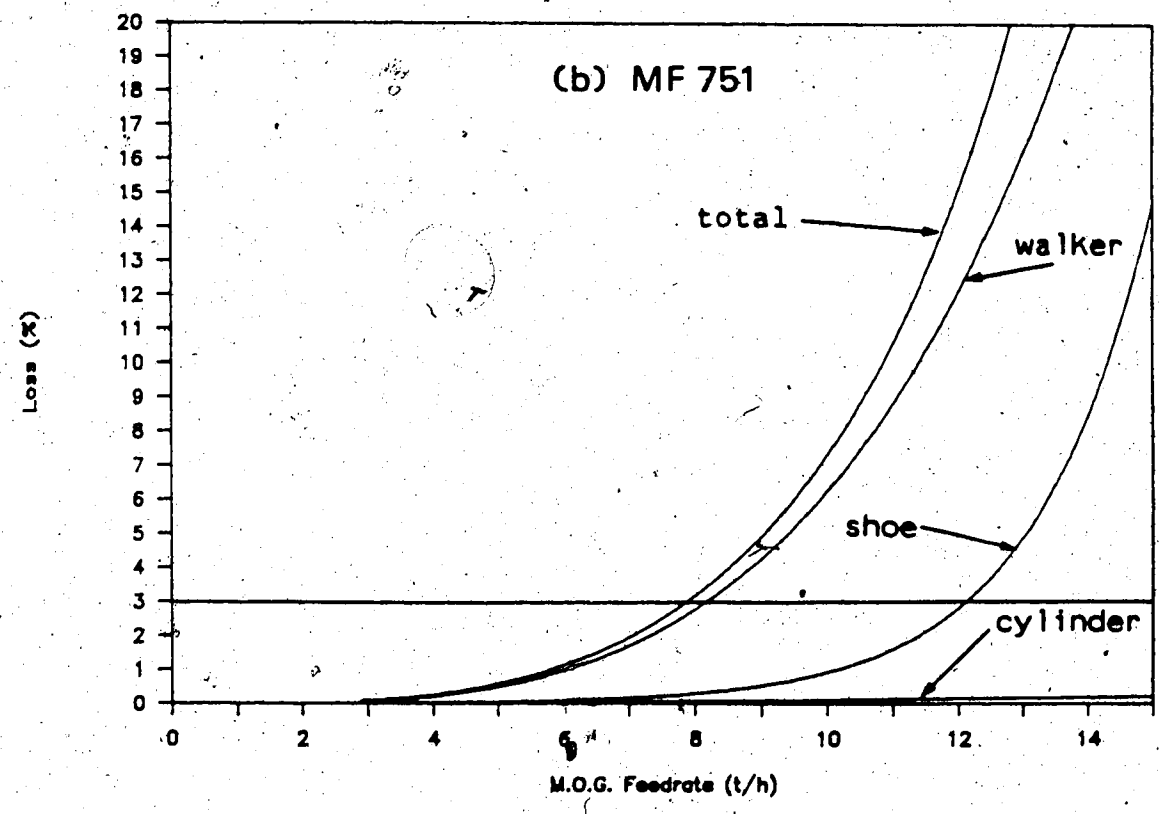
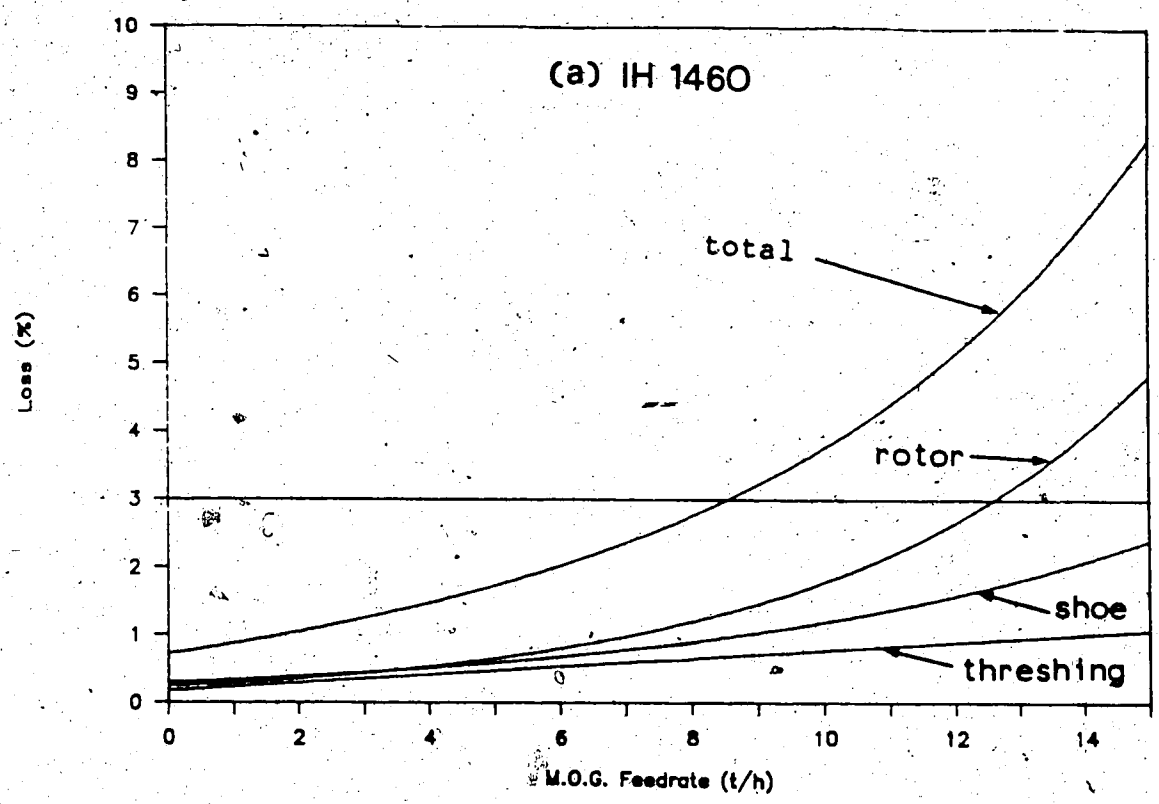


Figure 1.3 Axial-Flow and Conventional Type Performance Curves in Barley. (adapted from PAMI, 1979, 1980)

Such a method is described in chapter 2.

## 2. STRAW WALKER GRAIN LOSS

As illustrated by Figures 1.3(a) and 1.3(b), the most significant portion of the total harvester loss is the separation loss. This thesis is concerned with the measurement of separation loss for a conventional combine with straw walkers. Similar characteristics exist for separation in axial-flow combines, thus, the work in this thesis may also apply to axial-flow harvesters (Lunty, 1986). Since walker loss is the dominant contributor to total loss, a measure of walker loss gives an indication of total harvester loss. Straw walker loss is also easiest to control with feedrate as a consequence of ground speed alteration.

### 2.1 Governing Phenomenon

The straw walkers attempt to separate lodged kernels of grain from the associated straw by an oscillatory action. The oscillation also moves the straw rearward with the assistance of toothed walker edges. Optimum walker oscillation frequency has been found to be between 190 and 210 RPM for 50mm crank throw, and about 150 RPM for 75mm crank throws, with an optimum rearward slope of 8° to 20° from the horizontal under normal operating conditions (Boyce *et al.* 1974, Reed *et al.* 1972). Higher speeds tend to move the straw mat rearward faster with fewer oscillations for separation, resulting in a poorer separating motion. The walker slope determines the speed at which the straw mat is

moved rearward, with lower slopes having faster movement. The optimum angle and RPM results in an optimum amount of grain and straw on the walkers at any one time and thus maximizes the separator efficiency. The overall length of the walker also determines efficiency, with a longer walker ultimately saving more grain.

Separation curves for straw walkers were obtained by Reed *et al.* (1970) and Boyce *et al.* (1974). The latter showed that maximum separation occurred at about one third of the way along the walker due to the fact that not all of the crop was in contact with the walkers until completely slowed down by the first curtain (Figure 1.1). The grain separation then fell off rapidly in an exponentially decaying fashion. The former developed an equation to describe a grain-remaining curve:

$$G_r = G_o \exp(-bL) \quad 2.1$$

where:  $G_r$  = grain remaining on the walkers (kg),  
 $G_o$  = grain applied onto the walkers (kg),  
 $L$  = length of the walkers (m), and  
 $b$  = constant, (attenuation coefficient, Wang, 1984).

Reed *et al.* (1970) went on to describe a walker half-length, similar to a half-life of a radioactive decay, in order to describe the walker efficiency. The half-length described the length of a walker that would separate exactly one-half of applied grain. Typical separation data according to Boyce *et al.* (1974) are shown in Figure 2.1 as a separation curve, while a grain remaining curve is shown in Figure 2.2 for the same data. The data is given in Appendix III, Table 14.1. Units for the separation curve are percent



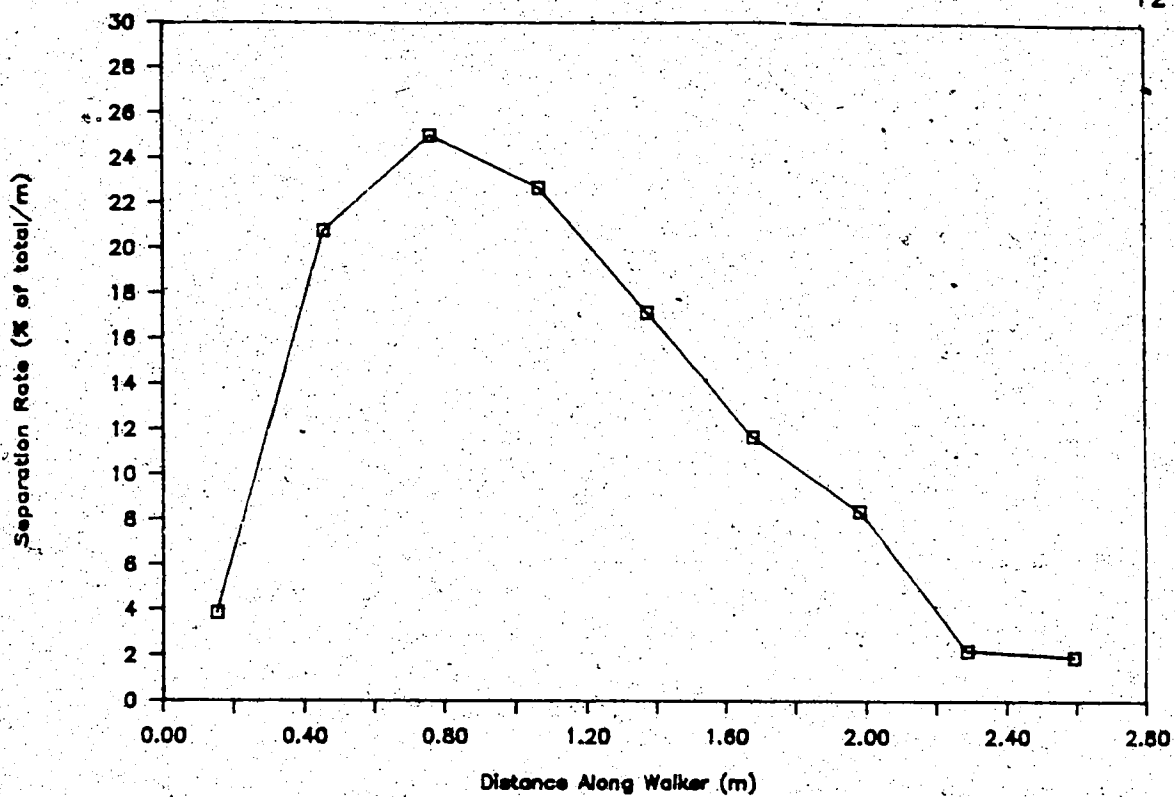


Figure 2.1 Separation Curve. (adapted from Boyce *et al.* 1974)

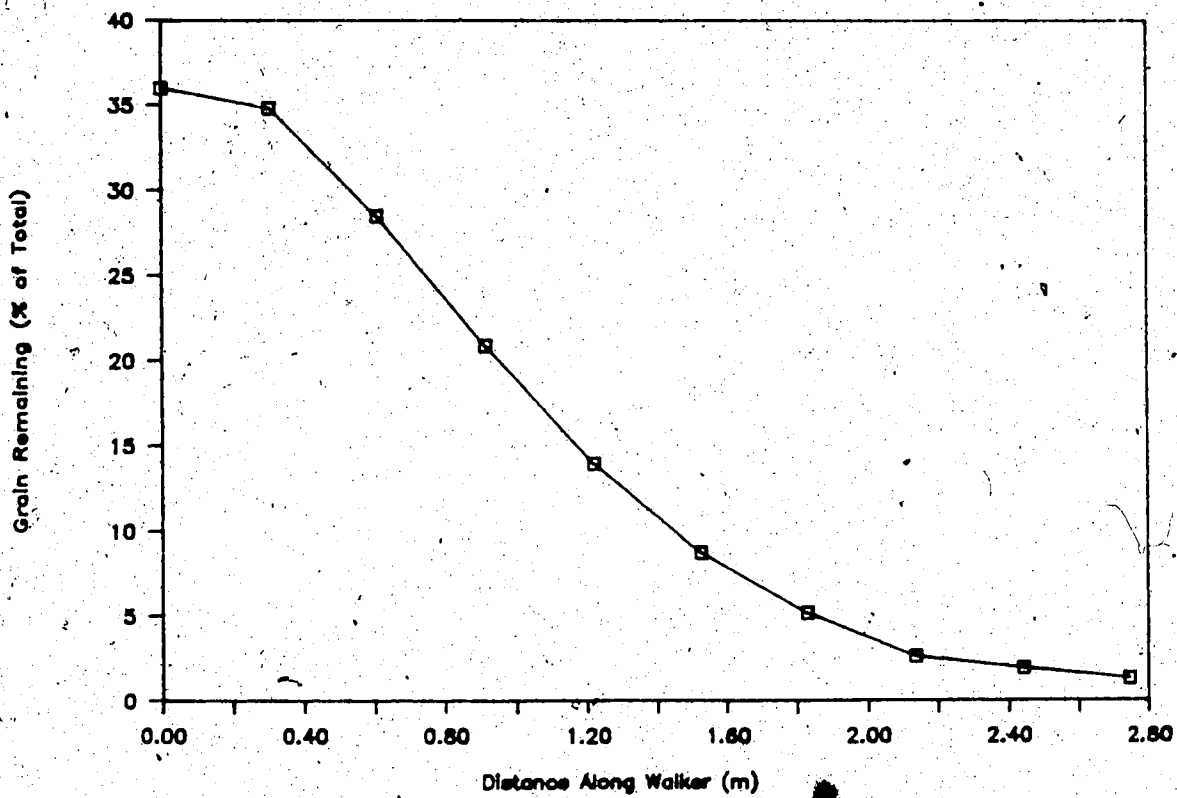


Figure 2.2 Grain Remaining Curve. (adapted from Boyce *et al.* 1974)

of total grain separated per metre of walker length versus distance along the walkers. The grain remaining curve is an integration of the separation curve, hence the units are percent of total versus distance along walker, with the value of grain remaining at the end of the walker being the percentage of walker loss. The grain remaining curve, obtained from Boyce *et al.* 1974, is of the general shape described by Reed *et al.* (1970), with values of  $G_0 = 80.63\%$ ,  $L = 2.745$  metres, and  $b = 1.52$ , being determined from a least squares regression. The regression gave an  $R^2$  of 0.978. The first two points represent a portion of the separation curve different from the other points. Little separation occurs until the straw is slowed down by the first curtain and full contact is made with straw walker. Consequently, the first two points were ignored when fitting the exponentially decaying curve to the grain-remaining curve. Therefore, the equation after Reed *et al.* (1970), would be:

$$G_r = 80.63 \exp(-1.52X) \quad 2.2$$

where:  $X$  = distance along walker (m).

The equation is valid for  $X$  between 0.60 and 2.745 m. The establishment of the grain remaining curve on an operating harvester would be difficult since the amount of grain applied to the straw walkers would be unknown.

Gregory and Fedler (1986) developed an equation for predicting grain separation on straw walkers based on Fick's Law of Diffusion and the fraction of open space in the straw

mat.

$$G_f = G_i \exp(-(bV_a W B_{dnog}/M)(L_s/L_d))L \quad 2.3$$

where:  $G_f$  = final mass of grain on walker (kg),  
 $G_i$  = initial mass of grain on walker (kg),  
 $b$  = constant, varies with grain size and vibration energy,  
 $V_a$  = average velocity over length  $L_s$  in direction of interest,  
 $L_s$  = average length of open space in material (m),  
 $B_{dnog}$  = bulk density of material other than grain ( $\text{kg/m}^3$ ),  
 $M$  = rate of flow of material other than grain ( $\text{kg/s}$ ),  
 $L$  = length of walkers (m), and  
 $L_d$  = length of diffusion (m).

This thesis will be concerned with the separation curves obtained by the measurement of actual separation rates along the walker.

## 2.2 Factors Affecting Walker Loss and Separation Curves

The most important factor affecting losses is feedrate (Reed *et al.* 1968). The relationship has been illustrated in Figures 1.3(a) and 1.3(b) with the harvester losses as a function of feedrate. The moisture content of both grain and straw also affect losses. The threshing efficiency of the cylinder is reduced at high moisture content, thus increasing the load on the straw walkers. Also, grain is not easily shaken from a mat of wet straw due to the increased density and higher effective coefficient of internal friction between grain and straw. In barley, if the material is extremely dry, bridging of grain and awns due to static electricity may prevent grain from being shaken through the

straw.

The losses over the straw walkers also are affected by the ratio of M.O.G. to grain, since a thick straw mat with grain dispersed throughout does not promote efficient separation (Reed *et al.* 1970). A thick straw mat is not agitated sufficiently, especially at the top surface, to induce the kernels to fall through. A thin straw mat offers less resistance to separation with an increased opportunity for grain to separate from greater agitation and more space to fall through (Gregory and Fedler, 1986).

Straw length affects separation with the tendency of long straw to behave as a continuous mat preventing adequate separation (Reed *et al.* 1970). Shorter straw enables the grain to be shaken out effectively. The orientation of crop material when entering the harvester influences the loading characteristics on the straw walkers (Reed *et al.* 1968, 1970). An uneven distribution of heads in the swath, commonly concentrated either to one side or the center, tends to overload parts of the walker system without utilizing the remainder to full capacity. A similar nonuniformity of walker loading occurs when operating on hillsides; the lower side being overloaded and the higher side under capacity.

A common contribution to loss over straw walkers is operator error. If an improper cylinder/concave adjustment is made, the walkers may become overloaded because of poor separation at the concave. A compromise must be reached

between threshing capacity and crop damage in order to optimize the threshing unit. Also, operators may run the harvester at under- or over-capacity and, thus, lower efficiency (Leflufy and Stone, 1983).

The separation curve is also affected by the presence and positioning of walker curtains which slow down the crop material to keep the straw mat in contact with the walkers. Boyce *et al.* (1974) conducted field tests to determine the influence of curtains on the separation curve. The conclusion was made that curtains, especially the front set, are critical to adequate separation.

### 2.3 Measurement of Walker Loss

Currently, measurement of walker loss is attempted by placing a single grain loss sensor at the discharge end of the straw walker. Huisman (1983) has proposed a method of measuring walker loss by measuring the separation rates along the entire walker length. Walker loss subsequently can be obtained from the separation curve. The grain-remaining curve, as in Figure 2.2, gives the amount of grain loss by the value at the end of the walker. That is, the grain remaining in the straw once the straw has left the walker assembly is considered as loss. This approach seems simple except for the fact that on a continuous measurement system, the initial value of grain onto the walker ( $G_0$ ) would not be known from the separation data alone. Knowing  $G_0$  would be critical in that this parameter positions the curve with

respect to the vertical axis and ultimately determines the value of grain loss. An error in estimating  $G_0$  would result in substantial misrepresentation of the loss actually occurring.

The separation curve obtained solely from separation data can be used for the calculation of end loss. By integrating under a separation curve with respect to distance along the walker from the discharge end to infinity, the value of grain loss is obtained (Lunty, 1986). This integration can be accomplished only by first obtaining a curve that accurately extrapolates the separation data beyond the walker length. The extrapolation is best accomplished by an exponential-type decay. Ignoring the first two data points, mentioned previously, the data used to generate Figure 2.2 were fitted to an exponential equation of the following form:

$$S_v = A \exp(BX) \quad 2.4$$

where:  $S_v$  = separation rate (% of total/m),  
 $A$  = constant (%/m),  
 $B$  = constant related to sharpness of decay, and  
 $X$  = distance along walker (m).

The least squares regression was:

$$S_v = 113.83 \exp(-1.53X) \quad [R^2=0.729] \quad 2.5$$

To calculate loss from the walkers,  $S_v$  is integrated from the end of the walkers to infinity:

$$\begin{aligned} L_v &= \int_L^\infty S_v \\ &= \int_L^\infty A \exp(BX) dX \end{aligned}$$

$$=(\exp(B \cdot \phi) - \exp(BL))A/B$$

$$= -\exp(BL)A/B$$

2.6

where:  $L_v$  = walker loss (%), and  
 $L$  = length of walker (2.745 m for these data).

In this case the walker loss was calculated to be 1.14% which differs from the figure for measured walker loss, (1.30%) by 0.16%. Of course, if the number of data points considered was reduced, the fit would be better ( $R^2$  of 0.870 and 0.913 if three and four points were ignored respectively), but the trend of the data would not be utilized fully in the fitted equations and thus the accuracy of loss calculation would be poorer. The difference of 0.16% can be attributed to a number of conditions present in the particular circumstances of the data acquisition.

The influence of the rear curtain on the separation curve is illustrated by the slight 'bump' in the curve at about 2.0 metres along the walker as shown in Figure 2.2. The separation characteristics are affected significantly at this point and would tend to introduce error in the calculation. This shows, also, that relying on the end separation rate for loss measurement would not be as accurate as including data from the whole walker length.

The data gathering method utilized very large sampling areas (0.305 metres \* walker width) making the average separation rate calculated for each area in possible error with that separation rate actually occurring at the center

of the area. The accuracy would have been better if point separation rates were used rather than collection tray averages. Consequently, a method of point-separation rate measurement seemed to offer a better basis for the real-time calculation of walker losses.

### 2.3.1 Measurement of walker loss with end-placed sensors

By placing sensors only at the end of the walkers the entire separation curve is approximated by the end separation. Lundy (1986) showed the problems encountered with such an arrangement by comparing two substantially different loss situations with the same end separation rate (Figure 2.3). The end separation rates are identical in the figure, yet the overall separation curves are not. Consequently, the losses illustrated in each case are in fact different, with identical end separation rates.

Current grain loss monitors give an indication of loss but do not quantify the loss in real units. The usual method for use of grain loss monitors is to calibrate them so that a given level of loss results in a corresponding meter reading. This calibration involves operating the combine while collecting effluent as well as a meter reading, requiring a calibration crew of approximately fifteen people (Wood and Kerr, 1980). Even after calibration, the loss monitors merely indicate a presence of loss without giving a reading of actual loss (Gullacher and Smith, 1979). The calibration so performed is valid only for the time and



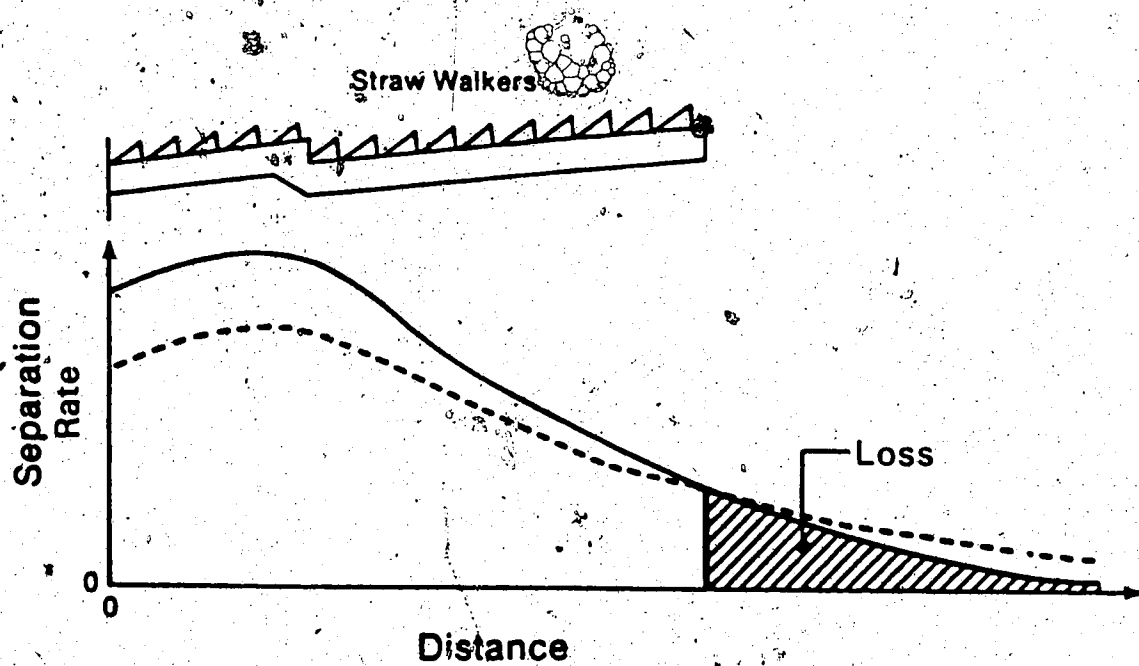


Figure 2.3 Differing Losses with the Same End Separation.  
(adapted from Hulsman, 1983)

conditions of calibration, with changes in crop and field irregularities affecting the accuracy of calibration. As a consequence, frequent calibrations would be necessary but are very seldom performed in a harvest situation. As a result, the monitor becomes inaccurate and unreliable and is often ignored.

### 2.3.2 Measurement of the separation curve

A method has been suggested by Huisman (1983) and attempted by Luntz (1986) where the separation rate curve is measured with multiple sensors along the walker length. Several point-separations are measured, creating a separation curve from which the walker loss can be calculated.

An approach to determine placement of sensors was sought which would give an adequate amount of information together with ease and simplicity of loss calculation and data processing. Thus, the walker was laterally divided into four quarters with a sensor situated at the rear end of each quarter below the open grate of the walker surface. This distribution of sensors would give an adequate representation of the exponentially decaying portion of the separation curve as well as the end separation. Loss calculations could then proceed as for the data evaluated in section 2.1 using four point-separation rates.

## 2.4 Objectives

The objectives of this study were to create a system which would accurately measure loss via the separation curve on a conventional combine. Multiple sensors beneath the straw walkers would be used to measure the separation curve. An exponentially decaying curve would be fitted to the data, and the integral of the curve from the end of the walker to infinity would yield the grain loss. The process would involve the development of a system capable of rapid data acquisition under the harsh conditions of a harvester environment. The system would be tested in both laboratory and field conditions and would be able to provide separation data for the calculation of walker loss.

The sensor signal, used to detect grain impacts, would be investigated both in analog and digital techniques for the purpose of adopting an adequate system for impact detection by a microprocessor. The sensor properties would be studied to determine the best angle of orientation to the grain trajectories. The measurement system would be tested to ensure little influence from chaff and straw.

The objective of the laboratory tests was to determine the ability of the sensor system to measure grain contacting the sensor, and ultimately measure the separation curves in hopes of calculating a loss.

The field test objectives were to obtain a working system on an actual harvester that could measure the separation curves and also result in a loss calculation. The

system should not be affected by change in harvesting conditions since the entire separation curve would be measured for all conditions.

### 3. AVAILABLE METHODS FOR MONITORING GRAIN LOSS

Many companies sell grain loss monitoring equipment. Some manufacture harvesters and supply monitors usually made by others as extra equipment. Others are independent manufacturers, selling directly to farmers. Regardless of which system is considered, all exhibit a similar overall strategy and utilise acoustic sensors.

#### 3.1 Sensors

There are several shapes of transducers suggested by Reed (1978) which may be mounted in specific locations on the harvester. Three types of sensors are categorized; pad, full width and longitudinal types, with the pad type being most common. All types of these sensors work on the same principle of acoustically detecting an impulse when contacted by a particle. The surface of the sensor, or sounding board, is a durable surface to which a piezoelectric crystal is attached (Reed *et al.* 1968). This crystal has the property of generating an electric potential when subjected to a mechanical strain. The sensor is situated to intercept kernels of grain being lost, which contact the surface causing minute strains in the crystal and consequently a train of electrical pulses. A single kernel impact on a sensor would exhibit a typical fundamental signal as shown in Figure 3.1 (Gullacher and Smith, 1979).

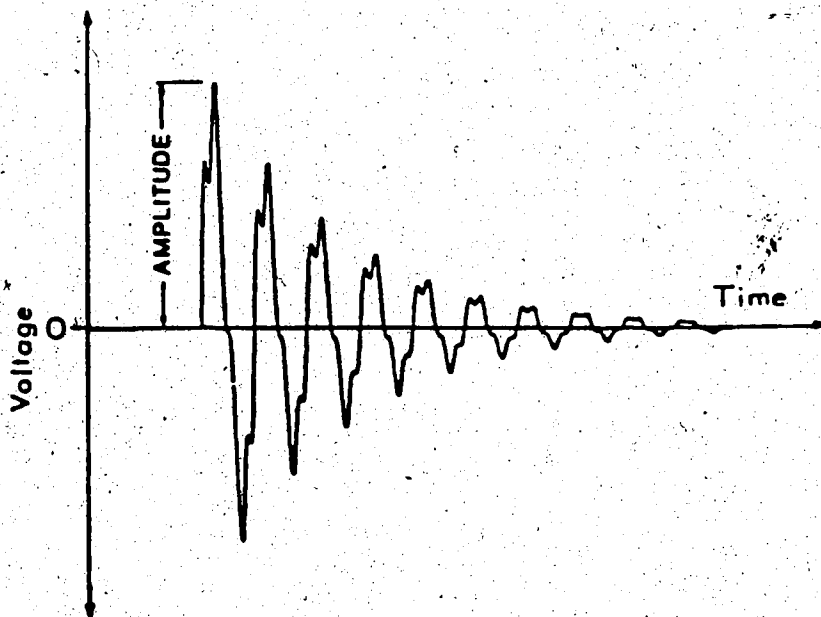


Figure 3.1 Fundamental Sensor Signal. (adapted from Gullacher and Smith, 1979)

Two characteristics of the fundamental signal are the amplitude of the initial pulse and the frequency of oscillation. The electric potential generated by the crystal is approximately in proportion to the time-rate of energy impartation by the impacting particle (Reed et al. 1968). The total energy imparted is influenced by the hardness, mass and velocity of the particle. The conservation of energy for a collision in an inelastic situation assuming that one object is immovable is given by:

$$\text{KE Before Impact} = \text{KE After Impact} + \text{Impact Energy} \quad 3.1$$

$$\text{Impact Energy} = (v_1^2 - v_2^2)M/2, \text{ J} \quad 3.2$$

where: KE = kinetic energy (J),  
 M = mass of the particle (kg),  
 $v_1$  = velocity component perpendicular to the sensor surface before impact (m/s), and  
 $v_2$  = velocity component perpendicular to the sensor surface after impact (m/s).

The time rate of energy impartation is obtained by taking the derivative of the impact energy with respect to time.

$$\text{Time-Rate of Energy Impartation} = \frac{d}{dt} ((v_1^2 - v_2^2)M/2) \quad 3.3$$

From this analysis, one can easily see that mass and velocity of the particle strongly influence the time rate of energy impartation. The hardness of the particle determines the duration of the impact and thus influences the rate of energy transfer. A hard particle will have a short duration impact, yielding a high amplitude, high frequency signal. A large particle would create a high amplitude impulse of long duration. A high velocity would create a larger deformation of the sensor surface and thus produce a high amplitude

signal of long duration. In a gravity-induced fall of a particle onto the sensor surface, the height of drop would influence the velocity of impact. After the impact, the sensor surface vibrates, producing the signal form shown in Figure 3.1. The vibration gradually decays due to friction in the sounding board material and eventually dies out. It is not clear why the resonant frequency would not be the same regardless of particle impact type. A typical grain signal lasts for about 7.5 milliseconds with an initial amplitude of less than one volt.

### 3.2 Monitor Operation

Current grain loss monitors employ a number of different techniques for analyzing the fundamental signal from the grain loss sensor. The monitor evaluates the signal to determine when a particle of interest has struck the sensor. Evaluation methods include discrimination of particles that are non-grain by the amplitude of impact signals and/or analysis of characteristic frequency groups (Gullacher and Smith, 1979). The frequency analysis is primarily effective in small seed crops such as canola, where the gross physical properties of the seeds and non-seeds only differ slightly (Gullacher and Smith, 1979).

For every detection of a grain kernel impact, a square voltage pulse is generated and processed by a frequency-to-voltage converter that converts a train of such pulses into a direct current potential proportional to the



frequency of impacts. The voltage is displayed with an analog meter, providing the operator with information concerning loss. Adjustments are available for calibration, sensitivity of discrimination and for the selection of which sensors to enable. Some monitors employ ground speed sensors in order to relate the loss readings to area of ground covered.

### 3.3 Limitations of Monitor Accuracy

Under conditions of high impact rates, kernel pulses tend to overlap either partly or wholly, and the monitors are not able to distinguish between them. The monitor becomes saturated and, consequently, does not indicate the full extent of the impact losses (Gullacher and Smith, 1979, Wood and Kerr, 1980). Monitors attempt to account for this saturation by employing compensation in the form of electronic circuitry or by fitting the meter with a non-linear scale (Gullacher and Smith, 1979). A typical representation of saturation effects is given in Figure 3.2. The saturation is primarily due to the physical constraints of the sensor/kernel impact. The time between the overlapping impacts is too short to allow the monitor to distinguish between them.

Even when a monitor has been calibrated to a manufacturer's specifications, the reading on the meter may not coincide proportionally to the actual loss rate of the harvester. One contribution to this distortion, especially

at high feedrates, is the inaccuracy of measuring loss only by sensors at the discharge end of the walkers and shoe. If the separation curve, as described in section 2.1. is altered slightly by changing conditions, the monitor may be thrown out of calibration due to a change in the percentage of effluent sampled (Gulacher and Smith, 1979). Figure 3.3 shows a typical relationship between meter reading and actual harvester loss for a properly calibrated loss monitor immediately after calibration.

A description of the design and testing of a system to measure accurately the walker loss from a harvester accurately using multiple location grain loss sensors follows.

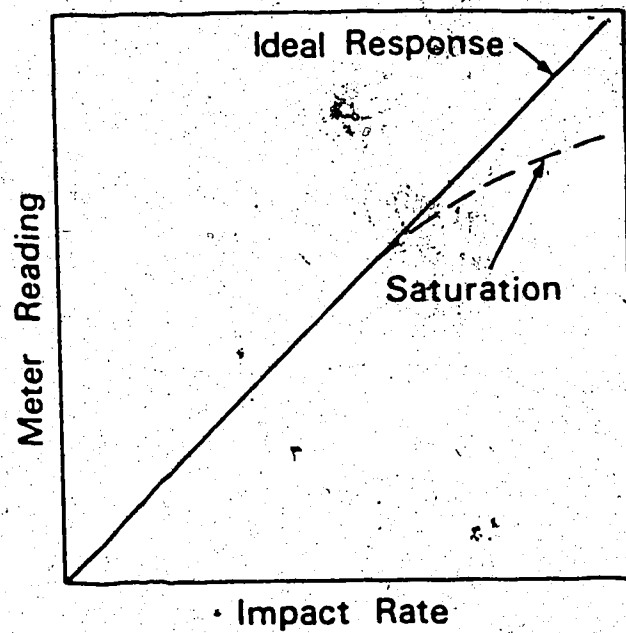


Figure 3.2 Sensor Saturation Effects. (adapted from Gullacher and Smith, 1979)

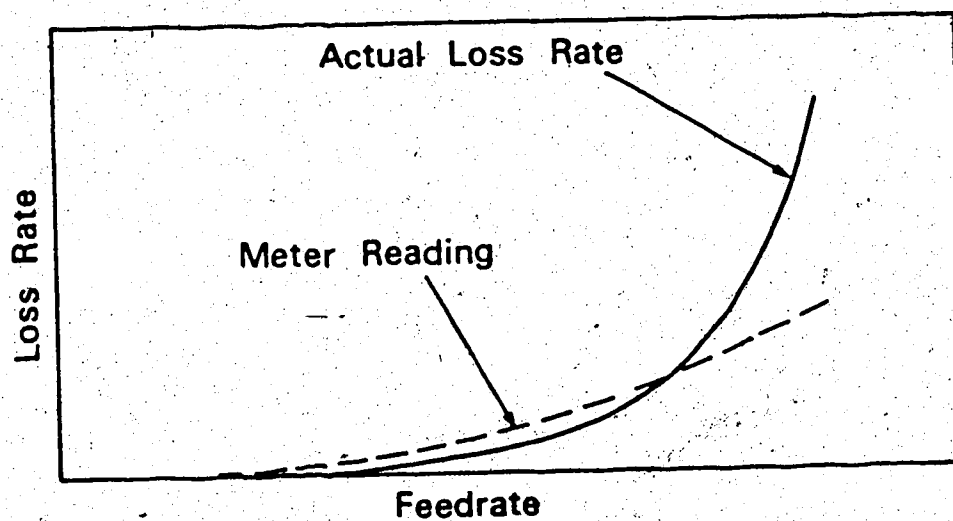


Figure 3.3 Monitor Inaccuracy. (adapted from Gullacher and Smith, 1979)

#### 4. FUNDAMENTAL SENSOR SIGNAL PROCESSING

A complete system for utilizing grain loss sensors is described in the following section. The grain loss sensors used throughout this thesis were manufactured by Baker Engineering Enterprises Ltd. (BEE), Edmonton, Alberta, and measured 75 by 150 mm.

##### 4.1 Advantages of a Microprocessor Base

A microprocessor, along with a select complement of peripheral devices, is the brain of a microcomputer system. The microprocessor can be programmed to perform functions and interact with the outside world. The system is able to collect data from sensors, analyze them according to programmed instructions and display information or activate control devices. A microprocessor-based grain loss monitor has several advantages over the highly dedicated analog circuitry of current grain loss monitors. A microprocessor system is flexible in operation since the function is only limited by the creativity of the programmer. The same microprocessor system could be used for various functions on the machine (Moller, 1985), or one part of an existing computer system could be employed specifically for loss analysis.

The microprocessor system can interpret a large quantity of data in a very short time. Complicated analyses may be computed that would be cumbersome to accomplish using a purely analog system. Several sensors could be monitored

simultaneously for separation curve determination. The inherent immunity to electrical noise of a digital system partially eliminates the concern of noise that would cripple an analog system into unreliability. The microprocessor system could be used on a harvester and operate under harsh field conditions.

The interrupt feature is a valuable tool of the microprocessor. An interrupt is caused when an event produces a voltage change on the interrupt input of the microprocessor. This interrupt triggers the microprocessor to jump to the interrupt handling routine of the program in order to service the condition. For example, an interrupt could occur when a grain kernel strikes a sensor, resulting in a register incrementation. After the interrupt is completely serviced, the program execution returns to the main operating instructions.

Another advantage of the microprocessor is the opportunity for operator input via a keyboard or simple switches. Several functions or parameters could be inserted such as width of cut and density of grain. The microprocessor system excels in versatility alone.

#### 4.1.1 Description of chosen microprocessor system

A specific system was chosen based on the Motorola 6802 microprocessor (Motorola Semiconductor Products Inc., Austin, Texas). The microprocessor was the brain of an MEK6802D-5 microcomputer evaluation board. The circuit

diagram of the microprocessor evaluation board can be found in Motorola, Inc. (1980). The circuit diagram of additional components can be found in Appendix I, Figure 12.1. Several features and adaptations of the system are discussed below.

The system had appropriate complementary components, including a peripheral interface adapter (PIA) and an asynchronous communications interface adapter (ACIA) enabling bidirectional communication with the outside world. Also, data could be entered via a hexadecimal keyboard under user control. A six digit seven-segment light emitting diode (LED) display was used to examine the system's operation without the need of an expensive logic analyzer. The system was easily programmed in assembly language with an assembler available on the MTS computing system at the University of Alberta (Motorola M6800 Cross Assembler, Release 1.1, Motorola Inc., Austin, Texas, 1974). The assembly language is written in mnemonics, with the assembler converting the mnemonic commands into hexadecimal format for use by the microprocessor. The system also included a cassette audio tape interface (300 Baud Kansas City Standard), which allowed for the transfer of hexadecimal information from memory to tape and *vice versa*. Also, the system allowed for substantial access to memory locations for the addition of extra peripheral devices needed from time to time. The system was compact, enabling use in a confined space such as an operator enclosure.

Several changes or additions were made to the standard MEK6802D-5. An RS-232-C port was implemented on the board to enable communication with higher order computers, the University of Alberta's mainframe computer in the Department of Computing Services, and an IBM personal computer. The former provided assembled versions of written programs while the latter could send as well as receive data. Listings of the communication programs appear in Appendix II, section 13.1.

On-board random access memory (RAM) was supplemented with additional RAM to house lengthy programs from time to time. Total RAM was 3K\*8bit and user programmable ROM was 2K\*8bit in the altered microprocessor system. A power supply with voltage regulation and current protection was used when operating the system from a harvester's cigar lighter outlet. Voltage regulation was accomplished with a 7808 voltage regulator pasted to a large heat sink in order to dissipate the excess energy at a maximum of 1.2 amperes and 8.0 volts direct current.

#### 4.2 Digital Signal Processing

Utilizing the speed and versatility of the microprocessor system, an attempt was made to digitize the fundamental sensor signal from a particle impact in order to accurately determine whether the particle was grain or non-grain. By analysis of the characteristic frequencies and amplitudes of the sensor signals, non-grain impacts could be

disregarded and, thus, only the true grain impacts would be counted. Preliminary efforts towards this end showed that software designs, hardware limitations and speed requirements were beyond the capabilities of the microprocessor system used. The system had an eight bit data bus and a slow (3.579 MHz) timing clock. Since grain loss sensors exhibit saturation effects above about twenty impacts per second, and based on the requirement of at least four grain loss sensors in use, eighty impacts per second would be the upper limit. Each impact signal would last about eight ms. This left only 340 ms per second for the processing of these data, to calculate the loss and to execute the display routine. This approach could only be accomplished with a more advanced system than the system chosen. The description of a system which digitizes the fundamental sensor signal is found in Appendix V.

#### 4.3 Analog Signal Processing

Due to the complexity involved and lack of processing ability of the available microprocessor system, a simpler analog-based system conjunct with the microprocessor system was developed. The particle discrimination was accomplished using mostly analog electronics with data being processed by the microprocessor.

As in the digital processing described in Appendix V, the fundamental signal from the sensor was the starting point for processing. Several stages of signal conditioning



were utilized to extract only impacts caused by grain and to interface the analog-based circuits with the microcomputer. The circuit diagram of the system to be described is shown in Appendix I, Figure 12.3 with the block diagram shown in Figure 4.1.

The fundamental sensor signal was of small amplitude and able to source little current, therefore, a voltage follower with gain (1/4 - LM324 quad operational amplifier) was used to amplify the signal and, at the same time, provide current for the remainder of the circuit. The amplification was adjusted so that any expected sensor signal would just cause 'slamming' of the amplifier.

The next stage of conditioning was frequency discrimination. From oscilloscope measurements, the dominant characteristic frequency of a barley impact was about 3000 Hz. Barley was chosen as the grain of interest because of the availability of test materials as well as to continue the work of Luntz (1986). Also, barley is more difficult to discriminate from non-grain contaminants because of the 'pointed' shape and somewhat soft covering. In order to concentrate only on the dominant frequency, a second order, active bandpass filter was implemented to attenuate the low frequencies of gross machine movements, impacts of straw and other contaminants and the high frequencies of machine vibrations and electrical noise. A narrow band of acceptable frequencies were passed by the filter which had a Q-factor of about 5. A rectifying diode was placed in the circuit

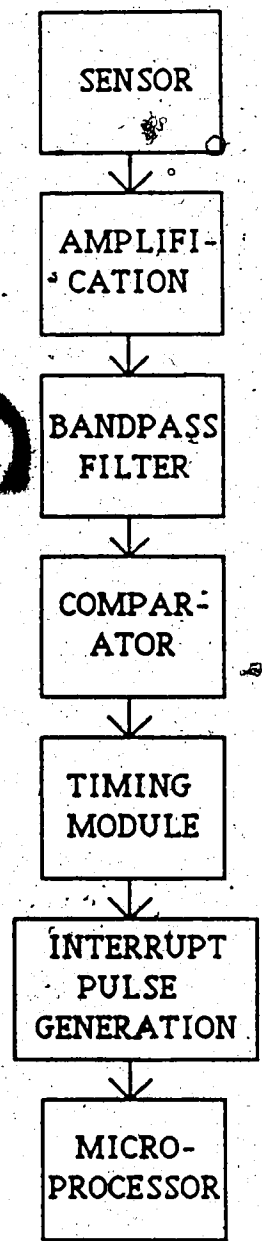


Figure 4.1 Analog Signal Processing Block Diagram.

following the filter to allow only the positive side of the filtered signal to proceed.

If a signal of sizeable amplitude passed the filter, a grain impact was assumed to have occurred since the frequency was allowable and the signal was adequately strong for a grain particle to have caused the signal. Since some non-grain particles may create impacts of the correct frequency, discrimination on the basis of amplitude, or strength of signal was carried out. Laboratory experiments determined the correct adjustment of the comparator (1/4 LM324 quad operational amplifier) which would give a +5.0 volt output if the input voltage was above that for an acceptable kernel impact. Several single kernel impacts were studied with a minimum drop height of 4 centimetres, the height assumed for the development of sufficient speed for a minimum impact energy expected in practice. The comparator was adjusted to act when the voltage level exceeded that for a drop height of less than 4 centimetres. The signal attained at this point would be similar in shape to Plate 16.1.

In order to obtain a single pulse for a single kernel, a monostable, configured from a 555 timer module, was triggered on the first rising edge of the signal from the comparator. The timer was connected to appropriate peripheral timing components to yield a positive pulse for the duration of a typical kernel impact of about 7.5 milliseconds. The maximum duration of a maximum energy

impact was assumed to be always less than this time, hence, the system would never count a single impact as two impacts. However, should two impacts occur less than 7.5 milliseconds apart, enough of the second impact signal would remain to deliver two pulses for two kernels (Figure 4.2). If several kernels fell at exactly the same time, the count would likely be less than expected as explained in section 3.3 when dealing with saturation effects. The probability of two or more impacts occurring close enough to register only one impact pulse is small if a sufficiently small area of the separation area is sampled as suggested in section 2.3. Illustrations of saturation effects are dealt with in the next section on system tests.

The monostable pulses from the timer module are representations of single kernel impacts, but were not directly compatible with the microprocessor interrupt system. The microprocessor system requires very short duration negative pulses (about 1 - 3 microseconds). To obtain this pulse on the rising edge of the monostable pulse, an inverter was used in a half-monostable configuration. The duration of the pulse used was given by the RC timing circuit and was about 2.2  $\mu$ s which was adequate for interrupt purposes.

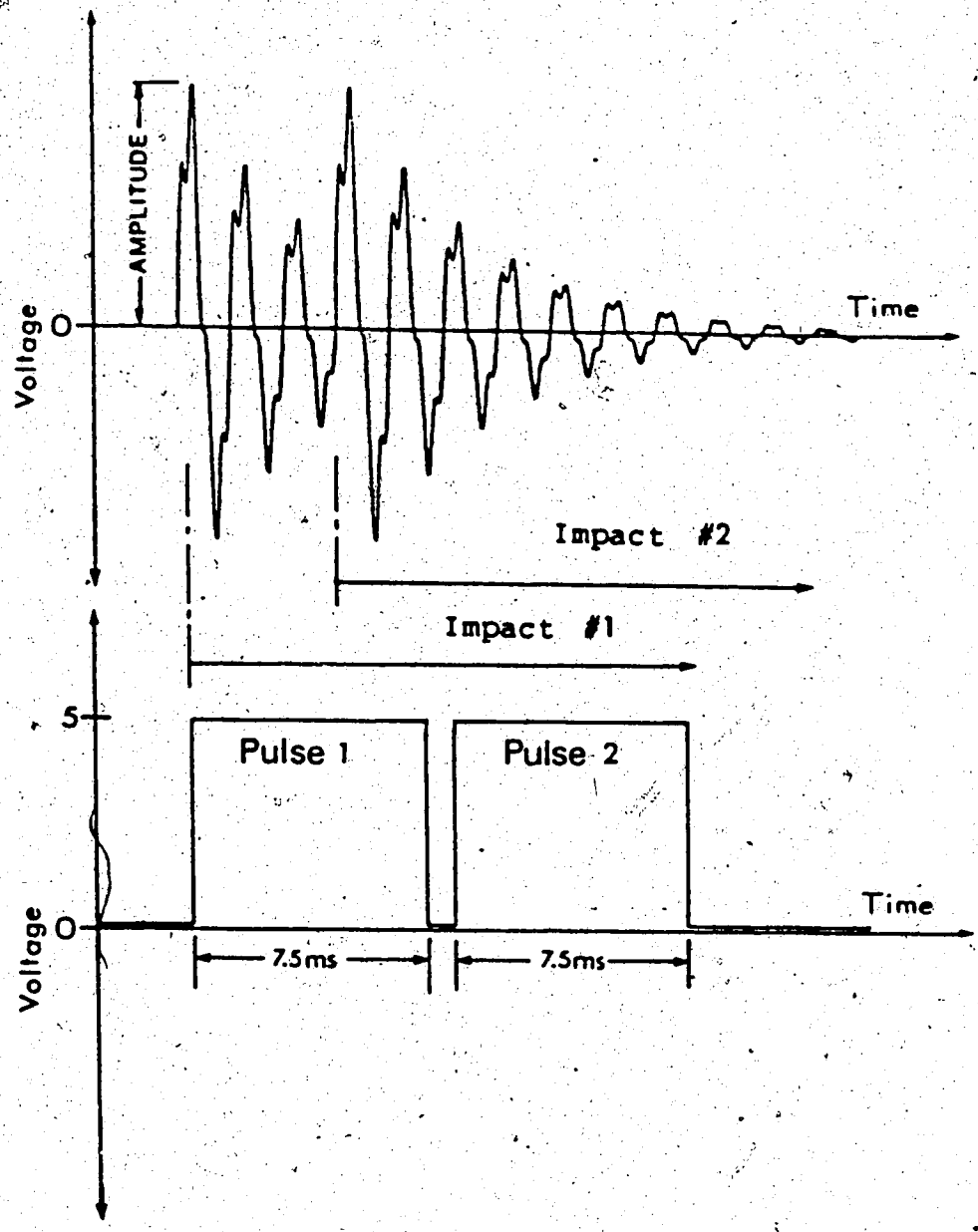


Figure 4.2 System Response to Two Overlapping Impacts.

#### 4.4 Analog Signal Processing Tests

Several tests were carried out using the system described in section 4.3 connected to the microprocessor system as described in section 4.1.1. These tests involved two basic areas, single and multiple sensors, with the majority of tests being carried out on the single sensors. Emphasis was placed on the consideration of mounting angle and location of impact on the sensor surface. The single sensor tests employed one program throughout (Appendix II, Section 13.3), while the multiple sensor tests involved a greater amount of hardware and software.

##### 4.4.1 Single sensor tests

The basic tests involved with the single sensor were to determine the adequacy of the analog conditioning conjunct with the microprocessor when counting impacts of barley kernels. The short negative pulses as referred to in section 4.3 were connected directly to the microprocessor interrupt pin. The system would then be interrupted every time a kernel impact occurred. On every impact, a counter was incremented in the microprocessor's memory.

The experiments involved dropping one hundred kernels of barley, randomly selected from a bin, onto a sensor pad over times ranging from 1.5 to 20 seconds. This resulted in impact rates of 5 to 67 kernels per second. The same one hundred kernels were collected and used for all subsequent runs.

A vibratory conveyor was utilized to deliver the grain onto the sensor. The organization of the kernels on the conveyor's tray determined the time for all one hundred kernels to fall (Figure 4.3(a)). The times were measured by a handheld digital stopwatch (Model X511WB, Innovative Time Corporation, Carlsbad, CA) and represented the time from fall of the first kernel to the last. Consequently, the rates of impact are averages for the entire time period, with actual time intervals being greater or less for consecutive kernel impacts.

Twenty four trials were carried out for each test, representing a large range of impact rates, in order to determine the system's accuracy at different rates. Seven different impact orientations were examined to determine the optimum orientation of the sensors when attached to a harvester. Wang (1984) suggested that  $45^\circ$  was the preferred orientation. The orientations considered here consisted of three angles of impact,  $10^\circ$ ,  $45^\circ$  and  $80^\circ$  between the sensor surface and the direction of fall. Three locations of impacts were considered, top, middle and bottom, referring to the lateral thirds of the sensor. Since the angle of  $10^\circ$  yielded a very small area for grain to contact, only one location of impact was possible, thereby making a total of seven configurations (Figure 4.4). The seven configurations were designated 80T, 80M, 80B, 45T, 45M, 45B and 10M.

Another test was performed on the single sensor apparatus. Grain was mixed with chaff and straw particles in

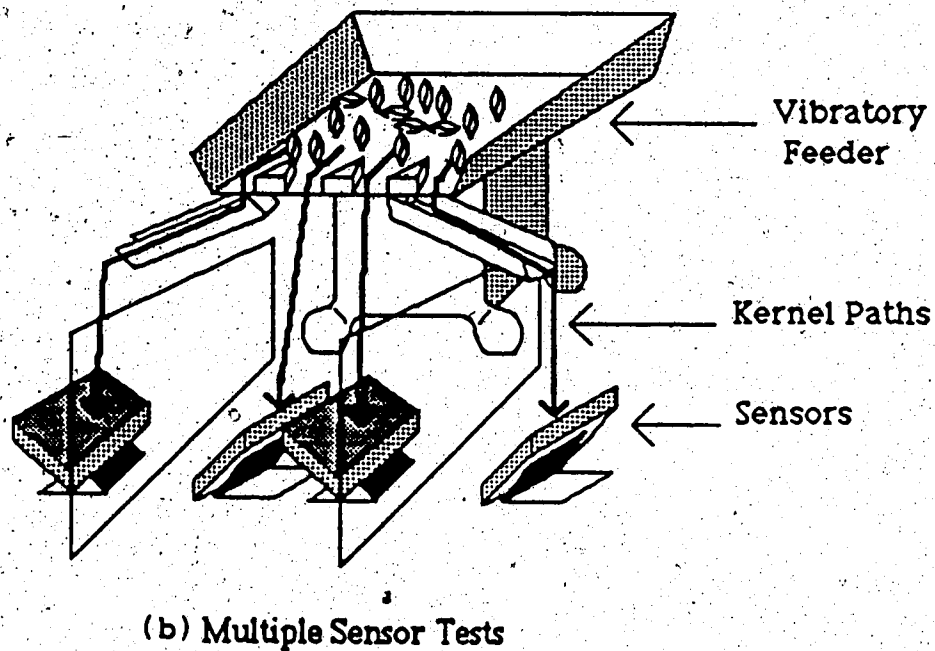
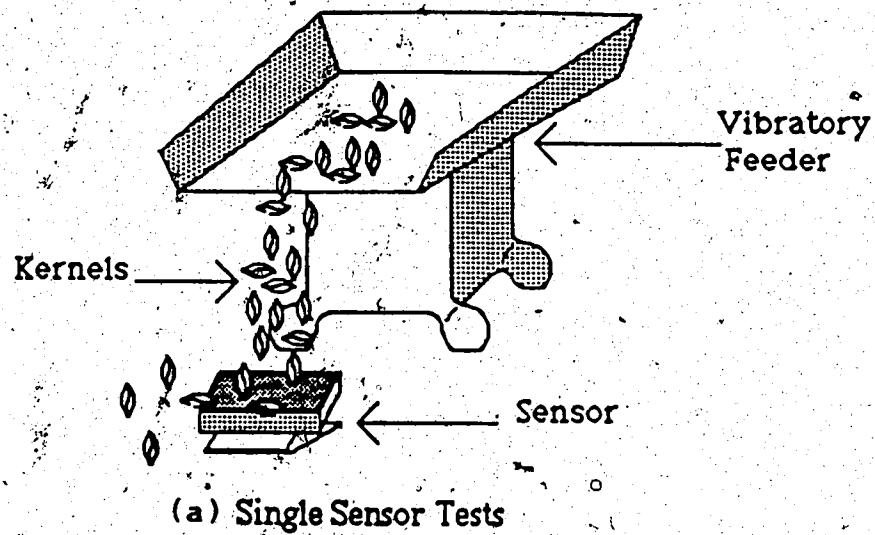
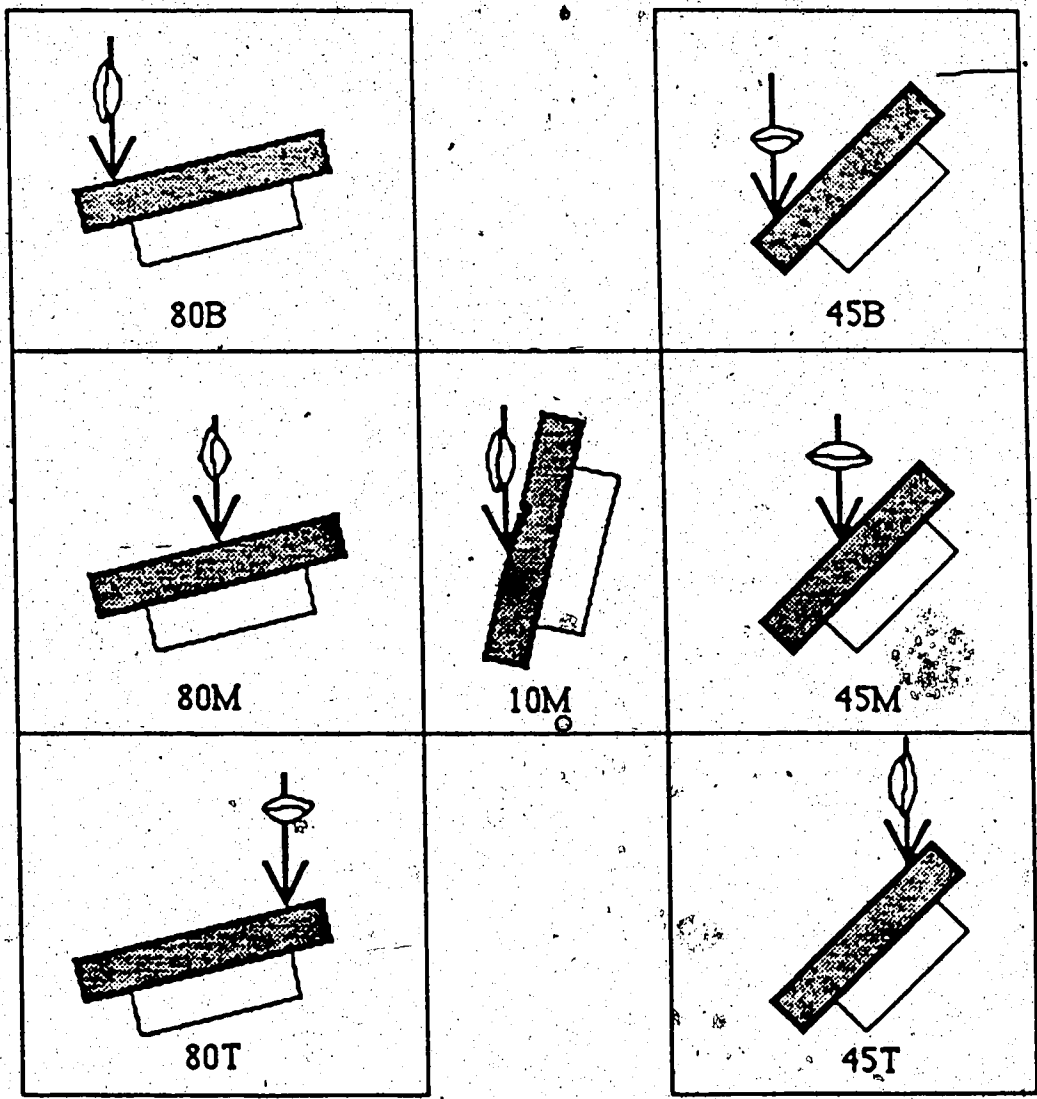


Figure 4.3 Vibratory Conveyor.





\* Figure 4.4 Impact Orientations.

a composition consistent with that which would be present in the space below the straw walkers of a harvester. The composition was established from first hand experience of the author. The test was carried out using the configuration of 45° and middle third, anticipating that 45° was the best attitude, and was identified as 45GSC.

Data for the orientation and location of grain impacts for a single sensor are given in Appendix III, Table 14.2. The data were analyzed with the objective of obtaining the best possible orientation of the sensor pad. A regression analysis was carried out on all data to arrive at an equation that described the response of a single sensor system. An equation of the form  $Y = A + B/X$  consistently gave the best fit of all equations when Y was numbers of counts out of one hundred and X was the time for the one hundred kernels to fall. The parameter 'A' is the number of counts expected if the time for the one hundred kernels to fall approached infinity.

Regression data for these trials are given in Table 4.1 along with regressions for combined groups of the 45° and 80° trials.

Table 4.1 Sensor Orientation Test Data Regressions.

Equation Form:  $Y = A + B/X$   
 Y = number of impacts counted, and  
 X = time for 100 impacts to occur (s).

Trial	A	B	R <sup>2</sup>
10M	113.7	-69.16	0.875
45B	99.1	-39.28	0.700
45M	112.4	-63.44	0.793
45T	102.1	-44.79	0.876
80B	105.2	-48.60	0.462
80M	109.1	-60.92	0.827
80T	114.7	-61.95	0.629
45GSC	97.5	-67.70	0.683
45GSCW	103.8	-75.65	0.683
MULT	91.7	-28.08	0.452

The combined groups better emulated the conditions expected in the field. The combined groups included bottom, middle and top data and were identified as 45BMT and 80BMT. A typical plot of the data for trial 45M is shown in Figure 4.5. The plots for other trials were similar in shape with a small difference in the ultimate values of the count when the time for one hundred kernels to fall was large. This can also be seen by comparing the 'A' parameter for the regressed curves. Of interest is the comparison between trial groups which would represent anticipated conditions in a field test. The groupings of all runs in each of two angles is shown in Figure 4.6. As illustrated by the plot, the curve of 45BMT maintains closest proximity to the one hundred count level when the time for fall is large. For this reason, the 45° angle of impact was chosen as the orientation of best accuracy.

Both the 10° and 80° orientation trials showed an artificially high number of counts for the same one hundred kernels. When the particle-sensor interface was observed closely, two unique phenomena at the 10° orientation were observed. The first one occurred if the barley kernel would strike the sensor and then roll or slide down the sensor as shown in Figure 4.7(a). The sliding or rolling action would tend to draw out the length of the electrical impulse created or cause a second impulse. The somewhat pointed shape of the kernel made this phenomenon highly dependent on which part of the kernel struck the sensor. The second case,

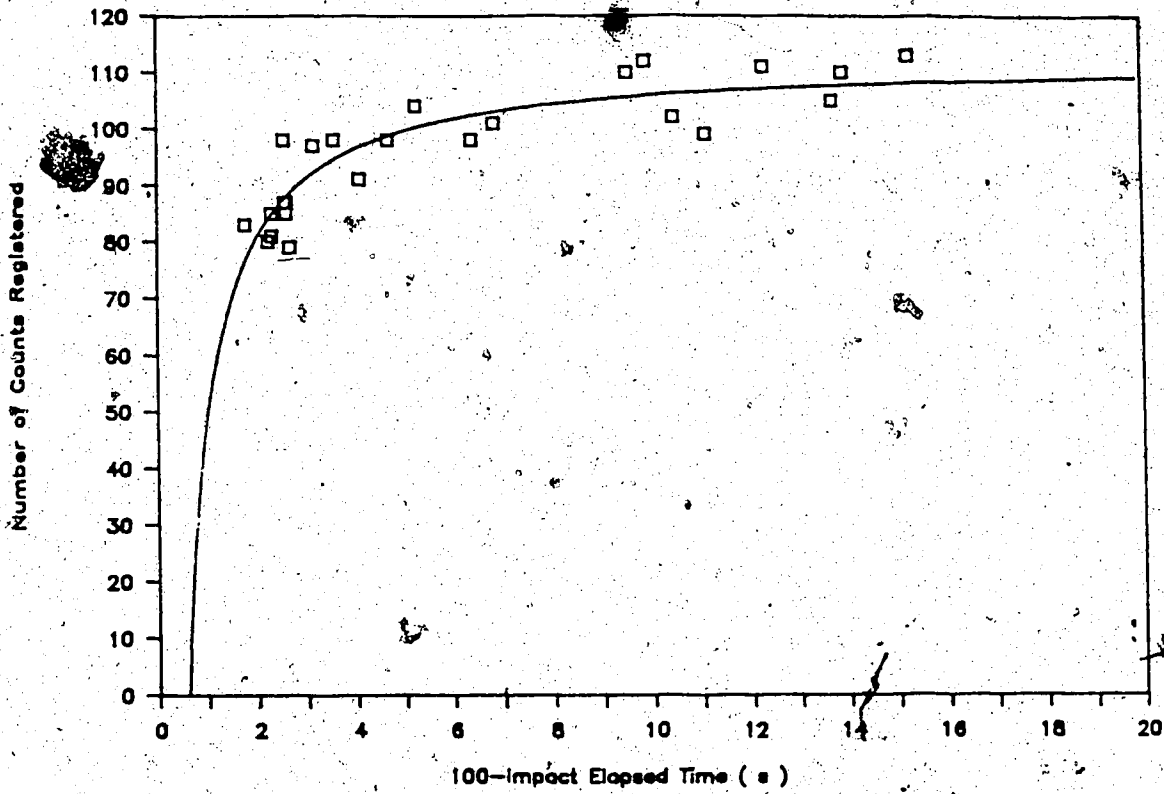


Figure 4.5 Single Sensor Impact Counting. (45M)

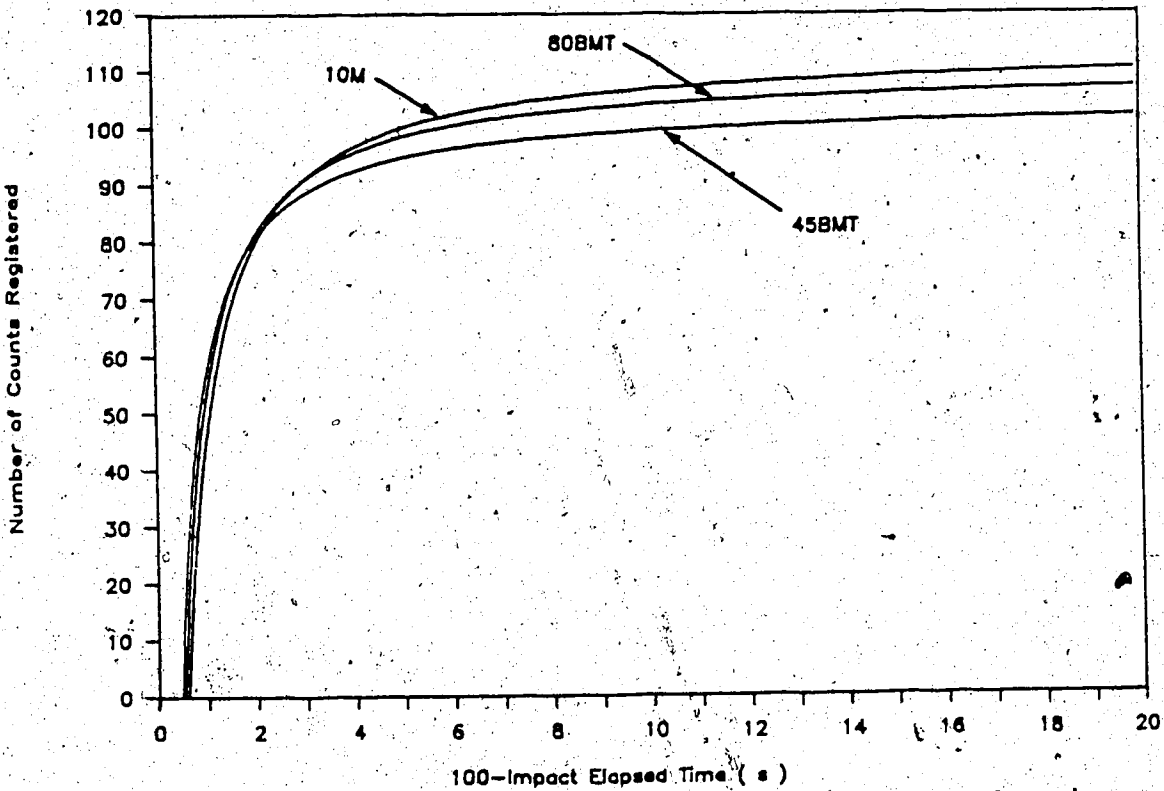


Figure 4.6 Single Sensor Impact Counting. (45BMT, 10M, 80BMT)

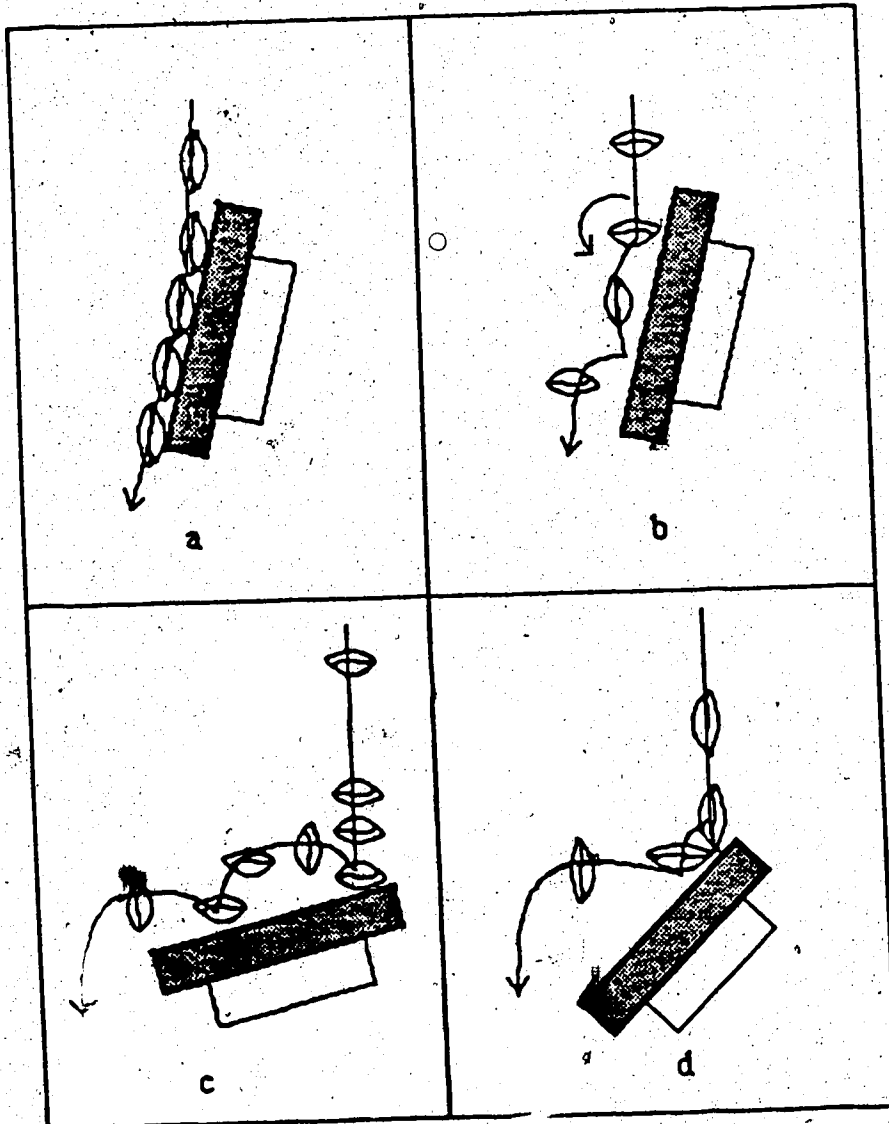


Figure 4.7 Phenomena Causing Double Counts.

as shown in Figure 4.7(b), occurred when the kernel struck the top portion of the sensor, and, because of the low angle of impact, was not thrown far enough away to clear the bottom portion of the sensor pad. The kernel then would cause a second impact and count twice.

The combined  $80^\circ$  orientation displayed the same latter phenomenon as the  $10^\circ$  trial. The very small slope would create a high bounce covering very little horizontal distance (Figure 4.7(c)), Consequently, the probability for the kernel to contact the sensor surface again was higher. Trial 80T had the highest 'A' parameter of all the  $80^\circ$  trials, showing the increased presence of this phenomenon in creating double counts when the top portion of an angled sensor is contacted.

In all trials, including the  $45^\circ$  trials, double counts would occur without any prevention or detection by the system. The double counts occur when the barley kernel strikes the pad with one of the pointed ends, turns over and strikes the pad again with the side (Figure 4.7(d)). As often as two counts may occur for one kernel, one count may occur for two kernels. If two kernels impacted the sensor surface at the same time, their intended causal vibration may not be cumulative, in fact, they may counteract one another due to a phase difference. The counteraction may not totally eliminate the total signal, but may reduce the vibration such that only one count may register. Since no quantification of these latter two phenomena was made, they

were assumed to be random and act to negate each other due to the unpredictability of the kernel position upon impact. Therefore, for a sample of adequate size, their combination affects the count little.

The chaff and straw, when dropped on the sensor alone, produced no counts by the system. The electrical signals created were of the wrong frequency range or had too little energy to command a count. Nonetheless, if the nodes of the straw stalks were to strike the sensor pad directly, a count may occur. Other contaminants such as wild oats also could mimic the physical characteristics of grain and would not be distinguished by the system.

After each trial the number of kernels collected were counted to ensure that one hundred impacts had occurred. For the trial of grain with chaff and straw added, only ninety-six kernels were collected. In order to use the data comparatively with the others, the number of counts and the time for the fall were increased by the appropriate amount as if one hundred kernels were applied. The data for the weighted trial is given under the identification of 45GSCW in Appendix III, Tables 4.2 and 4.1. The weighted data were then regressed and plotted, together with the 45BMT curve in Figure 4.8. The two equations plotted are similar in shape and magnitude with no apparent difference. The system, counting only the grain, performed the same in clean grain samples as it would in an effluent of grain, straw and chaff.



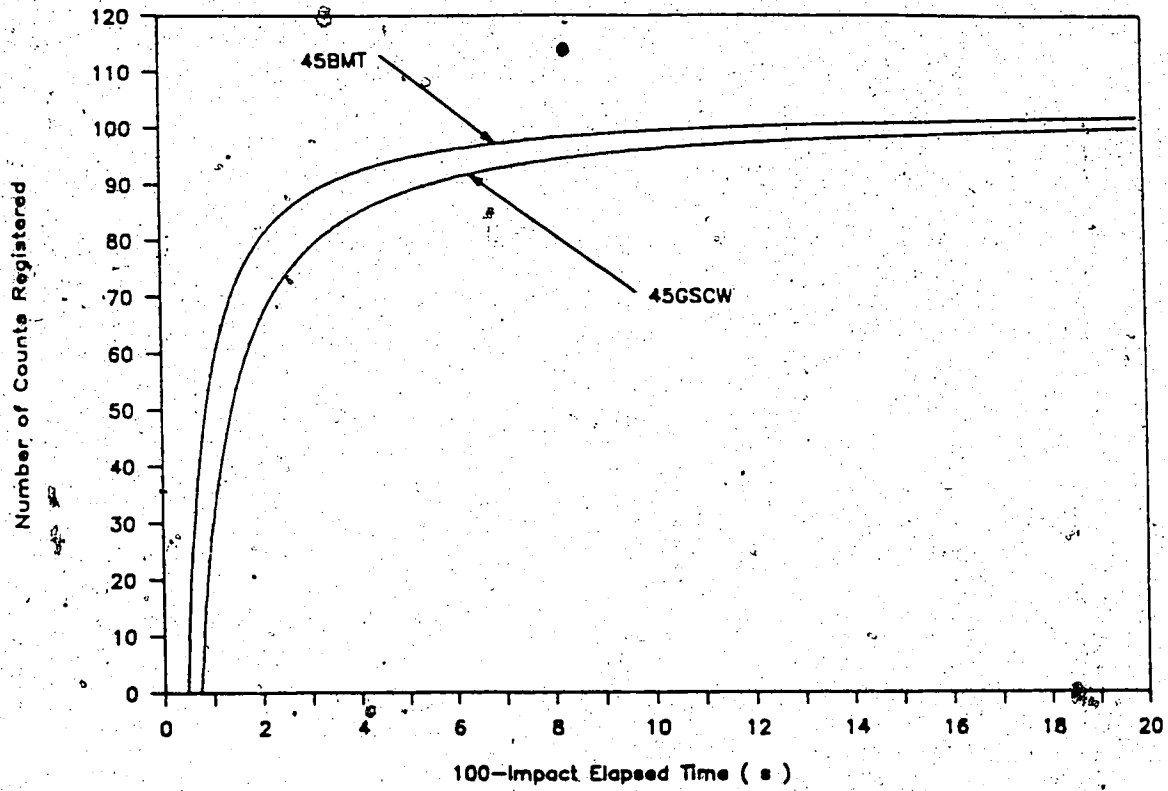


Figure 4.8 Single Sensor Impact Counting. (45BMT, 45GSCW)

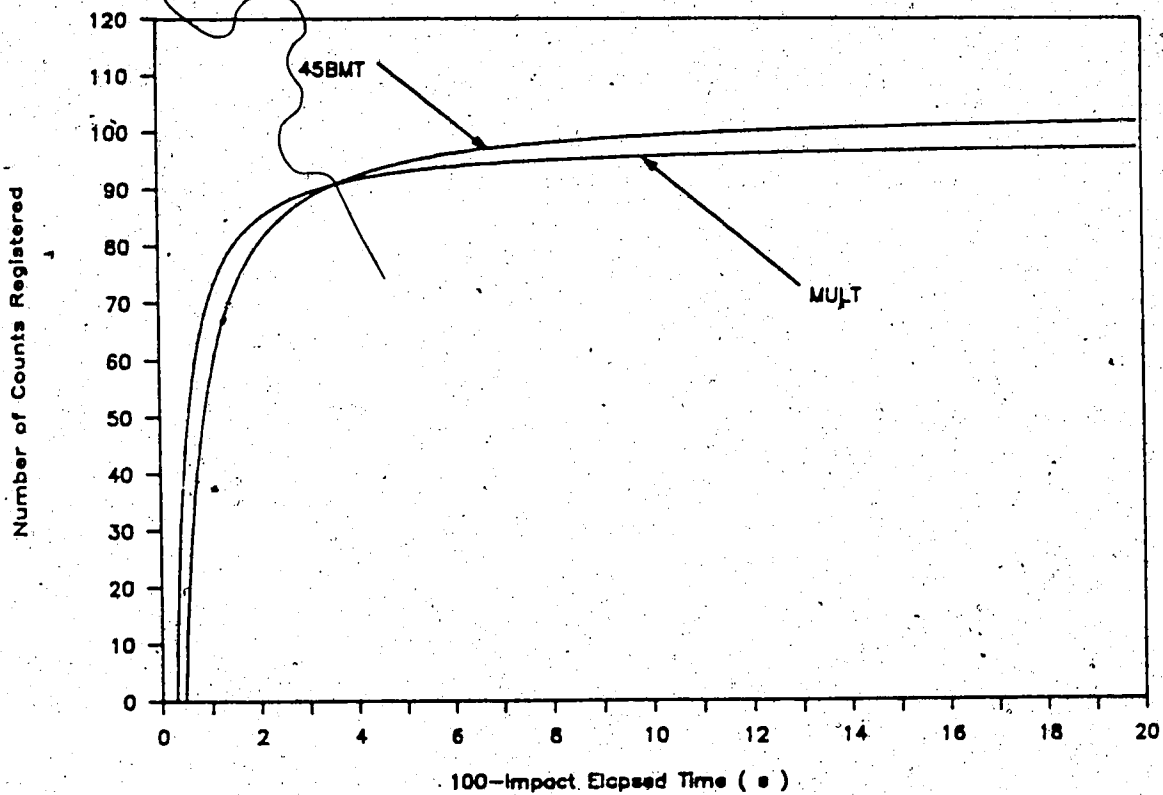


Figure 4.9 Multiple Sensor Impact Counting. (45BMT, MULT)

#### 4.4.2 Multiple sensor tests

In order to implement the system described in section 4.3 into a method of measuring a separation curve, four sensors would have to be monitored. The basic approach was similar to that with one sensor, but involved monitoring four sensors simultaneously. Both hardware and software must increase in complexity to accommodate four interrupt sources for one interrupt port. In order to determine the originating sensor experiencing an impact when four are connected at once, a PIA was used (M6821, Motorola Semiconductors Inc., Austin, Texas). The PIA has four control lines (designated as CA1, CA2, CB1 and CB2) available as inputs for interrupt signals. The particular function of these lines is determined on program initialization. The function used here was to cause an interrupt on the microprocessor whenever there was an interrupt on any of the control lines. When an interrupt occurs this way, the microprocessor can poll the registers within the PIA to determine the origin of the interrupt. An appropriate counter then can be incremented. Details of this process are given in the program listing in Appendix II, section 13.4. Since each interrupt signal is only 2.2 microseconds in duration, kernel impacts on different sensors greater than 2.2 microseconds apart would be recognized. Compared to the 7.5 millisecond length of each impact, a very small possibility exists for the signals on two sensors to overlap. The chances are far greater for two

kernels on the same sensor to overlap than for two on different sensors.

The same vibratory conveyor was used to apply barley kernels to the multiple sensors as in the single sensor tests, with four paths constructed so that all sensors would be contacted by grain at the same time (Figure 4.3(b)). The same one hundred kernels were applied to the sensors with an arbitrary amount to each sensor. The time was recorded as before, as well as the individual sensor counts. The sensors were situated in the 45M position with the trial identified as MULT.

The multiple sensor test was evaluated in the same manner as the single sensor tests, using the total count of four sensors as the data. The data were regressed and are compared to 45BMT in Figure 4.9. The curves differ little, hence the system was considered to operate well, accurately measuring the impacts on individual sensors. The small difference is attributed to experimental error in stopwatch operation and non-uniform spacing of kernel impacts. individual sensors. This multiple sensor system was adopted along with the 45° orientation as the basis for further tests in the laboratory and field. Overall, the system performed well, counting grain kernels with an accuracy of  $\pm 10\%$  up to a rate of 35 kernels per second.

## 5. LABORATORY TESTING OF MULTIPLE SENSOR SYSTEM

The system described previously had an eventual application on an actual harvester in field conditions. Prior to such an implementation, careful laboratory testing of the system's operation using a full-scale harvester straw walker system was performed. The testing provided data needed to evaluate performance as well as insights into the method of measuring the separation curve on the actual harvester. A similar attempt to measure straw walker separation characteristics on a laboratory test apparatus was performed by Lundy (1986). The author modelled the following experiment after Lundy (1986) in hopes of expanding previous work and as a means of comparison.

Several objectives were foremost in this testing. A separation curve was to be obtained with the developed microprocessor system. The grain contacting the sensors beneath the walkers was to be collected in order to correlate the measured counts with actual impacts. The computed separation curves were to be compared with those obtained from grain collected beneath the entire length of the walkers. The measurement system was to be tested to determine if the grain actually contacting the sensors was detected accurately enough to provide data for loss calculation.

### 5.1 Description of Testing Apparatus.

The equipment for the laboratory test was located at the Agricultural Engineering Research Facility at the University of Alberta's Ellerslie farm. The test apparatus consisted of a set of straw walkers to which grain and straw were applied in various amounts in order to collect data from the resulting separation.

The open-bottomed straw walkers (Figure 5.1) were a mounted set of three sections from a Massey Ferguson #205 combine. The overall dimensions of each walker section was 240 mm wide by 2745 mm long, and each had offset crank throws of 50 mm. The walkers were powered by a 370 W electric motor through a chain and sprocket reduction to yield an oscillation rate of 195 cycles per minute. Six collection trays, numbered 1 through 6, were situated beneath the walkers from front to back with an additional tray, numbered 0, located in front of the walkers. Trays 1 through 6 collected the material passing through the walkers, while the tray numbered 0 collected the grain and straw that were thrown ahead of the walkers. During the course of a trial, effluent straw was removed from the rear of the walker assembly to prevent flow impediment and discharged into a chaff blower wagon.

Straw throughputs of 35, 45, and 55 kg per minute were accomplished by means of a conveyor belt 15.5 m long and 915 mm wide. The conveyor was driven by a 746 W, variable speed motor at approximately 0.34 m/s (1.24 km/h). At this speed,

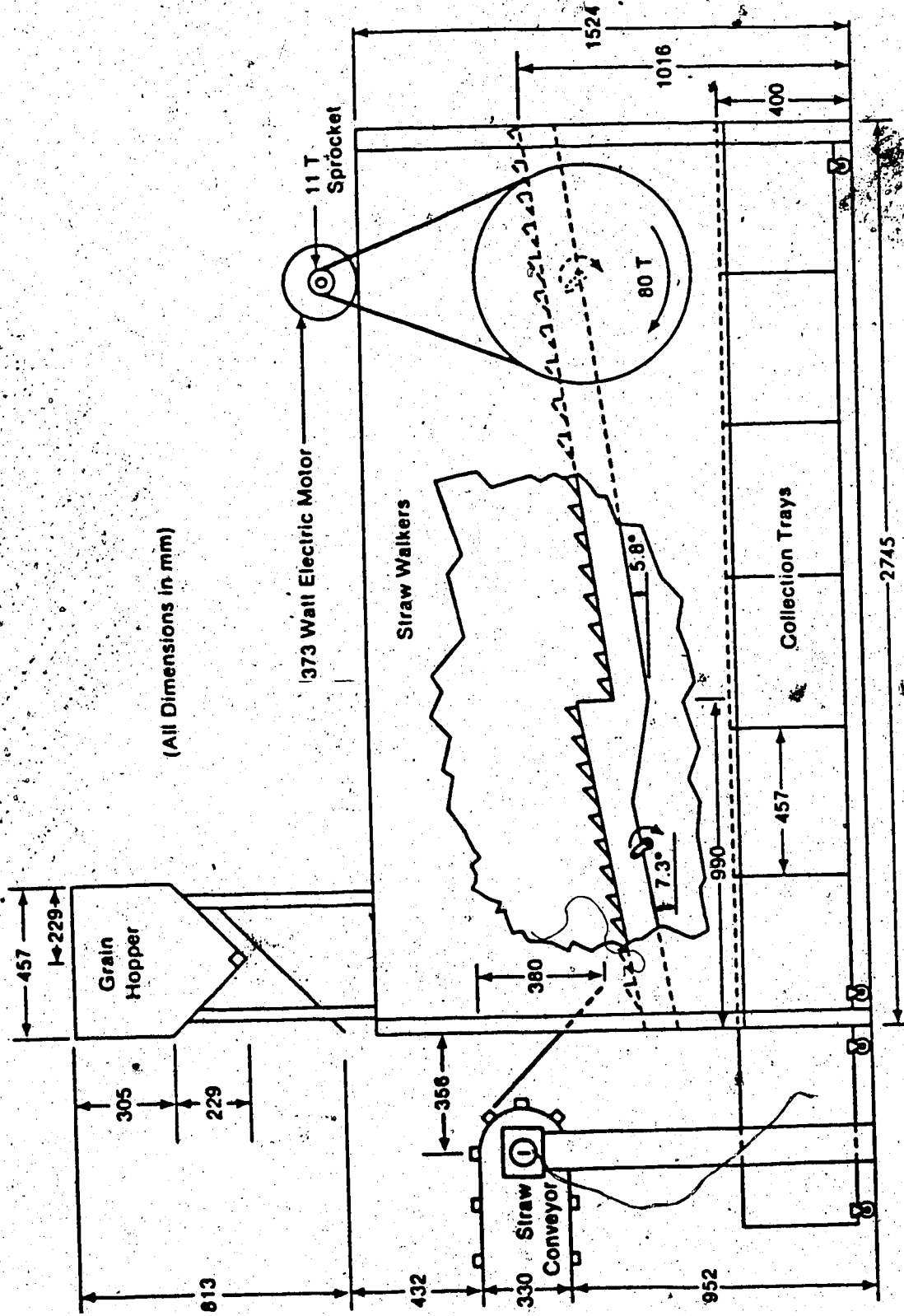


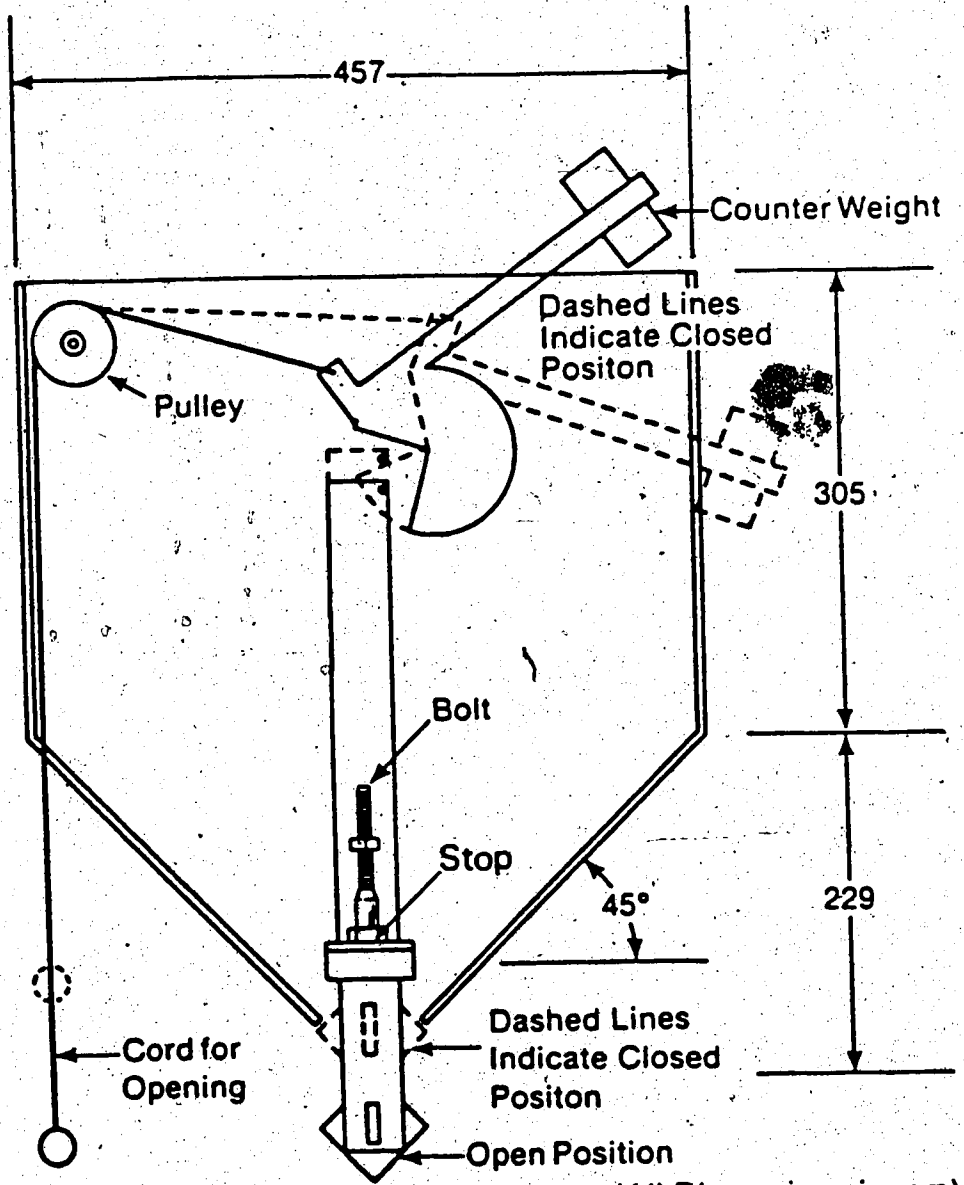
Figure 5.1. Side View of Laboratory Apparatus. (adapted from Luntz, 1986)

the straw was carried by the walkers with no congestion or sparsity. The duration of a run was 45 seconds. A large wooden box suspended by a spring scale attached to a moveable crane allowed easy weight measurement of straw for each trial. The straw was spread uniformly along the width and length of the conveyor.

Grain was applied to the straw entering the straw walker assembly by a gravity flow hopper (Figure 5.2). The gate of the grain delivery box was adjusted by means of a screw and stop. Various placements of the screw adjustment gave gate openings delivering different amounts of grain. The number of turns of the adjusting screws gave an indication of grain delivery rate. Four grain rates were used in the experiment: 15, 20, 25 and 30 kg per minute, which corresponded to 3.2, 3.6, 4.2, and 5.2 turns open respectively. The calibration curve for the hopper is shown in Figure 5.3. The hopper was filled with 40 kg of barley before each run, with the weight remaining after 45 s of grain flow being measured to determine the actual weight used. The grain hopper was opened as the straw contacted the walkers and closed after 45 seconds had elapsed.

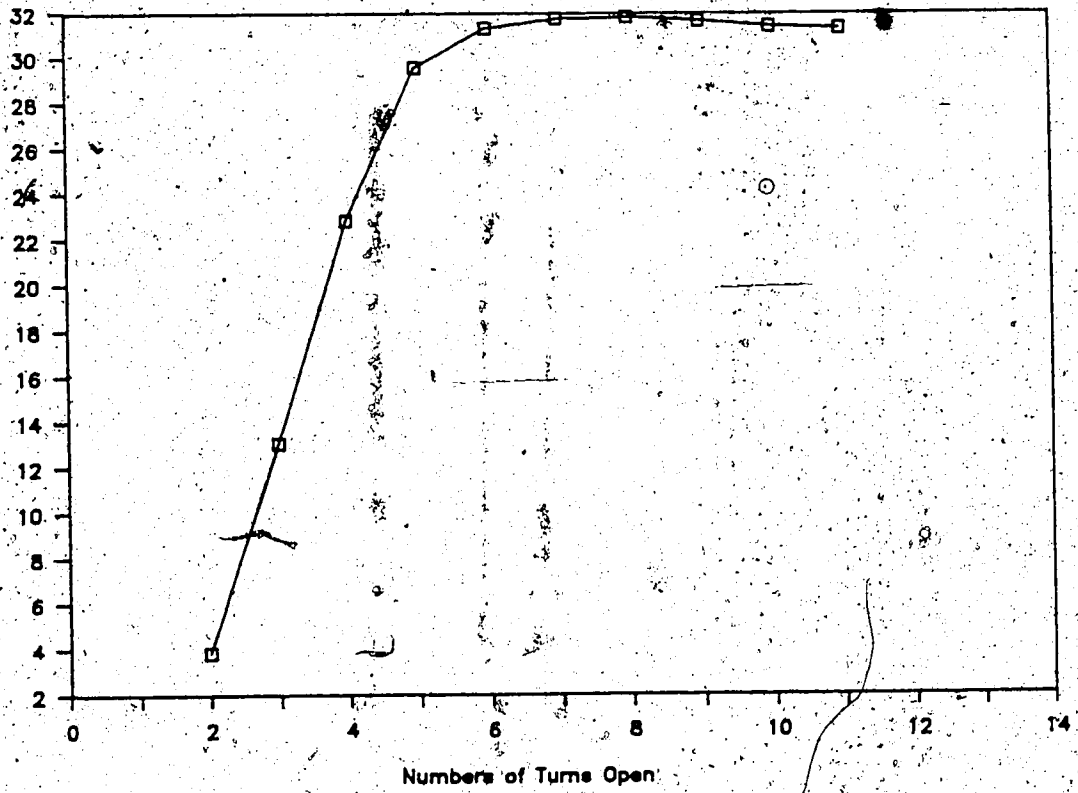
## 5.2 Description of Measuring System.

The measurement system comprised the microprocessor-based multiple sensor system as (described in section 4.4.2) mounted on the straw walker assembly. The sensor placement was chosen so that the separation curve



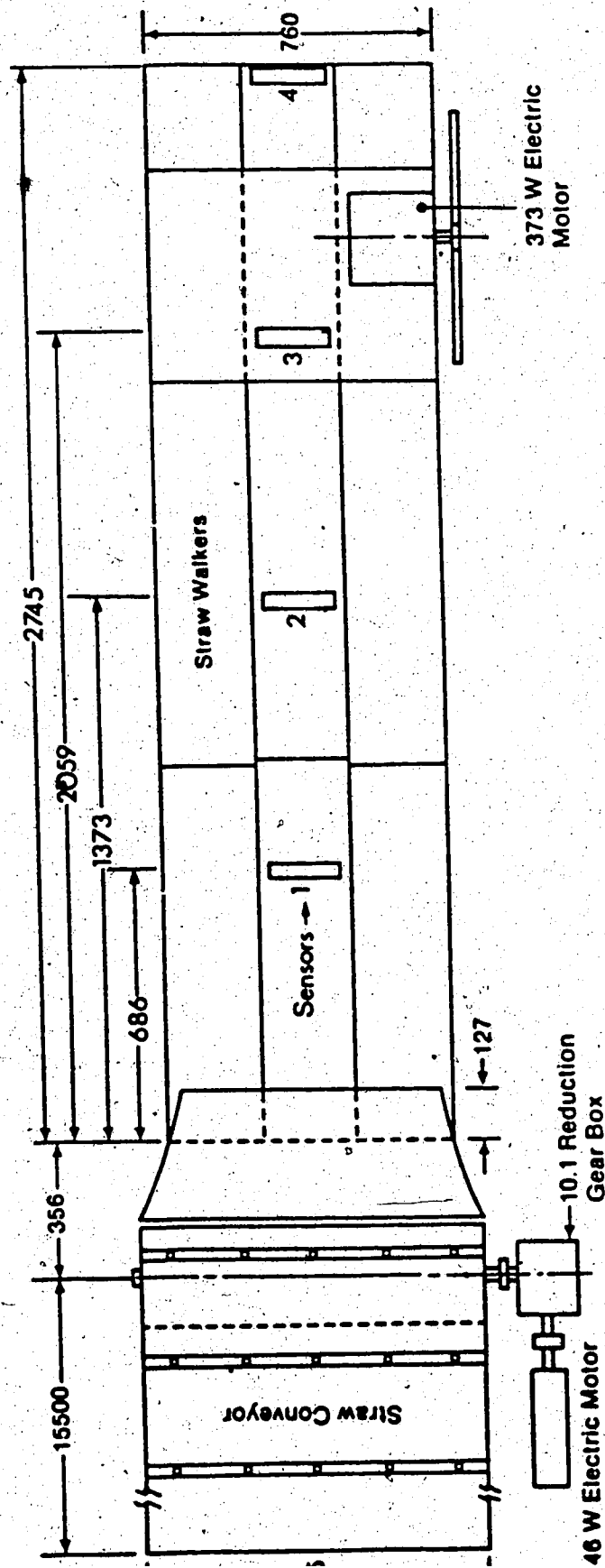
(All Dimensions in mm)





under the walkers would be represented accurately for a variety of operating conditions. As suggested in section 2.3.2, the walker area was divided into four quarters with a sensor placed at the rear of each quarter (Figure 5.4). Sensors were mounted on the center walker section only.

Several methods of sensor mountings were attempted before one was selected. The final arrangement involved sampling a walker section of known area and location, locating the sensor at the optimum angle of  $45^\circ$ , and collecting the material that contacted the sensor without influencing the count in any way. The adopted arrangement, shown in Figure 5.5, met all the criteria and adapted well to mounting on the walker's bottom surface. The sampling area was 108 mm by 28.6 mm for the front sensor and 108 mm by 38.1 mm for the rear three sensors. The difference in the two areas was due to the design of walker perforations in the initial and final sloping sections of the walker (Plates 5.1 and 5.2). Each sample area enclosed two perforations in the center of the walker. The sampled area was fixed in location and whatever material fell through the walker perforations contacted the sensor by a chute and collected in a bag. A deflector and a long narrow collection bag were used to prevent the bouncing of kernels within the sensor housing that could cause double counts. In addition, flaps were installed to direct the material striking the top of the sensor housing to the collection tray to which the material was originally destined.



(All Dimensions in millimeters)

Figure 5.4. Sensor Placement. (adapted from Luntz, 1986)

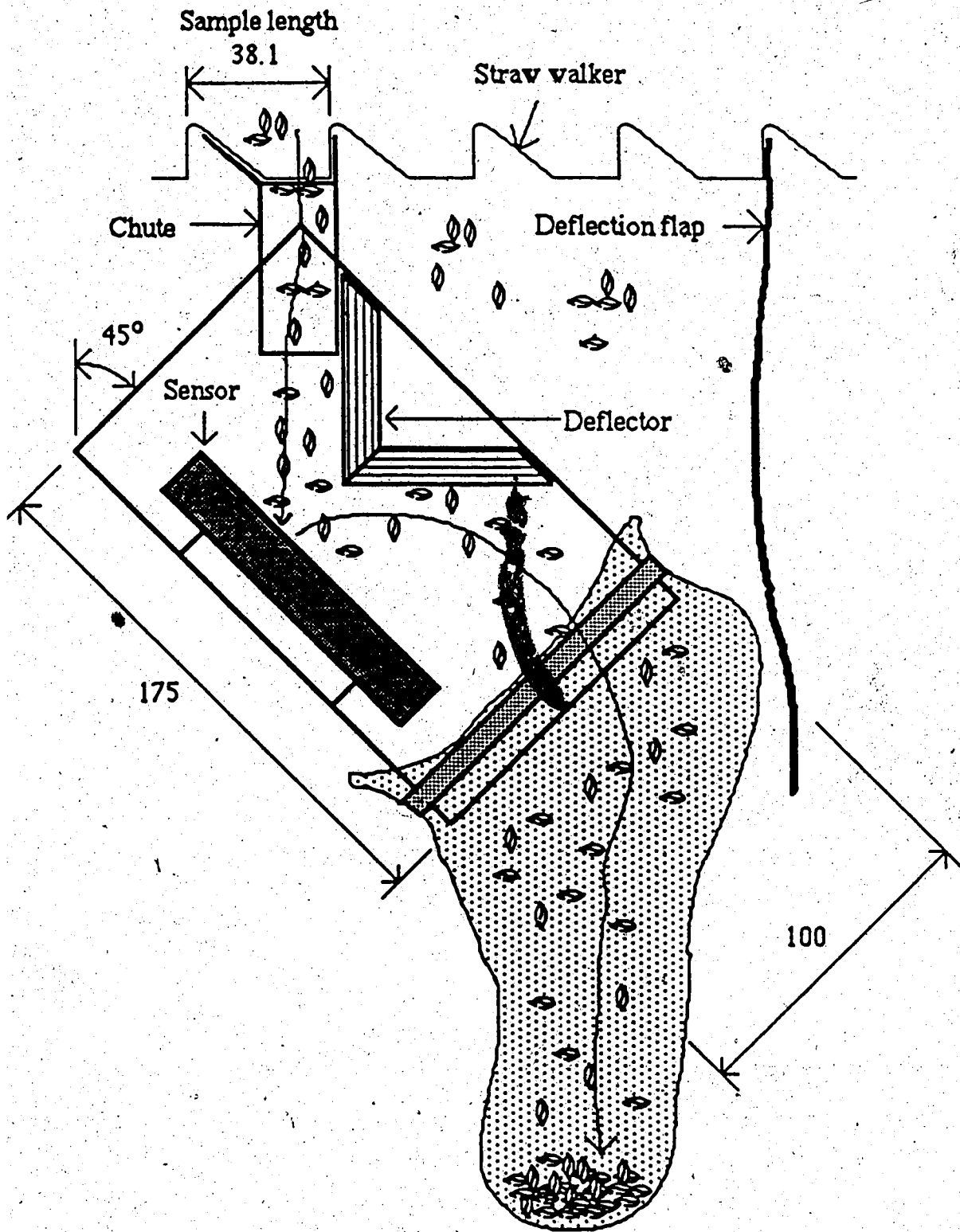


Figure 5.5 Laboratory Sensor Housing. (All dimensions in

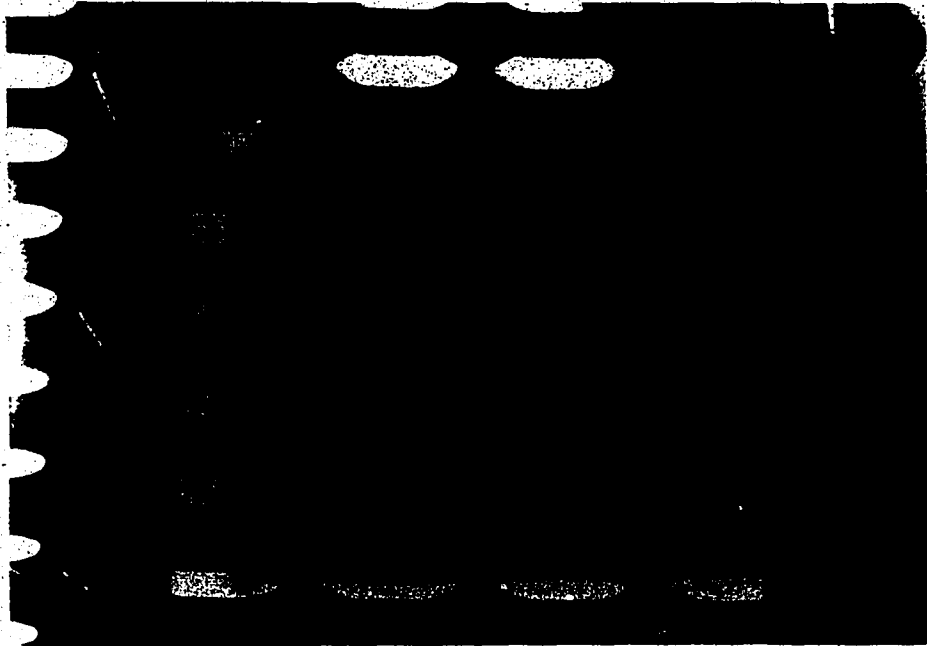


Plate 5.1 Front Section Walker Perforations

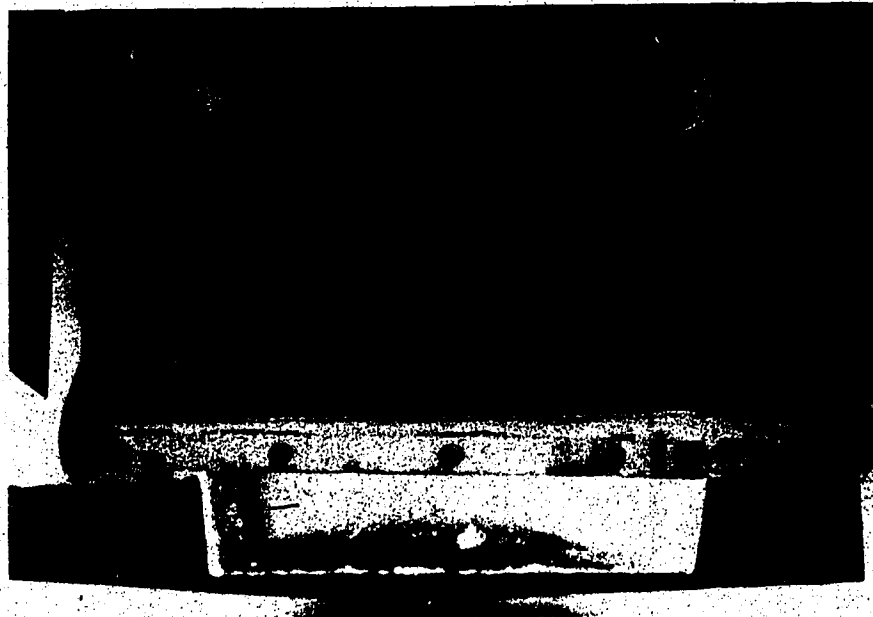


Plate 5.2 Rear Section Walker Perforations

The electronic monitoring system was exactly the same as that used for the multiple sensor test of section 4.4.2. Shielded cable, approximately 18 metres in length, was used to connect the sensors to the microprocessor system that was housed in a protective cabinet. This simulated the lead length required for the field test on a harvester. The system was designed to count the number of impacts occurring on all four sensors simultaneously while saving the data in memory.

### 5.3 Description of Materials.

The straw used in this experiment was barley straw purchased from a local farmer in the form of large round bales. The round bales were chosen due to availability, small amount of straw damage by the baler and the good quality of a large percentage of each bale. The straw was baled in the fall of 1985 and stored uncovered until used. The outside of each bale was discarded, leaving the unweathered interior for use. Average moisture content was 8.7 % wet basis as determined by the standard oven drying procedure outlined in ASAE (1983).

The grain used for this experiment was obtained from the department of Animal Science, University of Alberta and had a moisture content of 14.2 % wet basis according to a grain moisture meter (Model 919, Labtronics Manufacturing, Winnipeg, Manitoba). The barley averaged about twenty-two kernels per gram and was clean, with no contamination from

chaff or weeds.

#### 5.4 Experimental Design.

The main purpose of this experiment was to test the accuracy of the grain measurement system with the intention of obtaining a grain separation curve. The various rates of grain and straw throughput, outlined in section 5.1, would yield twelve different separation curves. The twelve ratios of grain to straw were between 0.27 and 0.86 with total throughput ranging from 50 to 85 kg per minute. A complete listing of throughput data appears in Appendix III, Table 14.3.

In addition to the single runs at each combination of throughputs, an initial run, with straw only, was performed to reveal the amount of grain in the straw applied. The amount was considered to be negligible and was ignored. The remaining twelve runs were randomized.

The null hypothesis of this experiment states that the mean of the ratio of number of impacts counted to the number of kernels collected for all tests and sensors was equal to one. The expected mean of the population of all such ratios is one. Equivalently, the alternate hypothesis would be that the mean of the sampled ratios from above was not equal to one. This describes a two-tailed t-test.

$$H_0 ; \mu = 1.0$$

$$H_A ; \mu \neq 1.0$$

For a normally distributed population, the 't' statistic as given by Steele and Torrie (1980) is:

$$t = (M - \mu)(n^{1/2})/s \quad 5.1$$

where: M = mean of sample size n,  
 s = standard deviation of sample, and  
 $\mu$  = specified value of population mean

This simple statistical analysis will yield a degree of confidence with which the system can be evaluated.

A comparison of separation curves for sensor and collection data was made for all twelve runs. Calculation of grain loss from collection and sensor data was compared using the method of section 2.3.

### 5.5 Experimental Procedure.

Several trial runs were made on the apparatus prior to actual testing to establish a procedure. The operator also became familiar with the time constraints involved in operating the system.

A typical run involved many individual procedures. The conveyor and straw walker system was cleaned thoroughly of all material remaining from the previous run. Collection bags were secured below the individual sensors followed by the placement of collection trays beneath the walkers. The 40 kg of barley was placed in the hopper and the screw stop adjustment made for the next run. Straw was selected, weighed and then placed on the conveyor. The straw walker system and chaff blower wagon then were started. The microprocessor system was activated and checked to ensure



proper operation. The conveyor then was started, with the grain application commencing as soon as the straw came in contact with the walkers. Time was monitored for 45 seconds, at the end of which the grain was shut off. During the entire run, straw was removed from the discharge end of the walker assembly and thrown manually into the chaff blower wagon.

Immediately after the grain was shut off, the microprocessor was shut down and the remainder of equipment halted. Memory in the microprocessor was examined for the collected data which was recorded manually. Grain remaining in the hopper was removed and weighed so that the actual application rate was known. Collection tray and bag material were placed in labelled storage bags with gross weights measured and recorded. All grain weights were measured with a digital electronic scale (Sartorius 3807-MP6). The samples were sealed and stored, pending the completion of all runs. Subsequently, samples were cleaned and weighed. A fanning mill from the Department of Plant Science, University of Alberta was used to clean each sample.

## 6. LABORATORY TEST RESULTS AND DISCUSSION

The data for the laboratory tests are given in Appendix III. Relevant data are compiled in various groupings to illustrate several trends and relationships.

### 6.1 Impact Counting Accuracy

The data for the impact counting accuracy determination was collected from sensor counts and collection bags during the twelve runs described in chapter 5. The weight (in grams) of clean grain from each bag was multiplied by twenty-two kernels per gram to calculate the number of kernels collected, since the counting of individual kernels proved too time consuming. A plot of number of counts versus number of kernels collected is shown in Figure 6.1 and shows the best fit straight line through the origin. The ratios of number of kernels counted to the number of kernels collected were calculated for all 48 collections made and are given in Table 6.1.

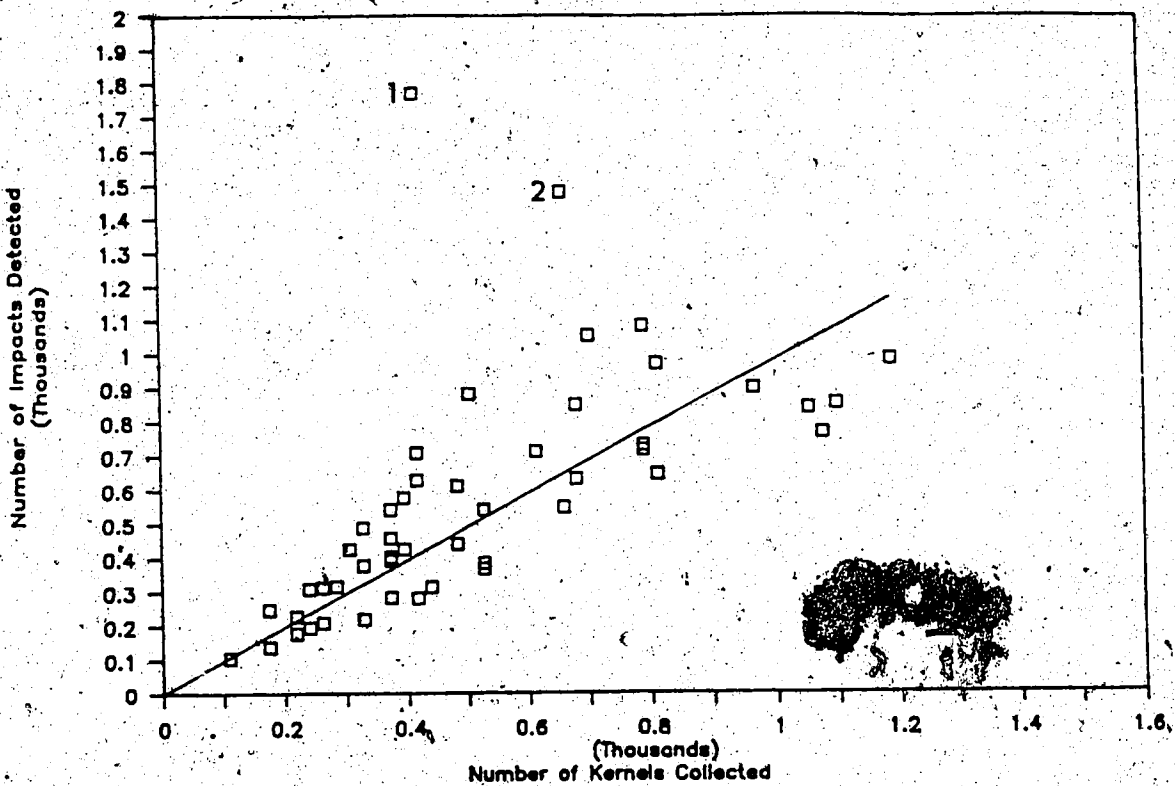


Figure 6.1 Impacts Counted versus Kernels Collected.

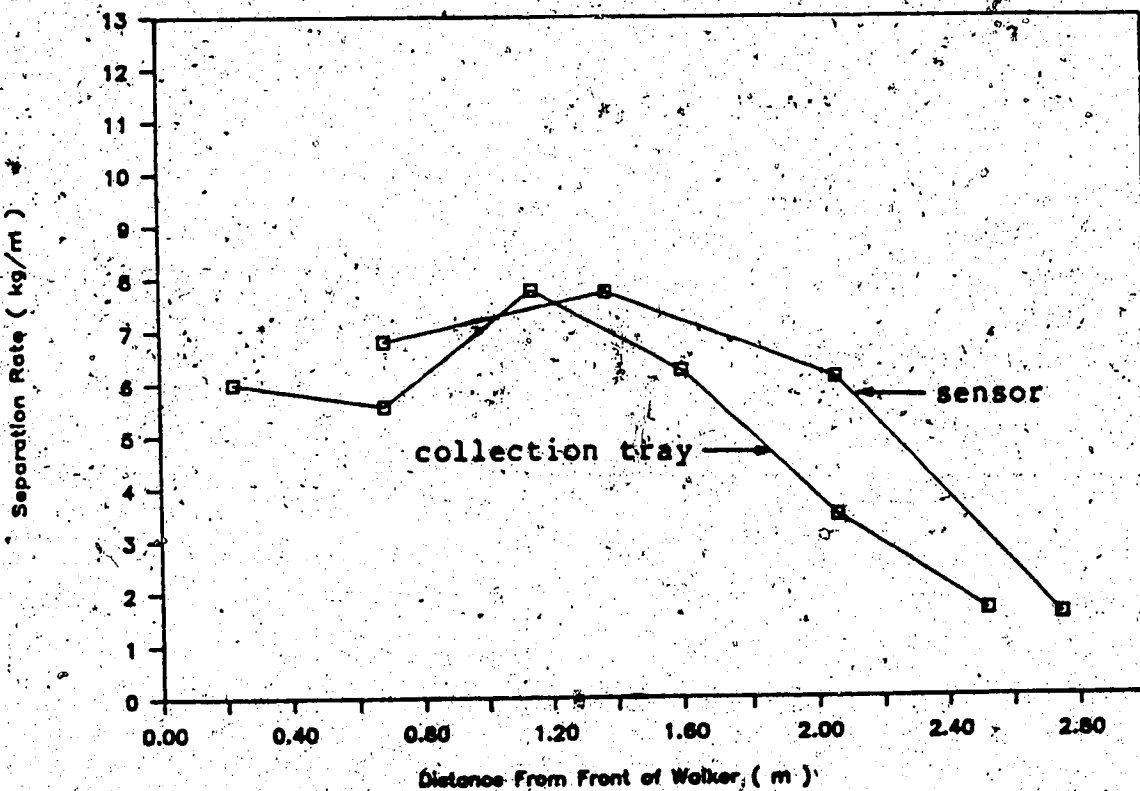


Figure 6.2 Typical Laboratory Separation Curve. (Run #5)

Table 6.1 Laboratory Collection Bag Data.

Col (g)	Col (#)	Cnt (#)	<u>Count</u> Collect	Col (g)	Col (#)	Cnt (#)	<u>Count</u> Collect
5	110	104	0.945	8	176	137	0.778
8	176	247	1.403	10	220	176	0.800
10	220	227	1.032	11	242	194	0.802
11	242	308	1.273	12	264	209	0.792
12	264	312	1.182	13	286	317	1.108
14	308	426	1.383	15	330	219	0.664
15	330	377	1.142	15	330	489	1.482
17	374	283	0.757	17	374	392	1.048
17	374	403	1.078	17	374	458	1.225
17	374	543	1.452	18	396	426	1.076
18	396	578	1.460	19	418	281	0.672
19	418	628	1.502	19	418	709	1.696
19	418	1770	4.234	20	440	314	0.714
22	484	440	0.909	22	484	611	1.262
23	506	882	1.743	24	528	367	0.695
24	528	384	0.727	24	528	542	1.027
28	616	713	1.157	30	660	548	0.830
30	660	1479	2.241	31	682	631	0.925
31	682	850	1.246	32	704	1053	1.496
36	792	717	0.905	36	792	732	0.924
36	792	1081	1.365	37	814	646	0.794
37	814	971	1.193	44	968	900	0.929
48	1056	842	0.797	49	1078	769	0.713
50	1100	855	0.777	54	1188	985	0.829

Two collections, numbered 1 and 2 on Figure 6.1, were ignored since the collection bags became tangled during the course of the run, causing rebounding of grain kernels within the housing and artificially high counts. The 't' statistic as described by equation 5.1 was calculated to be 1.3615 with  $M = 1.0589$ ,  $\mu = 1.0$ ,  $n = 45$  and  $s = 0.2934$ . With 45 degrees of freedom, the sample events would be accepted as part of the population with mean equal to 1.0 at the level of  $\alpha = 0.10$ . The 90% confidence interval places the mean of the population, from which the sample was taken, between 0.9862 and 1.1316.

## 6.2 Separation Curve Analysis

Separation data is given in Appendix III, Table 14.4, and separation curves for both sensor and collection methods are plotted in Appendix IV, Figures 15.1-12. A typical sample separation curve is shown in Figure 6.2. This shows clearly the general relationship between the two measuring methods. The six-point curves are from the collection tray data, while the four-point curves are from the sensor data. Units of the curves are kg/m per run duration (45s) versus distance along the walker in metres. The separation rate was calculated from raw data by applying the appropriate conversions for the area of straw walker sampled.

Several interesting points can be made concerning the shapes of the two curves and their differences. The sensors received data only from the middle walker, while the trays

collected data from the entire width of the system. The tendency for the straw to bunch along the center line is the cause of the shift in the sensor separation curve rearward as compared to the collection data. The center line of straw is thicker than at the edges, causing separation to occur at the edges before the separation can begin at the center line. The grain did not penetrate the straw mat as quickly along the center line. The delay can also explain the tendency of the first sensor to consistently read less than the second sensor, the reverse of what one would expect. Another contribution to the delay is that the grain is applied to the surface of the straw only, and not dispersed evenly, throughout the depth, as would be the case in a harvester situation.

Besides the delay as described above, the curves for the sensor and collection data are comparable both in magnitude and shape. The sensors may have recorded a higher separation due to the bunching of straw and grain along the system centerline. Consequently, the conclusion was made that the microprocessor measurement system was indeed capable of measuring a separation curve in conditions prevalent on a harvester.

### 6.3 Loss Calculations

The calculation of loss from the collection and sensor separation curve data, as well as the actual measurement of the applied grain was done. The actual loss was calculated

as the difference between the grain applied to the walkers and the grain collected in the collection bags and the collection trays 1 through 6. The grain collected in tray numbered 0 was subtracted from the applied grain since that grain did not fall through the walker surface. Loss was calculated by the integration of an extrapolated exponential curve on the trailing edge of the separation curve as described in section 2. For the tray collection, the regression of the exponential curve was done on the last four trays, while only the last three points of the sensor data were used because of the delay described previously. The calculated and actual losses for each run are given in Appendix III, Table 14.5, while the loss comparison is presented graphically in Figure 6.3. There were no regressions that fit the ratios of calculated to collected losses to a high degree.

The calculated losses per run in units of kilograms did not correspond well to the weighed losses. The differences were due primarily to the inability of the straw walker apparatus, using the procedure described, to emulate the separation response that is expected of a walker system in an actual harvester. Differences across the walker width were present because of the uneven feeding of the walkers. The application of the grain to the top surface of the straw added uncertainty in the separation characteristics.

Although the loss calculations did not fit well with the application amounts, the microprocessor measurement

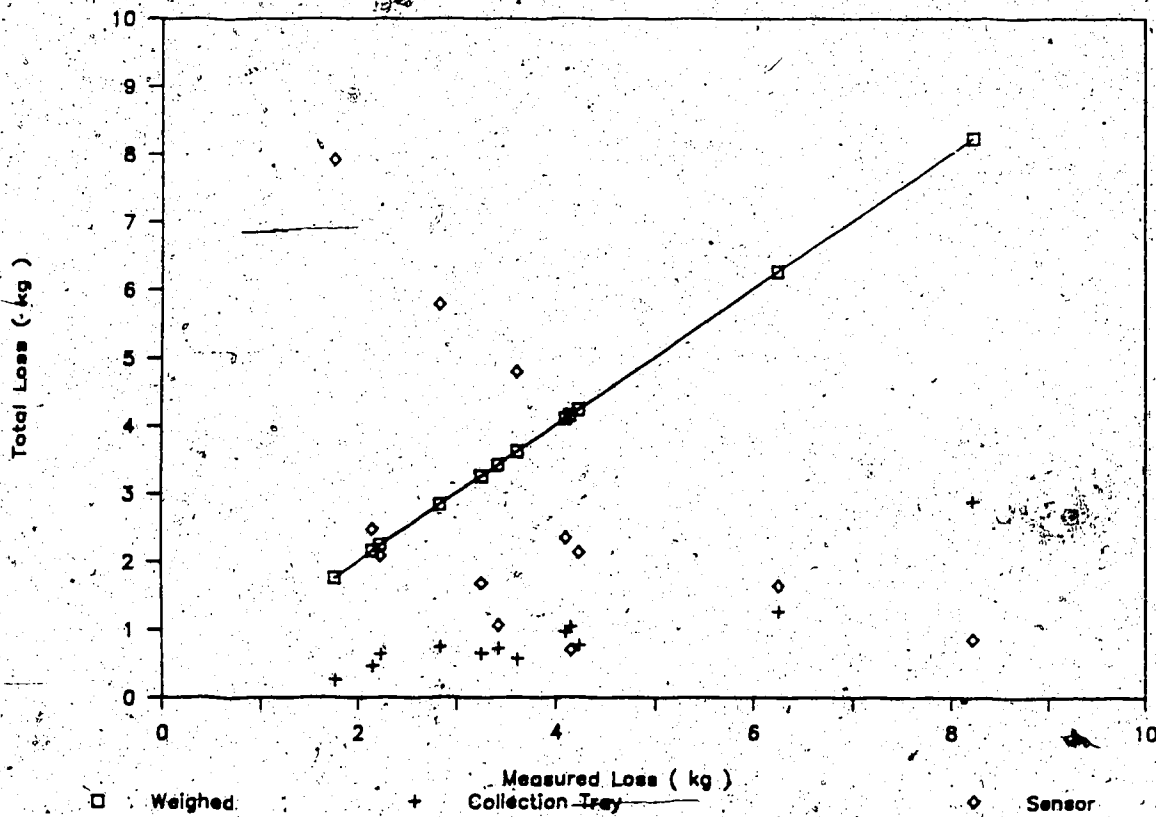


Figure 6.3 Calculated Versus Measured Losses.



system yielded comparable separation curves and the system was deemed adequate to proceed with field tests.

## 7. FIELD TESTING OF MULTIPLE SENSOR SYSTEM

A combine harvester was tested in actual field conditions with the multiple sensor system as previously described. Many steps involving the installation, operation and extraction of data were time consuming and organized to fit into the harvesting schedule of the farmers concerned. Because of this, only limited time for data acquisition was available. The field tests were done in the fall of 1986 near Boyle, Alberta, about 150 kilometres northeast of Edmonton.

### 7.1 Description of Equipment.

The harvesting unit comprised a Massey Ferguson model '751' conventional pull-type combine powered by a John Deere model '4640' two-wheel-drive tractor. A schematic of the combine is shown in Figure 1.1 and a view of the complete unit is shown in Plate 7.1. The capacity of the combine in barley, as determined by PAMI (1980) was 7.9 t/h at 3.0 % total loss. As illustrated by Figure 1.3(b), the greatest part of this tested loss was due to straw walker loss. The 1270 mm wide threshing cylinder operated at 1050 RPM for all tests conducted in this thesis. The straw walker assembly comprised six 30.6 mm long by 240-mm wide walkers which were open-bottommed. The Massey Ferguson design of walker perforations was consistent with the walker assembly tested in the laboratory, with the only difference being the length. Oscillation speed of the straw walkers was measured

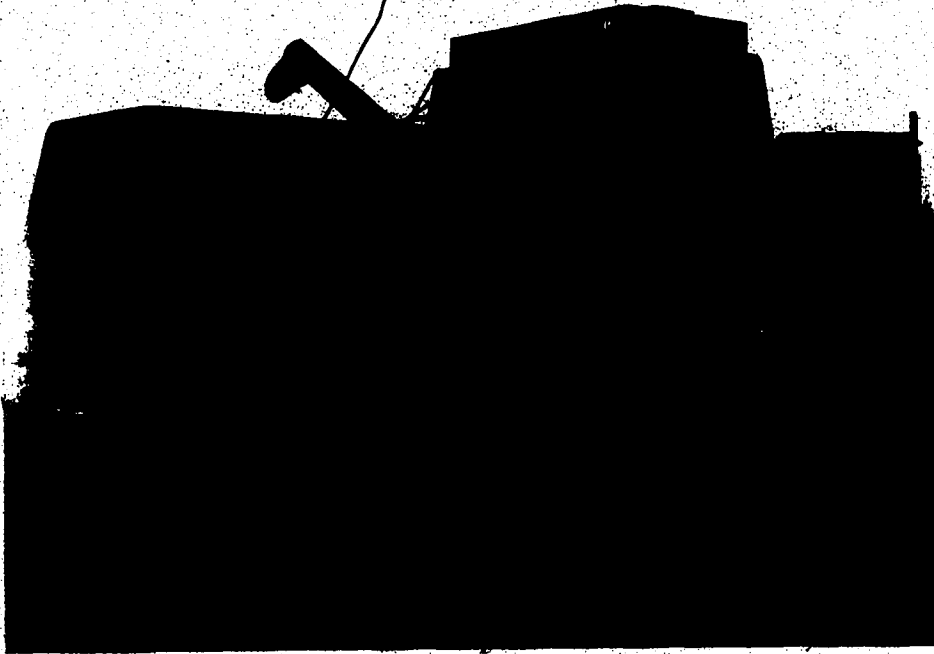


Plate 7.1 Field Test Machinery.



Plate 7.2 Microprocessor System.

to be 200 revolutions per minute. Separation curtains were located at 150 and 2400 mm from the front edge of the walkers. The curtains were in sections with one section over each walker. The tractor's electrical, mechanical, and hydraulic systems were used by the combine in normal operation.

Ground speeds were selected from the tractor's sixteen-speed mechanical transmission. Three speed selections were made with one speed above and one below the normal operating speed of the combine unit. The speeds chosen were 4.1, 5.8 and 7.2 km/h (1.1, 1.6 and 2.0 m/s respectively). Power was sufficient to maintain rated power take off speed under all loading conditions. The electrical system was twelve volts, negative ground, charged with an alternator.

Effluent from the straw walker and sieve assemblies were collected from the combine on 10 mil polyethylene sheets, 3.5 metres wide and 6.0 metres long. An electrically-controlled sheet roller was operated from the tractor enclosure. As the combine rolled along, the sheet was released, collecting only the straw walker effluent. A second sheet of polyethylene was pulled along under the combine and released immediately beneath the straw walker sheet to collect only the effluent from the sieves. Both collection sheets proved effective after a few trial runs. The collection sheets are shown in Plate 7.1.

## 7.2 Description of Measurement System.

The four sensors employed in the previous laboratory tests were used in the field tests. The software for the field test changed only slightly from the laboratory tests, in that a timing routine was implemented to operate the system for ten seconds at a time for each run. The program listing is given in Appendix II, section 13.5. The program was "burned" into an erasable, programmable, read only memory (EPROM), to ease the execution of the program. The microprocessor board was located in the tractor operator enclosure on a foam cushioned shelf (Plate 7.2).

The sensors were placed at the rear of the longitudinal quarters of the straw walkers in the laboratory tests. Plate 7.3 shows a view of the sensors on a removed walker. Since the combine was equipped with six straw walker sections, sensors were placed on the section third from the rear when viewed from the rear. This section was hoped to most accurately capture the average separation of the combine. Sample areas identical to those used in the laboratory were chosen to simplify mounting. The sensor housings were changed to fit the restricted area between the straw walkers and the grain conveyor pan immediately beneath. Also, no collection bags were used as the retrieval of such samples would be too labour-intensive. The 45° angle of impact was maintained as well as the shielding of sensors from grain from non-sample areas. A schematic of the sensor housing is shown in Figure 7.1.

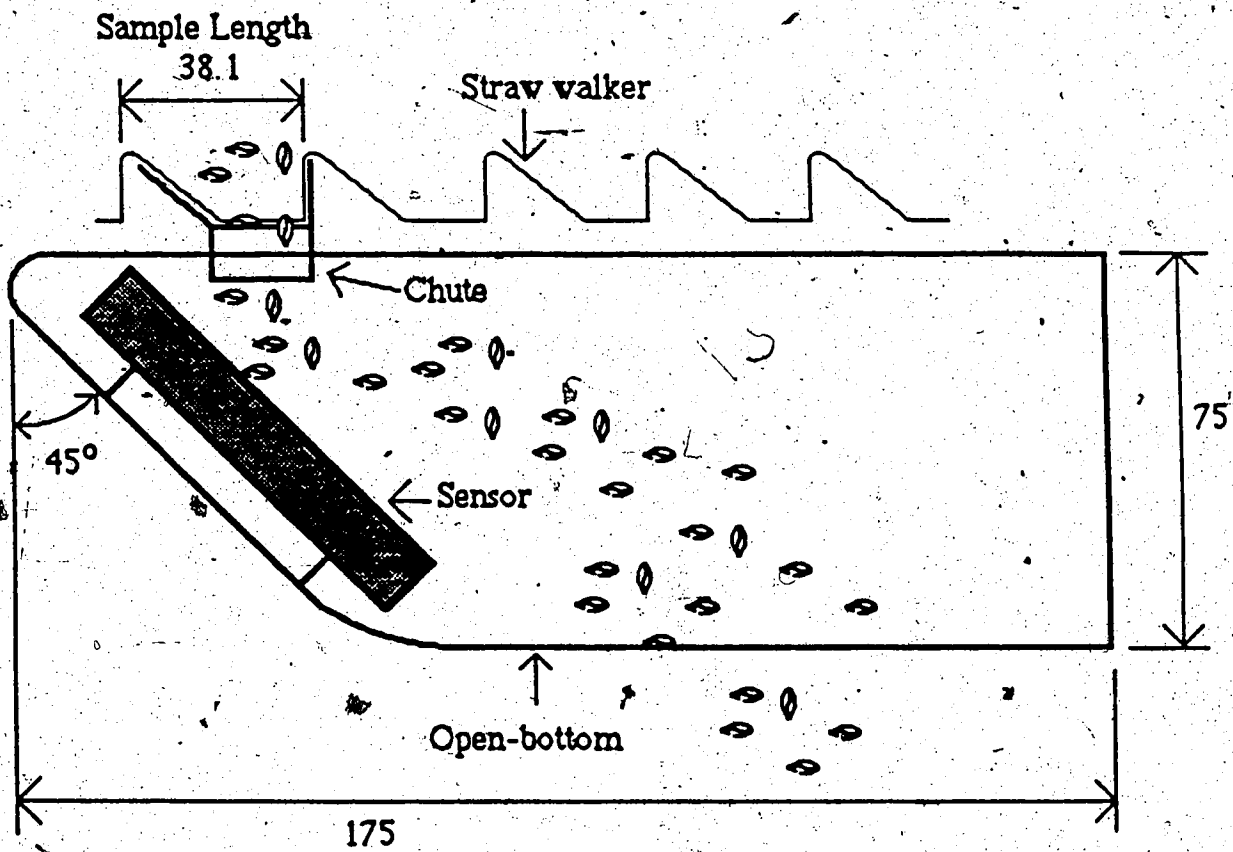


Figure 7.1 Field Test Sensor Housing. (all dimensions in mm)

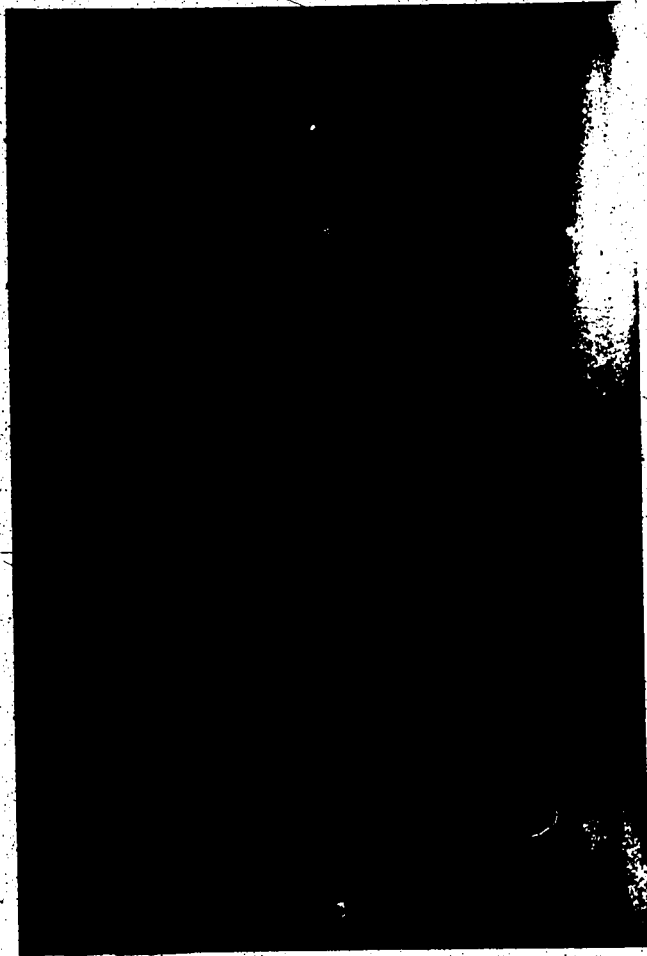


Plate 7.3 Location of Sensors.

The shielded cable from each sensor was grounded at a common point near the walker section rear and then routed along the combine length towards the tractor enclosure, using about 20 metres of cable in all. Great care was taken to ensure that the wires were adequately attached to the walker after the initial installation was destroyed after only ten hours of use. Efforts were made to ensure free passage of material around the leads and sensor housings so as to alter the separation characteristics as little as possible. Although the system was tested for only about two hours, the combine was used for about one hundred hours with the sensors installed.

In a preliminary test situation, interference was detected between the remote-controlled polyethylene roller and the sensor leads. The roller lines were relocated, eliminating the problem. Electrical power supply for the measurement system was supplied from the cigar lighter outlet of the tractor. The supply was regulated by an eight volt regulator as described in section 4.1.1. Voltage regulators internal to the microprocessor system further regulated the supply to five volts. A one-Ampere fuse was incorporated in the supply regulation to protect the system from any short circuit damage.



### 7.3 Material Description.

A fairly level piece of land was chosen for the site of the field test in order to inhibit any topographical influences. The land area was approximately 20 m by 150 m, comprised of four swaths from a 5.4-metre-wide swather. The area was reasonably free from weeds with a uniform crop stand as witnessed during the growing season. The surrounding 45 hectare field of Bonanza barley was harvested at a moisture content of about 17 %, while the tests were performed only when the grain moisture content reached 14.2 % wet basis. The swaths were in good condition, surviving ten mm of post-swathing precipitation. Average yield of the plot section was determined to be 2.5 t/ha. The barley's density was 920 kg/m<sup>3</sup> with an average of 34 kernels per gram. The straw was measured to have an average moisture content of 8.4 % wet basis. The average length of straw was 1.3 m and stubble was 150 mm high on average.

### 7.4 Experimental Design.

The main objective of this field experiment was to compare the loss as measured from the collected effluent with the loss calculated from the sensor measurement of the separation curve. The sensors were the only method by which the separation curve could be measured since no provision was made to collect material under the straw walkers. The t distribution of a sample from a normally distributed population was used to determine the significance of the

mean of the ratio of calculated loss versus collected loss for all runs as in equation 5.1. The null hypothesis was that the mean of the ratio was equal to one, whereas the alternate hypothesis was that the mean of the ratio was not equal to one.

$$H_0 ; \mu = 1.0$$

$$H_A ; \mu \neq 1.0$$

In order to keep the environmental effects down to a minimum, the experimental trials were run in one day. Three speeds were chosen as stated previously, with three replications completed in each speed yielding a total of nine runs. The three speeds represented the ability to choose different feedrates close to the normal maximums and minimums encountered in practical harvesting. Since the crop density changed slightly from place to place within the test area, one metre samples of swath were taken at each location of a run. The order of the runs was randomized and were performed on two adjacent swaths in the center of the four available systems. In order to obtain an adequate amount of data for each run without consuming too much area, sample periods of ten seconds were chosen, with the collection sheets deployed during those ten seconds.

An additional ten runs were performed on the remaining crop area without any collection of effluent due to the amount of materials already collected and the time of day. The additional runs served as checks to the previous runs assuming a uniformity of crop across the test area. Only the

sensor readings were recorded for these additional runs.

### 7.5 Experimental Procedure.

Before the runs were performed, trials were conducted to organize the procedures and collection methods. The first task was to adjust the combine to field conditions. The adjustments to cylinder, cleaning shoe and fan were made by the owner to ensure a representative combine setting was obtained. No attempt was made to adversely adjust the combine to exhibit any unusual characteristic.

One trial involved operating the measurement system with the combine operating at rated speed with no input. The combine was driven across the field at normal operating speeds. Loaded trials involved determining the procedures for the test team in operating the collection sheets. Once a procedure for a run was adopted, the normal runs began.

Before each run, a one metre sample of swath immediately ahead of the combine was collected, bagged and sealed, to be used at a later date for feedrate determination. The polyethylene sheets were rewound and positioned for sampling. The combine then was operated at rated speed and the measurement system checked. Once the system was operating correctly, the test began.

Moving into the crop, the system was activated when the combine was fully loaded and effluent began to appear at the rear. The remote controlled polyethylene sheet was deployed, prompting the sieve collecting sheet to be released. The

combine continued on, depositing effluent on the sheets. Care was taken to ensure that the wind would not disrupt the placement of collected material. The combine was stopped and allowed to clear after the ten-second data acquisition process had elapsed.

The grain count data then were obtained from the microprocessor and recorded manually. One metre samples of straw walker and sieve effluent were collected, bagged and sealed for future examination. The test machinery then was ready for the next run.

The collected grain, straw and chaff was threshed and/or separated by equipment in the Department of Plant Science at the University of Alberta. Weights of all components were recorded immediately after being measured by an electronic scale. The data then were grouped and analysed.

## 8. FIELD TESTING RESULTS AND DISCUSSION

Raw data recorded for runs 2-10 and 11-20 are given in Appendix III, Table 14.6, along with information obtained from the raw data. Twice during the test procedure, after runs 7 and 8, the system responded incorrectly from a buildup of straw and chaff inside one or two of the sensor housings. The sensor would continuously register counts, even when the combine ran empty. The sensor housings were all thoroughly cleaned and no further problem was encountered of this sort. Run 4 was highlighted by the passage of a porcupine through the harvester. The rodent's carcass interrupted or in some other way altered the sensor readings for that run. Consequently, the six runs remaining were considered to be 'good' out of the nine scheduled.

### 8.1 Separation Curves and Loss.

Separation rate curves were obtained from sensor data only (Table 8.1) and are plotted in Appendix IV, Figures 15.13-21. Data was converted from count data to separation rate (kg/m per duration of 10s run) by considering the area sampled and grain characteristics. Regression equations for the separation curves were calculated and loss calculated from the extrapolation and integration of the curve beyond the walkers. The equations and losses are given in Table 8.1.

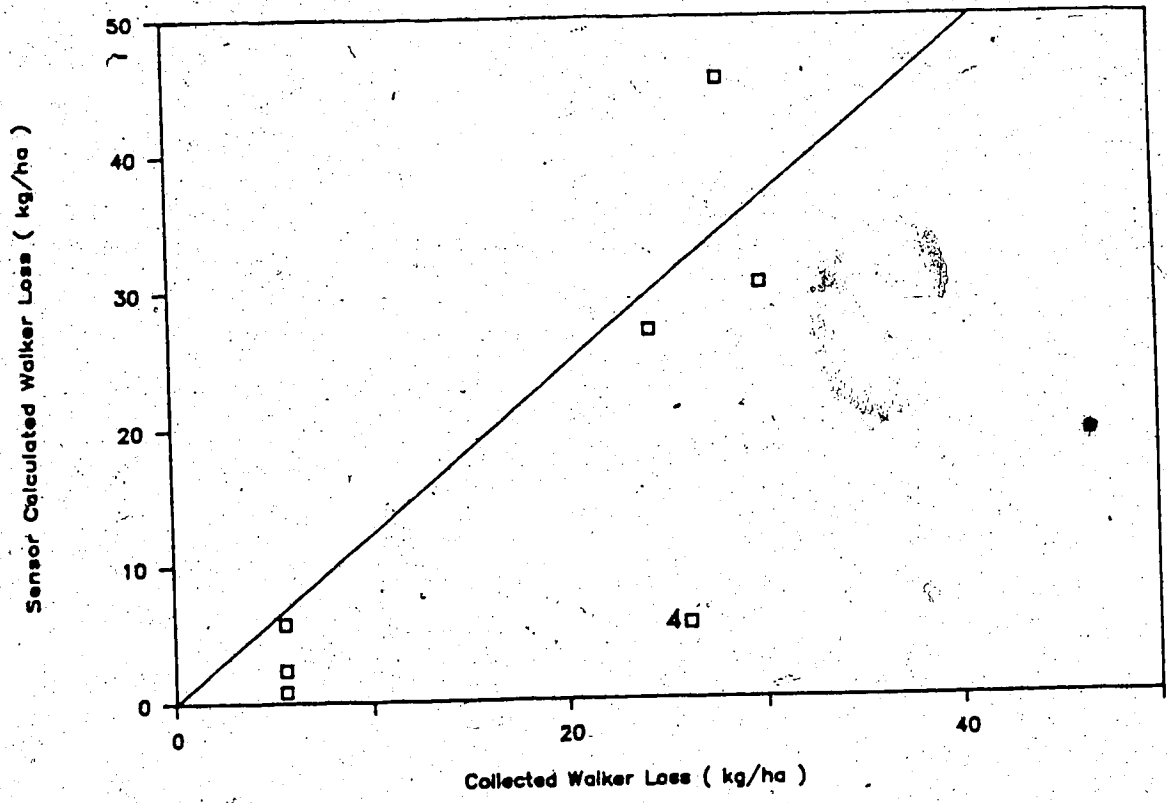


Figure 8.1 Sensor-Calculated Loss versus Collected Loss.

89

Table 8.1 Field Test Separation Data Equations and Losses

Separation Equation Form:  $Y = A \cdot \exp(B \cdot X)$   
 $Y$  = Separation Rate (kg/m), and  
 $X$  = Distance Along Walker (m)

Run (N)	Separation Rate (kg/m) e Sensor (location, m)				Separation Equation			Loss Calc (kg/ha)	Calc Means
	1	2	3	4	A	B	R <sup>2</sup>		
	(0.754)	(1.508)	(2.362)	(3.015)					
2	0.136	0.092	0.009	0.009	0.449	-1.382	0.838	0.854	1.147
3	0.136	0.092	0.018	0.018	0.314	-1.013	0.918	2.40	0.429
4	0.383	0.167	0.121	0.037	0.796	-0.950	0.970	5.53	0.211
5	0.198	0.148	0.065	0.111	0.236	-0.351	0.721	27.0	1.107
6	0.740	0.417	0.250	0.204	1.065	-0.577	0.976	30.4	1.013
7	0.518	0.195	0.232	0.389	0.373	-0.099	0.068	263	18.7
8	0.308	0.250	0.204	0.296	0.288	-0.050	0.070	463	16.48
9	0.333	0.185	0.157	0.148	0.374	-0.341	0.832	45.4	28.1
10	0.259	0.130	0.047	0.037	0.495	-0.909	0.992	5.77	5.6
11	0.296	0.222	0.092	0.036	1.024	-0.931	0.857	7.74	
12	0.308	0.222	0.204	0.175	0.491	-0.232	0.917	86.2	
13	0.184	0.157	0.268	0.417	0.162	-0.388	0.852	8.57	
14	0.209	0.092	0.036	0.101	0.297	-0.431	0.544	21.9	
15	0.222	0.194	0.092	0.083	0.487	-0.489	0.905	18.7	
16	0.567	0.370	0.602	0.546	0.656	0.053	0.049		
17	0.382	0.221	0.184	0.055	1.051	-0.766	0.896	15.9	
18	0.247	0.166	0.157	0.175	0.343	-0.144	0.548	127	
19	0.296	0.184	0.240	0.064	0.682	-0.542	0.538	16.3	
20	0.444	0.314	0.296	0.546	0.487	0.063	0.068		

The calculated loss versus measured loss is plotted in Figure 8.1 with the regression equation being:

$$Y = 1.2177 X$$
 8.1

where: Y = Sensor calculated walker loss (kg/ha), and  
X = Collected walker loss (kg/ha).

The porcupine altered data for Run #4, identified by the '4' on the graph and, consequently, was not used in the regression. Runs #7 and #8 do not lie on the graph and were not used in the regression since plugging of sensor housings occurred. The units of kg/ha for the walker loss were determined by applying the appropriate factors of area conversions. The tests ranged in total loss from 0.4% to 2.9%. Loss would average about 2% when operated by the owner under normal conditions. The ratio of calculated loss to measured loss then was averaged for all valid test runs. The ratios are given in Table 8.1.

By equation 5.1, the 't' statistic was 0.514 with M = 0.89,  $\mu = 1.0$ , n = 6, and s = 0.524 with five degrees of freedom. The null hypothesis is accepted with  $\alpha=0.10$ . The ratio of calculated to measured loss was within statistical proximity of the expected population mean of 1.0. The 90 % confidence interval places the population mean between 0.46 and 1.32 according to the sample data obtained. The statistic would indicate that the system measured the loss at a statistically significant level.

Referring to Figure 8.1, the slope of the best-fit line through the origin had a slope of 1.21. This shows that the



measurement of loss on average, tended to be higher than that collected in the effluent, illustrating again the influence of only sampling one walker. The combine pick-up mechanism tended to load the right-hand side of the combine more heavily when avoiding contact between the tractor tires and the swath. Consequently, walkers on the right hand side would be loaded with larger quantities of grain. Since the sensors were placed towards the right hand side, they experienced the same increase in grain. The location of the sensors is considered to be of critical importance.

The separation curves in Appendix IV show that an exponential decay does in fact occur and is measured consistently by the system. Except for the blockage problems of runs #7 and #8, the curves display the same general shape. The exponential regression was carried out for all four sensor locations for all runs. A high degree of correlation suggests that the system responded well to measuring separation data on a harvester. High correlations of fit were obtained, with  $R^2$  ranging from 0.721 to 0.992 for the valid runs with collection data.

## 9. CONCLUSIONS

Examination of grain loss sensor attitude with reference to grain contacting the surface revealed that the best orientation was at  $45^\circ$  to the direction of the grain trajectory. Tests showed that a microprocessor-based system developed could distinguish individual grain particles from straw and chaff, as well as from each other. The system could count grain kernels with an accuracy of  $\pm 10\%$  at a rate of about 35 kernels per second for single and multiple sensors at the optimum  $45^\circ$  attitude.

The collection of grain that contacted the sensors in the laboratory test showed a high statistical correlation between the number of kernels collected and the impacts counted. The 90 % confidence interval placed the ratio of impacts counted to kernels collected within 13% of the mean.

The laboratory separation apparatus did not provide very accurate separation data. The comparison of laboratory collected loss and calculated loss, both from tray collection and sensor data, showed no significant relationship. The method of applying grain and feeding straw was poor in that field conditions could not be closely duplicated. The applied grain was excessive when compared to separation rates in the field. Separation rates along the walker length reached 16 kg/m per minute in the laboratory, while actual field separation rates never exceeded 4.8 kg/m per minute.

The field test measurements of separation curves were performed successfully. The curves of all valid runs were of high-correlation exponential decays with a calculated loss statistically close to the measured loss rates. The worst fit had an  $R^2$  of 0.721, while the best was 0.992.

Loss calculations based on separation rate curves are accurate, provided the samples are point-samples of known area and location. The comparison of calculated to measured loss showed a statistically significant correlation at the level of  $\alpha = 0.10$  with limited data. The calculation of walker loss is simple once the exponentially decaying curve is extrapolated beyond the walkers.

Digitization of an electrical signal from a grain loss sensor is possible with a microprocessor-controlled analog-to-digital converter. The signal could then be analyzed to determine whether the signal was from a grain or non-grain particle. This analysis was not possible with the equipment available.

## 10. RECOMMENDATIONS

Recommendations are made for system improvement and procedural revamping.

### 10.1 Improvements to Sensing System

From tests in the laboratory and field, complications arose due to the monitoring of only one walker section. The recommendation is made to implement a multiple sensor system on more than one walker section, with monitoring all walker sections being ideal. The complete separation analysis could then be achieved without having to assume a constant separation across the walker width.

Software could be developed beyond the scope of this thesis to calculate the actual loss from the sensor data immediately. An internal calibration for the number of kernels per kilogram could be utilized in an on-going basis. A number of kernels could fall onto a sensor from the grain tank. The kernels could be collected and weighed, with the microprocessor calculating the number of kernels per kilogram from the data. This would avoid the necessity to enter crop parameters into the program as the crop quality changed.

The sensor housings should be modified to prevent the plugging which altered field tests #7 and #8. The housing cowls should incorporate more elaborate deflection techniques to minimize the plugging and disturbance to separation.

## 10.2 Improvements to Procedure

An improvement to the feeding characteristics of the laboratory apparatus is needed. Perhaps a walker system behind a threshing cylinder and concave is the only way to accurately mimic the conditions of a harvester.

The field tests should be increased in number and length. The samples for each run should be larger to eliminate the possibility of concentrated variation in crop properties. Larger samples of effluent would help to improve reproduceability of data.

A different material for collection sheets would help collection. The polyethylene sheets tended to slide on the stubble. As well, the effluent tended to slide on the sheets. Wind would catch the sheets easily if care was not taken. A canvas or rubber sheet is suggested as a better material.

## 11. REFERENCES.

- ASAE, 1983. Standard S358.1. Moisture Measurements - Forages. Agricultural Engineers Yearbook. Am. Soc. Agric. Eng., St. Joseph, Michigan.
- Audsley, E. and D.S. Boyce. 1974. A Method of Minimising the Cost of Harvesting and High Temperature Grain Drying. J. Agric. Eng. Res. 19:173-189.
- Boyce, B.H., R.T. Pringle, and B.M.D. Wills. 1974. The Separation Characteristics of a Combine Harvester and a Comparison of Straw Walker Performance. J. Agric. Eng. Res. 19:77-84.
- Gregory, J.M. and C.B. Fedler. 1986. Mathematical Relationship Predicting Grain Separation in Combines. Paper No. 86-1522 Am. Soc. Agric. Eng., St. Joseph, Michigan.
- Gullacher, D.E. and L.G. Smith. 1979. Grain Loss Monitor Performance. Paper No. 79-1579 Am. Soc. Agric. Eng., St. Joseph, Michigan.
- Huisman, W. 1983. Optimum Cereal Combine Harvester Operation by means of Automatic Machine and Threshing Speed Control. Doctoral Thesis. Agricultural University, Wageningen, The Netherlands.
- Leflufy, M.J. and G.T. Stone. 1983. Speed Control of a Combine Harvester to Maintain a Specific Level of Loss. J. Agric. Eng. Res. 28:537-543.
- Lunty, J.W. 1986. Measurement of Combine Straw Walker Grain Loss. Master's Thesis. University of Alberta,

Edmonton, Alberta.

McGechan, M.B. and C.A. Glasbey. 1982. The Benefits of Different Speed Control Systems for Combine Harvesters. J. Agric. Eng. Res. 27:537-552.

Moller, A. 1985. Application of Microprocessors Within Agriculture. Agri Contact, Hundested, Denmark.

Motorola, Inc. 1980. MEK6802D5 Microcomputer Evaluation Board User's Manual. Second Edition. Motorola, Inc., Austin, Texas.

Nyborg, E.O., H.F. McColly, and R.T. Hinkle. 1969. Grain Combine Loss Characteristics. Trans. Am. Soc. Agric. Eng. 12:727-732.

Palmer, J. 1984. Selecting Profitable Automatic Control Systems. Paper No. 84-1635 Am. Soc. Agric. Eng., St. Joseph, Michigan.

Phillips, P.R. and J.R. O'Callaghan. 1974. Cereal Harvesting - A Mathematical Model. J. Agric. Eng. Res. 19:415-433.

PAMI. 1980. Evaluation Report E3079B. Massey Ferguson 751 Pull-Type Combine. Prairie Agricultural Machinery Institute, Humbolt, Saskatchewan.

PAMI. 1979. Evaluation Report E3078A. International Harvester 1460 Self-Propelled Combine. Prairie Agricultural Machinery Institute, Humbolt, Saskatchewan.

Reed, W.B. 1978. A review of Monitoring Devices for Combines. Proceedings of the International Grain and

- Forage Harvesting Conference. Iowa State University, Ames, Iowa. September, 1977. Publication No. 1-78, Am. Soc. Agric. Eng.
- Reed, W.B., M.A. Grovum, and A.E. Krause. 1968. Combine Harvester Grain Loss Monitor. Paper No. 68-607 Am. Soc. Agric. Eng., St. Joseph, Michigan.
- Reed, W.B., G.C. Zoerb, and F.W. Bigsby. 1970. A Laboratory Study of Grain-Straw Separation. Paper No. 70-604 Am. Soc. Agric. Eng., St. Joseph, Michigan.
- Reed, W.B., G.C. Zoerb, and F.W. Bigsby. 1972. A Laboratory Study of Straw-walker Efficiency. Paper No. 72-638 Am. Soc. Agric. Eng., St. Joseph, Michigan.
- Steele, R.G.D. and J.H. Torrie. 1980. Principles and Procedures of Statistics. A Biometric Approach. McGraw-Hill Book Company. New York.
- Wang, G. 1984. A Study of Separation Characteristics of a Rotary Combine. Master's Thesis. University of Saskatchewan, Saskatoon, Saskatchewan.
- Wood, J.E. and R.P. Kerr. 1980. Evaluation of Grain Loss Monitor Performance. Paper No. 80-1541 Am. Soc. Agric. Eng., St. Joseph, Michigan.
- Wrubleski, P.D. and E.O. Nyborg. 1978. Prairie Agricultural Machinery Institute Field Evaluation of Grain Combines. Proceedings of the International Grain and Forage Harvesting Conference. Iowa State University, Ames, Iowa. September 1977. Publication No. 1-78, Am. Soc. Agric. Eng.



12. APPENDIX I CIRCUIT DIAGRAMS

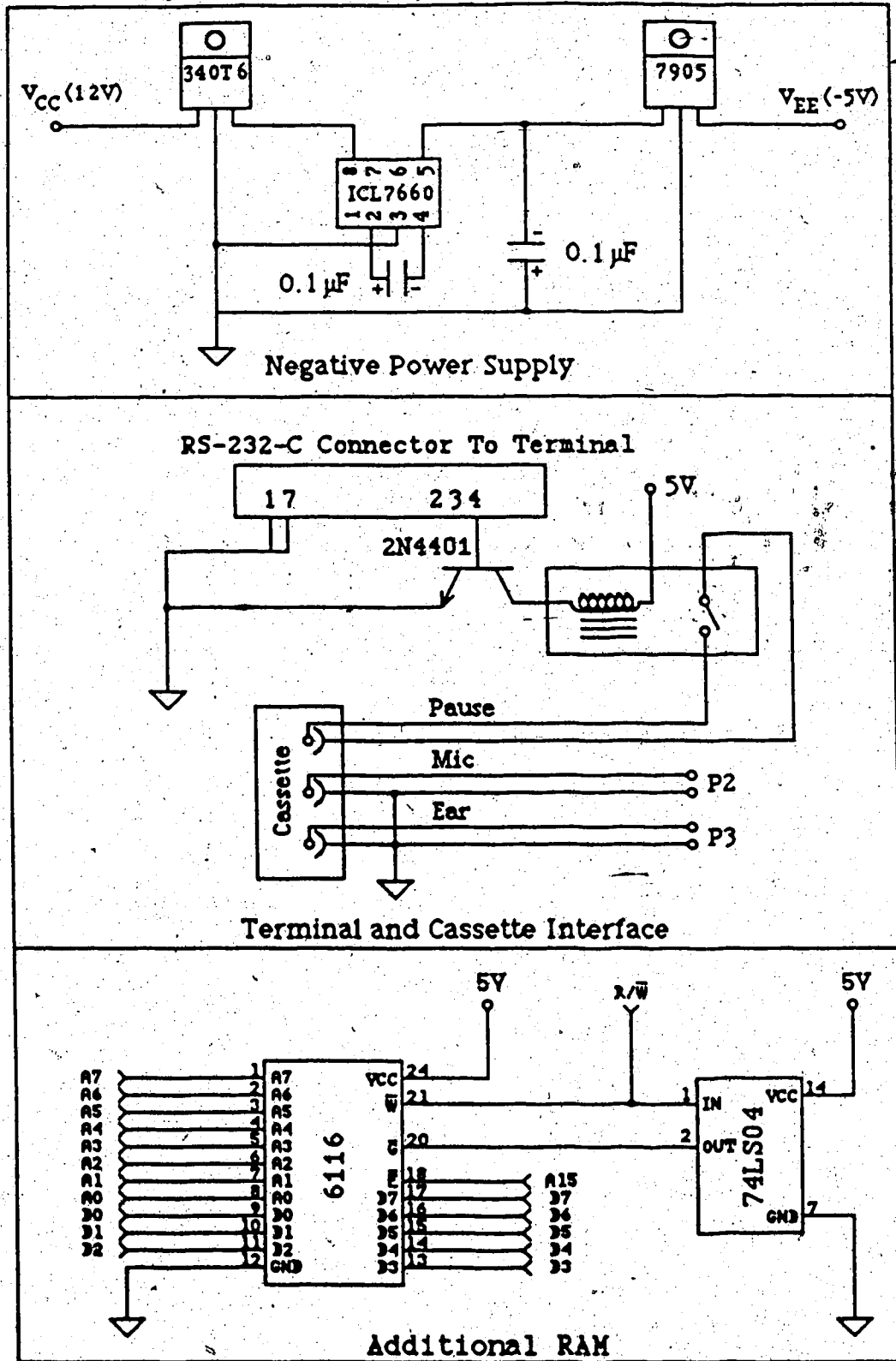


Figure 12.1 MEK6802-D5 Evaluation Board Additions.

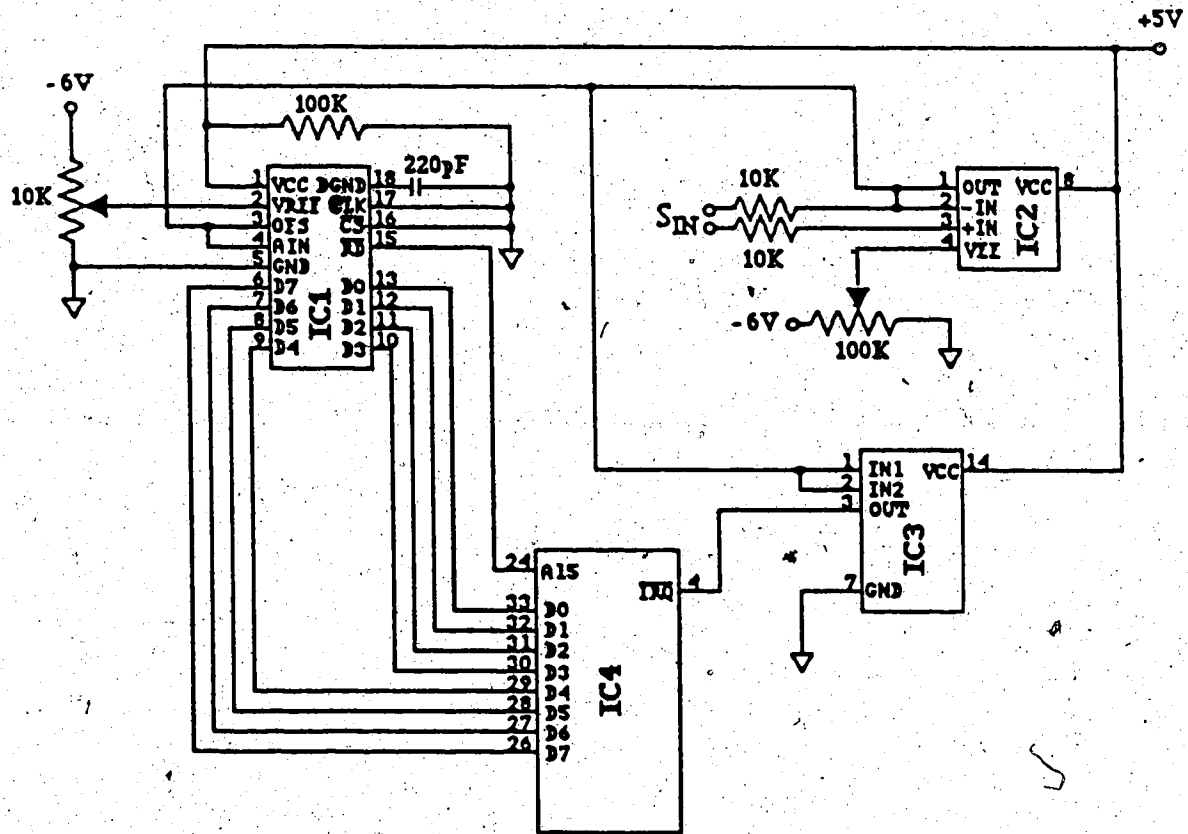


Figure 12.2 Digital Signal Processing Circuit. IC1, AD7574 analog-to-digital converter; IC2, 1458 dual operational amplifier; IC3, 74LS00, quad-NAND; IC4, MC6802 microprocessor; SIN, sensor input..

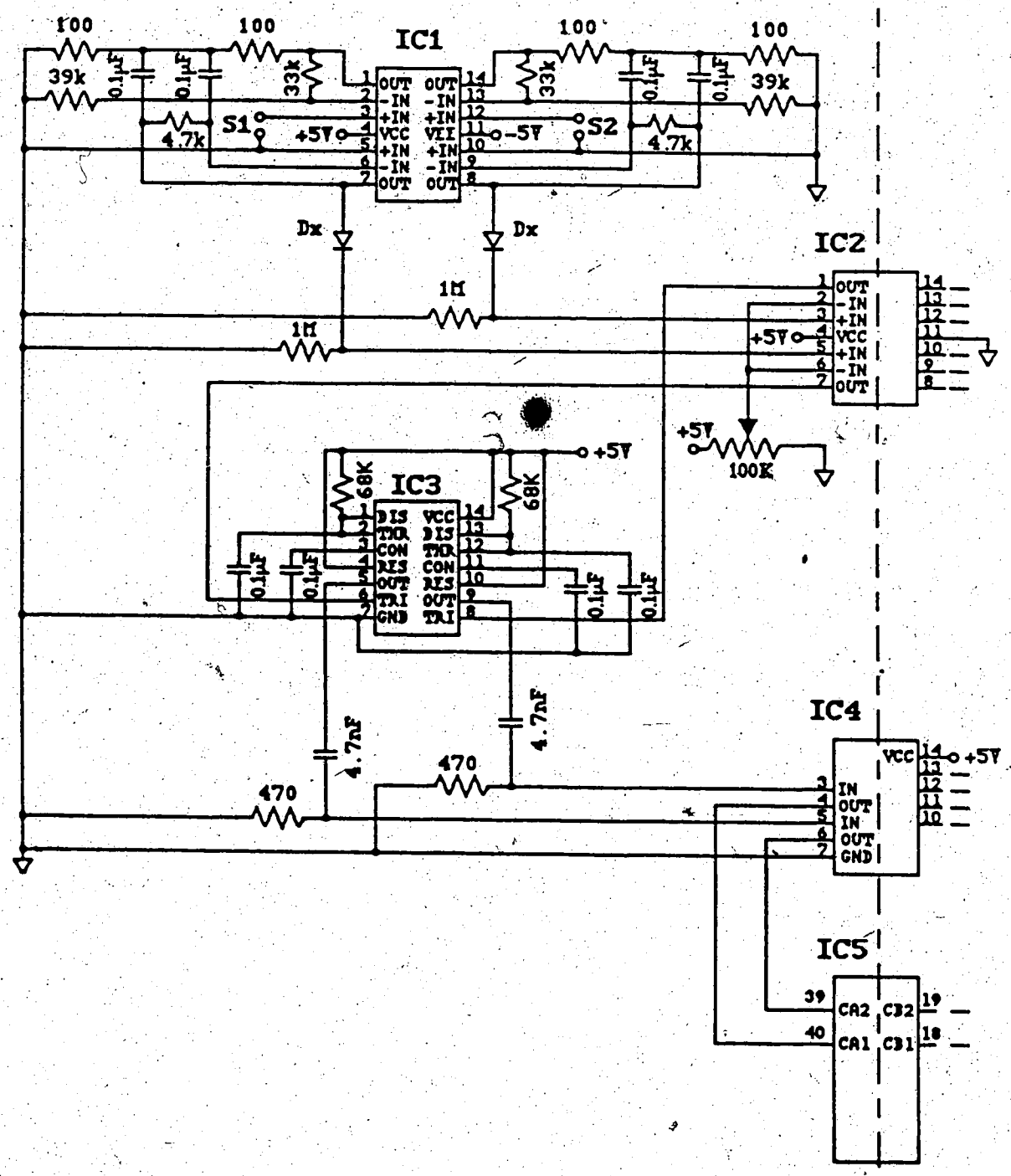


Figure 12.3 One Half of Analog Signal Processing Circuit. IC1, IC2 LM324 quad operational amplifiers; IC3, 556 dual timing circuit; IC4, 74LS04 hex-inverter; IC5, MC6821 peripheral interface adapter; S1, S2, sensor inputs.

# 13. APPENDIX II PROGRAM LISTINGS

## 13.1 Microprocessor Data Transfer Programs

### 13.1.1 Mainframe to microprocessor

NAM MTS

\*  
 \* THIS PROGRAM TRANSFERS ASSEMBLED PROGRAMS TO THE D5  
 \* FORM THE MAINFRAME COMPUTER VIA A MODEM AND ACIA  
 \* ALLOWANCE IS MADE FOR CASSETTE STORAGE OF PROGRAM  
 \*

CR EQU \$E700 ;ACIA STATUS AND CONTROL REGISTER  
 DR EQU \$E701 ;ACIA DATA REGISTER  
 PUNCH EQU \$F630 ;CASSETTE STORAGE SUBROUTINE  
 PROMPT EQU \$F024 ;PROMPT DISPLAY SUBROUTINE  
 BEGAD EQU \$E460  
 ENDAD EQU \$E462

\*  
 X10 ORG \$E800  
 BSR X1 ;BEGIN PROGRAM READ  
 LDAB #\$29 ;TURN ON CASSETTE  
 STAB CR  
 JSR X2

\*  
 JSR PUNCH ;TAPE STORAGE  
 LDAB #\$49 ;TURN OFF CASSETTE  
 STAB CR  
 BRA X3

X11 BSR X1  
 X3 JSR X2  
 JMP PROMPT ;DISPLAY PROMPT

X1 LDAB \$E3F1 ;E3F1=0 ?  
 BEQ X4 ;YES, X4  
 LDAB #\$FF ;NO, E3F1=00

X4 STAB \$E3F1  
 LDAB \$E3F2 ;E3F2=00

LDAB \$E3F3  
 BEQ X5 ;E3F3=0 ?, YES, X5  
 LDAB \$E40 ;NO, E3F3=40

X5 STAB \$E3F3  
 NOP  
 LDX \$0000  
 STX BEGAD  
 LDAB \$03 ;MASTER RESET  
 STAB CR  
 LDAB \$49  
 STAB CR

```

X7      JSR X6          ;READ CHAR
X9      CMPB #$53      ;CHAR='S'?
        BNE X7         ;NO, X7
        JSR X6         ;YES, GET NEXT CHAR
        CMPB #$31     ;IS CHAR=1?
        BEQ X8         ;YES, X8
        CMPB #$39     ;IS CHAR=9?
        BNE X9         ;NO, TRY UNTIL IT IS
        RTS

*
*
        ORG $E888      ;BEGINNING WITH TAPE STORAGE
        JMP X10

*
*
        ORG $E899      ;BEGINNING WITHOUT TAPE STORAGE
        JMP X11

*
*
X2      ORG $E8A0
        LDAB DR        ;READ DATA REG
X12     LDX #$4000     ;DELAY
        DEX
        BNE X12
        LDAB CR        ;CHECK IF ENTIRE SEND IS OVER
        ANDB #$03
        EORB #$02
        BNE X2
        LDAB #$07
X13     STAB DR
        LDAB CR
        ANDB #$02
        BEQ X13
        LDAB #$08
        STAB DR
        RTS

*
*
X8      LDAA #$01      ;PREVIOUS 2 CHAR WERE 'S1'
        BSR X14        ;OBTAIN COUNTER BYTE
        SUBB #$03
        STAB $E3F6
        BSR X14        ;READ PROGRAM DATA
        STAB $E3F4
        BSR X14
        STAB $E3F5
X18     LDX $E3F4
        BSR X14
        STAB 0,X
        SUBB 0,X
        ANDB $E3F1
        BEQ X15
        LDAA $E1
        BRA X16

```

```

X15  CPX  ENDAD      ;IS LINE OVER ?
      BLS  X17
      STX  ENDAD      ;YES
X17  INX
      DEC  $0076      ;NO, CONTINUE
      BGT  X18
      BSR  X14
      BNE  X19
      JMP  X7
X19  STAA  $E3F2
      TAB
      LDAA #E2
X16  BSR  X2
      BRA  X16
X6   LDAB  CR          ;STATUS REG
      ANDB #01        ;CHECK RDRF
      BEQ  X6          ;NO, WAIT
      LDAB CR          ;YES CHECK MODEM CARRIER
      ANDB $E3F3
      BEQ  X20
      LDAA #E3
      BRA  X16
X20  LDAB  DR          ;READ CHARACTER
      ANDB #$FF
      RTS
*
*
X14  BSR  X6
      CMPB #$40
      BLE X21          ;CHECK IF CHAR IS LETTER OR NUMBER
      ADDB #$09        ;CHANGE FROM ASCII TO HEX
X21  ANDB #$0F
      ASLB
      ASLB
      ASLB
      ASLB
      STAB $E3F5      ;STORE HEX IN E3F5
      BSR  X6          ;NEXT CHAR
      CMPB #$40        ;CHECK IF CHAR IS NUMBER OR LETTER
      BLE X22
      ADDB #$09        ;CONVERT ASCII TO HEX
X22  ANDB #$0F
      ADDB $E3F5
      ABA
      RTS
*
*
      END

```

### 13.1.2 Microprocessor program for IBM personal computer communication

#### NAM TRANSFER

\* THIS PROGRAM WILL ACCEPT OPCODE FROM THE IBM PC IN THE FIRST  
\* AND SEND DATA TO THE PC IN THE SECOND PART

\* PROGRAMMER RON LARSON

```

*
RESET EQU $F000 ;RESET OF SYSTEM AND DISPLAY PROMPT
CR EQU $E700 ;ACIA STATUS AND CONTROL REGISTER
DR EQU $E701 ;DATA REGISTER

```

\* THE FIRST PART

```

*
X1 ORG $E300 ;BEGINNING ADDRESS
RMB 2 ;STORAGE FOR INDEX REG ADDRESS

```

\* MASTER RESET

```

*
LDAA #$03
STAA CR

```

```

*
LDAA #$55 ;/16,8B,1ST,NPR,RTS HIGH,TRANS I DIS,I DIS
STAA CR

```

\* BEGINNING OF LINE READ

```

*
LOOP1 LDAA CR ;RDRF, IE. IS THERE A CHARACTER?
LSRA
BCC LOOP1 ;NO, WAIT FOR ONE.

```

\* COUNTER BYTE READ

```

*
LDAB DR ;YES STORE THE COUNTER BYTE
CMPB #$FF ;IF FF THEN LAST ROW AND THEN END (RESET)
BNE OVR ;NO, CONTINUE
JMP RESET ;DISPLAY PROMPT

```

\* HIGH BYTE ADDRESS

```

*
OVR LDAA CR ;NEXT CHAR ?
LSRA
BCC OVR ;NO, WAIT
LDAA DR ;YES, HIGH ADDRESS BYTE
STAA X1 ;STORE ADDRESS
DECB ;COUNTER DECREMENT

```

\* LOW ADDRESS BYTE

```

*
LOOP2 LDAA CR ;NEXT CHAR
LSRA
BCC LOOP2 ;NO, WAIT

```

```

LDA DR      ,OBTAIN LOW @ BYTE FROM THE PC
STAA X1+1  ,SAVE LOW BYTE
DECB       ,COUNTER DECREMENT
LDX X1     ,ADDRESS INTO X REG

```

```

* READING OF DATA INTO RAM

```

```

LOOP3 LDA CR      ,NEXT CHARACTER
      LSRA
      BCC LOOP3  ,NO WAIT
      LDA DR     ,READ DATA
      STAA 0,X   ,STORE DATA
      INX       ,GET READY FOR THE NEXT DATA
      DECB      ,DEC COUNTER
      BEQ LOOP1 ,NEXT LINE
      BRA LOOP3 ,NEXT DATA

```

```

* THE SECOND PART
* THE DATA TRANSFERED IS CONTAINED IN THE ADDRESS SPACE $E000
* $E3FF (ALWAYS) THE PC CAN THEN PICK OUT THE REQUIRED ONES.
ORG $E350
LDA #03    ,MASTER RESET
STAA CR

```

```

LDA #55    ,/16, 8BIT, 1 ST,NPR,RTS*HIGH,TRAN I DIS
STAA CR

```

```

LDX #E000 ,BEGINNING OF DATA
LOOP4 LDA CR ,CHECK TDRE
      BITA #02
      BEQ LOOP4

```

```

AGAIN LDA 0,X ,SEND DATA TO PC
      STAA DR
      JSR DELAY ,DELAY FOR PC TO CATCH UP
      INX
      CPX #E400 ,END OF DATA ?
      BNE LOOP4
      JMP RESET ,END

```

```

* THIS IS THE DELAY SUBROUTINE

```

```

DELAY LDA #09 ,FIRST COUNTER
HERE LDAB #FF ,SECOND COUNTER
HERE1 DEC B
      BNE HERE1
      DEC A
      BNE HERE
      RTS

```

```

*
END

```



### 13.1.3 IBM personal computer program for microprocessor communication

```

10
20
30 This is the IBM-PC Basic program to transmit and receive data with the
40 MC6802-D5.
50
60 Programmers Ron Larson, Peter Clark
70
80 CLS: KEY OFF
90 INPUT "Download program (d) or upload data (u) ";KS
100 IF KS="d" THEN 160
110 IF KS="u" THEN 540
120 GOTO 90
130
140
150
160 Subprogram to transfer ASCII codes to the MC6802-D5 for program download.
170
180
190
200 AS="0123456789ABCDEF"
210 INPUT "Enter the file name for downloading":FILENAME$
220 PRINT "***** Start D5 processing incoming program *****":PRINT "Type E800 GO
230 INPUT "Are you ready ":RS
240 IF LEFT$(RS,1)="y" THEN 250 ELSE 230
250 PRINT "Downloading commences..."
260 OPEN FILENAME$ FOR INPUT AS #1
270 OPEN "COM1:9600,N,8,1,RS,CS,DS,CD" AS #2
280 IF EOF(1) THEN 500
290 LINE INPUT #1, STINS: PRINT STINS:" "
300 IF (LEFT$(STINS,4)<>" S1") THEN 280
310
320 Skip first two blanks and 2 characters. Get length of STINS into L.
330 Send length of string as the first byte for processor (L-1)
340
350 SL$=MID$(STINS,5,1): SR$=MID$(STINS,6,1): GOSUB 480: L=L-1
360 PRINT #2, CHR$(L-1): "this is length of current line
370
380 Print line converting every two hex characters skipping last one
390 which is the checksum. J is position in string STINS.
400
410 FOR I=1 TO L-1:J=7+(I-1)*2:SL$=MID$(STINS,J,1):SR$=MID$(STINS,J+1,1)
420 GOSUB 480: PRINT #2, CHR$(D):
430 NEXT
440 GOTO 280
450
460 subroutine to return decimal from two hex characters
470
480 D=(INSTR(AS,SR$)-1+(INSTR(AS,SL$)-1)*16)
490 RETURN
500 PRINT #2, CHR$(255):PRINT CHR$(7)
510 PRINT " ... done."
520 CLOSE
530 END
540 INPUT "Target file for data transfer on PC ":FS
550 OPEN FS FOR OUTPUT AS #2
560 PRINT "Enter limits as decimal count of memory location (E000=1)"
570 INPUT "Lower address limit (from base e E000)":V
580 INPUT "Upper limit " :W
590 PRINT "Stored address range is ";HEX$(V+57343!);" to ";HEX$(W+57343!)
600 INPUT "Are you sure ":OS

```

```
610 IF LEFT$(Q$,1)="n" THEN 570
620 IF LEFT$(Q$,1)<>"y" THEN 600
630
640
650
660 This subprogram accepts data from MC6802-D5 via standard RS-232
670
680
690 PRINT "***** Begin D5 data dump program sequence *****"
700 PRINT "Uploading commences....": PRINT "Type E850 GO on D5 kit"
710 I=0
720 DIM X(1024)
730 DIM S$(1024)
740 OPEN"COM1:9600,n,8,1,cs,ds,cd",AS #1
750 FOR I=1 TO 1024
760 S$(I)=INPUT$(1,#1)
770 X(I)=ASC(S$(I))
780 NEXT I
790 PRINT "done."
800 FOR N=V TO W
810 PRINT #2,N,X(N),HEX$(N+57343!),HEX$(X(N))
820 NEXT N
830 CLOSE
840 PRINT CHR$(7)
850 END
```

## 13.2 Digitization of Impact Program

NAM GR/ACIA.A19

\* THIS PROGRAM ATTEMPTS TO READ THE AMPLIFIED GRAIN  
 \* IMPACT ON THE SENSOR, DIGITIZE IT, AND THEN SEND  
 \* THE INFORMATION TO THE IBM/PC VIA THE ACIA

\* << SYSTEM >>

\*  
 MNPTR EQU \$E419  
 HEXBUF EQU \$E42C  
 DISBUF EQU \$E41D  
 PUT EQU \$F08B  
 DYSCOD EQU \$F120  
 UIRQV EQU \$E43C  
 \*

\*  
 ORG \$E000  
 CLI  
 LDX #INTER  
 STX UIRQV  
 LDX #CYCLIC  
 STX MNPTR  
 LDX #\$6D78 ;DISPLAY ST  
 STX DISBUF  
 LDX #\$7750 ;DISPLAY AR  
 STX DISBUF+2  
 LDX #\$7840 ;DISPLAY T-  
 STX DISBUF+4  
 JMP PUT

\*  
 CYCLIC NOP

RTS  
 INTER SEI

LDX #\$E100 ;START DATA SPACE  
 LOOP LDAA \$00 ;READ A/D  
 STAA 0,X  
 INX  
 CPX #\$E400  
 BNE LOOP  
 LDX #\$7954 ;DISPLAY E  
 STX DISBUF  
 LDX #\$5E00 ;DISPLAY D  
 STX DISBUF+2  
 LDX #\$0000 ;NO DISPLAY  
 STX DISBUF+4  
 RTI

\* THIS IS THE ACIA PORTION

\*  
 CR EQU \$E700 CONTROL/STATUS REG  
 DR EQU \$E701 DATA REG  
 \*

ORG \$E080  
 LDAA #\$03 MASTER RESET  
 STAA CR

\*  
 LDAA #\$15 /16, 8BIT, 1 ST,NPR,RTS\*LOW,TRAN I DIS  
 STAA CR  
 \*

\*  
 LDX #\$E100 ;BEGINNING OF DATA  
 LOOP2 LDAA CR CHECK TDRE  
 BITA #\$02  
 BEQ LOOP2

\*  
 AGAIN LDAA 0,X ;SEND DATA TO PC  
 STAA DR  
 JSR DELAY ;DELAY FOR PC TO CATCH UP  
 INX  
 CPX #\$E400 ;END OF DATA ?  
 BNE LOOP2  
 SWI ;END

\* THIS IS THE DELAY SUBROUTINE

\*  
 DELAY LDAA #\$0F ;FIRST COUNTER  
 HERE LDAB #\$FF ;SECOND COUNTER  
 HERE1 DEC B  
 BNE HERE1  
 DEC A  
 BNE HERE  
 RTS

\*  
 END

## 13.3 Impact Counting Program for Single Sensor

```

NAM CNT.SINGLE
*
* SYSTEM FOR COUNTING IMPACTS ON ONE SENSOR
*
* << SYSTEM >>
*
MNPTR EQU $E419
HEXBUF EQU $E42C
DISBUF EQU $E41D
PUT EQU $FOBB
DYSCOD EQU $F120
UIRQV EQU $E43C ; INTERRUPT VECTOR
KYFLG EQU $E41C
CNT EQU $E000;COUNTER
*
*
ORG $E001
CLR CNT ; START WITH COUNTER=0
CLI ; CLEAR INTERRUPT MASK
LDX #INTER
STX UIRQV
LDX #CYCLIC
STX MNPTR
JSR DYSCOD
JMP PUT
*
CYCLIC NOP
LDAB KYFLG ; NO KEY PRESSED, CONTINUE
BEQ RTS ; ELSE END
JSR DIS
RTS RTS
INTER INC CNT ; ON INTERRUPT, INCREASE COUNT
RTI
DIS LDAA CNT
SEI
STAA HEXBUF+2 ; DISPLAY COUNT
JSR DYSCOD
CLR KYFLG
RTS
END

```

## 13.4 Impact Counting Program for Multiple Sensors

NAM MULT

\*  
 \* THIS PROGRAM MERELY COUNTS THE NUMBER OF IMPACTS ON EACH  
 \* OF FOUR SENSORS  
 \* THE NUMBERS ARE STORED IN MEMORY LOCATIONS DIST  
 \* THROUGH DIST+7 IN TWO BYTE ARRANGEMENTS.

\*\*\*\*\*

\* ADDRESS EQUATES

\*  
 \*\*\*\*\*

\* INTERRUPT VECTOR

\*  
 UIRQV EQU \$E43C

\* PIA EQUATES

\*  
 DA EQU \$E480

CRA EQU \$E481

DB EQU \$E482

CRB EQU \$E483

\* MONITOR RAM

\*  
 MNPTR EQU \$E419

DISBUF EQU \$E41D

\* MONITOR ROUTINES

\*  
 PUT EQU \$F0BB

\* COUNTER VARIABLES

\*  
 X1 EQU \$00

XY EQU \$02

\*\*\*\*\*

\* PROGRAM INITIALIZATION

\*  
 \*\*\*\*\*

ORG \$0010

DIST RMB 8 ; COUNTERS FOR SENSORS

\* PROGRAM BEGINS

\*  
 ORG \$E888

SEI ; PREVENT INTERRUPTS WHILE INITIALIZING

```

*
* SET UP THE PIA
*
    LDX #IHNDLR
    STX UIRQV
    CLR CRA
    CLR CRB
    CLR DA ;SIDE A TO BE ALL INPUTS
    LDA A #%00001101
    STA A CRA
    STA A CRB

*
* CLEAR VARIABLES
*
    CLR DIST
    CLR DIST+1
    CLR DIST+2
    CLR DIST+3
    CLR DIST+4
    CLR DIST+5
    CLR DIST+6
    CLR DIST+7

*
* INITIAL START-UP
*
    LDX #$0050
    STX DISBUF
    LDX #$1C54
    STX DISBUF+2
    LDX #$0000
    STX DISBUF+4
    LDX #CYCLIC
    STX MNPTR
    CLI ;CLEAR THE INTERRUPT MASK
    JMP PUT ;GO TO PUT ROUTINE

*
* CYCLIC PART
*
CYCLIC NOP
END RTS
*****

*
* INTERRUPT HANDLING ROUTINE
*
*****
IHNDLR LDA A CRB ;DID S1 OR S2 CAUSE INTERRUPT?
    BITA #%10000000 ;CHECK IF S1
    BNE S1
    BITA #%01000000 ;CHECK IF S2
    BNE S2
    BRA IHNDL2 ;TRY A SIDE

```

```

*
S1    LDAA DB
      LDAA #$FF          ;MORE THAN ONE BYTE FULL ?
      CMPA DIST+1
      BNE NO
      INC DIST
NO    INC DIST+1        ;HIGH BYTE
      RTI

*
S2    LDAA DB
      LDAA #$FF
      CMPA DIST+3
      BNE NO2
      INC DIST+2
NO2   INC DIST+3
      RTI

*
IHNDL2 LDAA CRA          ;A SIDE, DID S1 OR S2 CAUSE INTERRUPT?
       BITA #%10000000 ;CHECK IF S1
       BNE S1A
       BITA #%01000000 ;CHECK IF S2
       BNE S2A
       RTI

*
S1A   LDAA DA
      LDAA #$FF
      CMPA DIST+5
      BNE NO3
      INC DIST+4
NO3   INC DIST+5
      RTI

*
S2A   LDAA DA
      LDAA #$FF
      CMPA DIST+7
      BNE NO4
      INC DIST+6
NO4   INC DIST+7
      RTI

*
      END

```



13.5 Field Test Program

NAM LAB

```

* THIS PROGRAM MERELY COUNTS THE NUMBER OF IMPACTS ON EACH
* OF FOUR SENSORS MOUNTED ON THE STRAW WALKER ASSEMBLY AT
* THE FARM. THE NUMBERS ARE STORED IN MEMORY LOCATIONS DIST
* THROUGH DIST+7 IN TWO BYTE ARRANGEMENTS.

```

\*\*\*\*\*

ADRESS EQUATES

\*\*\*\*\*

\* INTERRUPT VECTOR

UIRQV EQU \$E43C

\* PIA EQUATES

```

DA EQU $E480
CRA EQU $E481
DB EQU $E482
CRB EQU $E483

```

\* MONITOR RAM

```

MNPTR EQU $E419
DISBUF EQU $E41D

```

\* MONITOR ROUTINES

PUT EQU \$FOBB

\* COUNTER VARIABLES

```

X1 EQU $00
XY EQU $02

```

\*\*\*\*\*

\* PROGRAM INITIALIZATION

\*\*\*\*\*

```

ORG $0010
DIST RMB 8 ;COUNTERS FOR SENSORS

```

\* PROGRAM BEGINS

```

ORG $E888
SEI ;PREVENT INTERRUPTS WHILE INITIALIZING

```

\* SET UP THE PIA

```

LDX #IHNDLR
STX UIRQV
CLR CRA
CLR CRB
CLR DA ;SIDE A TO BE ALL INPUTS
LDA A #%00001101
STA A CRA
STA A CRB
* CLEAR VARIABLES
*
CLR DIST
CLR DIST+1
CLR DIST+2
CLR DIST+3
CLR DIST+4
CLR DIST+5
CLR DIST+6
CLR DIST+7
*
* INITIALIZE COUNTERS
*
LDAA #$FF
STAA X1
LDAA #$20
STAA XY
*
* INITIAL START-UP
*
LDX #$0050
STX DISBUF
LDX #$1C54
STX DISBUF+2
LDX #$0000
STX DISBUF+4
LDX #CYCLIC
STX MNPTR
CLI ;CLEAR THE INTERRUPT MASK
JMP PUT ;GO TO PUT ROUTINE
*
* CYCLIC PART
*
CYCLIC NOP
DEC X1
BNE END
COM X1
DEC XY
BNE END
SEI ;TIME UP
LDX #$0079 ;DISPLAY END
STX DISBUF
LDX #$545E
STX DISBUF+2
END RTS

```

```

*
* INTERRUPT HANDLING ROUTINE
*

```

```

*****
IHNDLR LDAA CRB          ;DID S1 OR S2 CAUSE INTERRUPT?
      BITA #%10000000 ;CHECK IF S1
      BNE S1
      BITA #%01000000 ;CHECK IF S2
      BNE S2
      BRA IHNDL2       ;TRY A SIDE
*
S1      LDAA DB
      LDAA #$FF          ;MORE THAN ONE BYTE FULL ?
      CMPA DIST+1
      BNE NO
      INC DIST
NO      INC DIST+1       ;HIGH BYTE
      RTI
*
S2      LDAA DB
      LDAA #$FF
      CMPA DIST+3
      BNE NO2
      INC DIST+2
NO2     INC DIST+3
      RTI
*
IHNDL2 LDAA CRA          ;A SIDE, DID S1 OR S2 CAUSE INTERRUPT?
      BITA #%10000000 ;CHECK IF S1
      BNE S1A
      BITA #%01000000 ;CHECK IF S2
      BNE S2A
      RTI
*
S1A     LDAA DA
      LDAA #$FF
      CMPA DIST+5
      BNE NO3
      INC DIST+4
NO3     INC DIST+5
      RTI
*
S2A     LDAA DA
      LDAA #$FF
      CMPA DIST+7
      BNE NO4
      INC DIST+6
NO4     INC DIST+7
      RTI
*
      END

```

14. APPENDIX III DATA

Table 14.1 Separation Data (adapted from Boyce et al. 1974)

Tray #	Collection (% total)	Separation Rate (kg/m)	Remaining (% total)
(start)			36.00
1	1.18	3.9	34.82
2	6.34	20.8	28.48
3	7.62	25.0	20.86
4	6.91	22.7	13.95
5	5.23	17.2	8.72
6	3.56	11.7	5.16
7	2.56	8.4	2.60
8	0.68	2.2	1.92
9	0.59	1.9	1.30

Table 14.2 Sensor Orientation Test Data.

10M Time Cnt (s) (#)	45B Time Cnt (s) (#)	45M Time Cnt (s) (#)	45T Time Cnt (s) (#)	808		80M		80T		45GSC		45GSCW		MULT			
				Time Cnt (s) (#)	Time Cnt (s) (#)	Time Cnt (s) (#)	Time Cnt (s) (#)	Time Cnt (s) (#)	Time Cnt (s) (#)	Time Cnt (s) (#)	Time Cnt (s) (#)	Time Cnt (s) (#)	Time Cnt (s) (#)	Time Cnt (s) (#)	Time Cnt (s) (#)	Time Cnt (s) (#)	Time Cnt (s) (#)
16.22 109	10.05 94	10.42 102	5.74 99	9.23 103	15.40 112	8.30 101	2.89 77	3.01 82	2.91 88	3.01 82	2.89 77	3.01 82	2.91 88	15 18 27 28			
2.72 88	2.44 81	2.57 87	9.26 103	4.11 100	3.85 86	2.22 83	3.28 78	3.42 83	1.18 76	3.42 83	3.28 78	3.42 83	1.18 76	12 23 19 22			
6.67 108	5.02 94	4.09 91	9.17 94	2.45 79	6.37 109	5.70 100	3.35 84	3.49 89	6.00 97	3.49 89	3.35 84	3.49 89	6.00 97	23 28 31 38			
2.16 88	16.50 100	11.07 99	2.10 78	12.92 96	2.25 86	3.19 102	3.53 72	3.68 77	1.86 88	3.53 72	3.53 72	3.68 77	1.86 88	27 25 16 20			
5.38 100	2.17 77	2.31 85	1.91 77	2.35 84	4.57 94	5.30 99	3.78 88	3.94 94	1.84 97	3.78 88	3.78 88	3.94 94	1.84 97	31 24 37 5			
7.01 99	10.04 93	6.39 98	5.56 98	2.74 93	2.17 85	9.12 107	3.88 74	4.04 79	2.49 86	3.88 74	3.88 74	4.04 79	2.49 86	21 17 12 36			
8.87 112	3.09 97	2.61 87	11.25 98	1.85 80	12.08 101	2.34 78	3.89 80	4.05 85	2.42 79	3.89 80	3.89 80	4.05 85	2.42 79	20 12 17 20			
3.76 90	5.96 89	13.69 105	21.46 96	3.09 95	11.00 102	2.78 95	4.41 80	4.59 85	3.70 91	4.41 80	4.41 80	4.59 85	3.70 91	17 13 28 33			
4.54 95	2.19 84	13.91 110	4.90 90	8.86 93	1.99 76	6.75 93	4.94 78	5.15 83	3.37 101	4.94 78	4.94 78	5.15 83	3.37 101	26 21 32 22			
2.04 83	7.70 91	2.60 85	2.27 84	5.80 81	2.00 82	12.08 100	5.29 89	5.51 95	3.18 94	5.29 89	5.29 89	5.51 95	3.18 94	33 12 19 30			
2.05 74	2.03 75	2.31 81	5.01 90	6.63 110	2.40 76	13.34 128	5.98 82	6.23 87	19.18 98	6.23 87	5.98 82	6.23 87	19.18 98	24 28 17 29			
2.05 85	5.37 93	3.58 98	5.71 98	8.18 110	7.48 98	9.98 99	6.2 84	6.46 89	14.17 99	6.2 84	6.2 84	6.46 89	14.17 99	30 16 22 31			
6.59 106	19.48 94	9.49 110	7.44 94	2.32 90	12.98 105	8.21 112	6.63 89	6.91 95	16.09 94	6.63 89	6.63 89	6.91 95	16.09 94	11 34 21 28			
2.54 82	2.60 77	4.68 98	16.48 101	2.41 80	2.88 84	2.09 82	8.63 89	8.99 95	10.86 99	8.63 89	8.63 89	8.99 95	10.86 99	16 37 20 26			
6.04 103	2.24 88	2.56 98	6.15 96	2.14 82	6.35 100	5.11 106	9.55 92	9.95 98	7.46 98	9.55 92	9.55 92	9.95 98	7.46 98	22 28 39 9			
5.42 104	4.03 91	3.16 97	1.84 78	6.86 94	2.01 78	2.30 87	9.93 79	10.34 84	5.41 90	9.93 79	9.93 79	10.34 84	5.41 90	21 16 17 36			
2.08 79	2.39 86	12.27 111	6.77 82	7.13 82	2.43 83	1.59 80	12.94 93	13.48 99	5.12 93	12.94 93	12.94 93	13.48 99	5.12 93	17 29 22 25			
9.78 108	5.60 86	5.26 104	16.37 97	3.98 89	5.18 97	9.35 114	16.64 91	17.33 97	3.69 84	16.64 91	16.64 91	17.33 97	3.69 84	17 19 21 27			
5.59 95	11.53 88	1.77 83	3.45 89	12.95 105	15.24 110	3.31 95	19.26 99	20.06 105	5.29 93	19.26 99	19.26 99	20.06 105	5.29 93	37 15 12 29			
7.60 100	4.95 94	15.24 113	6.22 94	4.67 97	10.06 101	3.32 105	6.65 117	20.45 111	4.11 84	6.65 117	6.65 117	20.45 111	4.11 84	23 31 17 13			
2.13 82	4.85 86	6.84 101	1.77 78	19.61 96	2.57 93	2.92 96	6.65 117		3.39 91	2.57 93	2.57 93		3.39 91	19 22 16 34			
6.48 96	9.63 94	2.23 80	6.23 85	3.06 82	4.36 93	2.92 96			9.93 97	4.36 93	4.36 93		9.93 97	25 27 23 27			
6.89 105	9.59 94	9.85 112	3.61 90	16.45 121	4.30 96	14.05 102			2.32 82	4.30 96	4.30 96		2.32 82	16 19 26 21			
10.43 111	1.84 77	2.67 79	13.41 100	1.91 83	12.74 99	13.99 115			2.72 81	12.74 99	12.74 99		2.72 81	24 22 18 17			

Table 14.3 Desired Laboratory Test Throughput Data.

Grain (kg/min)	Straw (kg/min)	Total (kg/min)	(t/h)	Grain/Straw
15	35	50	3.0	0.429
15	45	60	3.6	0.333
15	55	70	4.2	0.273
20	35	55	3.3	0.571
20	45	65	3.9	0.444
20	55	75	4.5	0.364
25	35	60	3.6	0.714
25	45	70	4.2	0.556
25	55	80	4.8	0.455
30	35	65	3.9	0.857
30	45	75	4.5	0.667
30	55	85	5.1	0.545

Table 14.4 Laboratory Separation Data.

Run #	Dry1	1	2	3	4	5	6	7	8	9	10	11	12
Grain (kg/min)	0.000	24.424	13.687	22.118	14.973	27.855	23.869	13.865	26.117	16.984	29.887	16.387	17.515
Straw (kg/min)	55.0	55.0	55.0	35.0	45.0	55.0	45.0	35.0	35.0	45.0	45.0	55.0	35.0
Tray Collect (g)	0	190	174	878	259	427	588	729	1332	1805	1531	655	1870
	1	1475	1085	3146	1636	2745	3200	2070	4840	2636	5725	1614	4128
	2	1505	1065	2655	1527	2549	2637	1588	3073	1899	3283	1604	2051
	3	2207	1350	2966	1787	3560	3110	1719	3415	2329	3507	2247	1759
	4	2190	1174	1828	1332	2867	2244	1134	2224	1562	2240	1552	1210
	5	1498	778	934	1332	1594	1277	612	1180	857	1194	849	565
	6	915	432	455	415	759	621	330	559	430	582	439	224
Bag Collect (g)	1	37	15	17	17	28	22	11	17	13	18	12	8
	2	37	18	23	19	36	32	15	31	19	30	19	14
	3	36	17	44	22	50	49	24	54	36	48	31	30
	4	8	5	24	10	15	19	11	24	12	20	10	17
Bag Collect (# kernels)	1	814	330	374	374	616	484	242	374	286	395	264	176
	2	814	396	506	418	792	704	330	682	418	660	418	308
	3	792	374	968	484	1100	1078	528	1188	792	1056	682	660
	4	176	110	528	220	330	418	242	528	264	440	220	374
Sensor Cnt (#)	1	646	377	458	543	713	440	308	403	317	426	312	247
	2	971	578	882	1770	1081	1053	489	850	709	1479	628	426
	3	717	392	900	611	855	769	542	985	732	842	631	548
	4	137	104	367	227	219	281	194	384	209	314	176	283
Tray Separation Rates (g/m)	1	n/a	2369	6869	3572	5993	6987	4520	10568	5755	12500	3524	9013
	2	n/a	2325	5797	3334	5566	5758	3402	6710	4146	7168	3502	4478
	3	n/a	2948	6476	3902	6773	6790	3753	7456	4867	7657	4906	3841
	4	n/a	2563	3991	2908	6260	4900	2476	4856	3410	4891	3389	2642
	5	n/a	3257	2039	1712	3480	2788	1336	2576	1871	2607	1854	1234
	6	n/a	943	993	906	1657	1356	721	1221	939	1271	959	489
Sensor Separation Rates (g/m)	1	n/a	3596	4368	5178	6799	4196	2937	3843	3023	4062	2976	2356
	2	n/a	4137	6314	12670	7738	7538	3500	6084	5075	10587	4495	3049
	3	n/a	2806	6442	4374	6120	5505	3880	7051	5240	6027	4517	3923
	4	n/a	744	2627	1625	1568	2011	1389	2749	1496	2248	1260	2026

Table 14.5 Separation Curve Equations and Losses.

Equation Form:  $Y = A \cdot \exp(bX)$   
 $Y$  = Separation rate (kg/m), and  
 $X$  = Distance along walker (m).

Run #	1	2	3	4	5	6	7	8	9	10	11	12
Tray Collection	11.68	8.63	33.39	14.60	33.08	29.00	16.03	36.91	21.28	37.04	21.05	25.30
	-0.660	-0.836	-1.37	-1.07	-1.14	-1.18	-1.22	-1.32	-1.21	-1.31	-1.20	-1.52
	0.800	0.891	0.983	0.953	0.891	0.949	0.983	0.971	0.951	0.979	0.959	0.914
Loss (kg)	2.89	1.04	0.567	0.723	1.27	0.963	0.461	0.746	0.635	0.776	0.551	0.257
Sensor	61.78	26.94	17.69	97.73	46.13	31.74	10.65	16.16	21.35	53.55	19.87	5.344
	-1.43	-1.25	-0.639	-1.50	-1.16	-0.963	-0.674	-0.579	-0.890	-1.13	-0.827	-0.298
	0.647	0.816	0.557	0.909	0.690	0.858	0.419	0.374	0.449	0.964	0.173	0.212
Loss (kg)	0.852	0.697	4.79	1.06	1.64	2.34	2.48	5.78	2.08	2.13	1.68	7.91
Actual Loss (kg)	8.220	4.152	3.619	3.422	6.261	4.103	2.156	2.899	2.240	4.237	3.258	1.760



Table 14.6 Field Test Data.

Run (#)	Speed (km/h)	Swath		Walker		Shoe		Expected		Feedrate (MOG) (t/h)	Walker (%)	Loss Shoe (%)	Sensor Counts			
		Grain (g)	MOG (g)	Grain (g)	MOG (g)	Grain (g)	MOG (g)	Grain (g)	MOG (g)				1	2	3	4
2	4.1	606	1182	3	1266	1	171	977	1437	5.89	0.3	0.1	11	10	1	1
3	4.1	1101	1639	3	903	2	304	807	1204	4.94	0.4	0.2	11	10	2	2
4	5.8	1271	1616	14	1060	11	211	991	1271	7.37	1.4	1.1	31	18	13	4
5	5.8	1184	1415	13	1458	2	234	1404	1692	9.81	0.9	0.2	15	16	7	12
6	7.2	1240	1400	16	1086	9	203	1134	1289	9.28	1.4	0.8	60	45	27	22
7	7.2	1304	1617	25	1242	10	255	1198	1498	10.78	2.1	0.8	42	21	25	42
8	7.2	1197	1380	15	1106	5	192	1129	1298	9.34	1.3	0.5	25	27	22	32
9	5.8	1269	1445	15	954	9	304	1107	1258	7.30	1.3	0.9	27	20	17	16
10	4.1	1345	1618	3	1039	2	184	1015	1223	5.01	0.3	0.2	21	14	5	4
11	4.1												24	24	10	4
12	5.8												25	24	22	19
13	7.2												15	17	29	45
14	4.1												17	10	4	11
15	5.8												18	21	10	9
16	7.2												46	40	65	59
17	4.1												31	24	20	6
18	5.8												20	18	17	19
19	7.2												24	20	26	7
20	7.2												36	34	32	59

15. APPENDIX IV LABORATORY AND FIELD SEPARATION CURVES

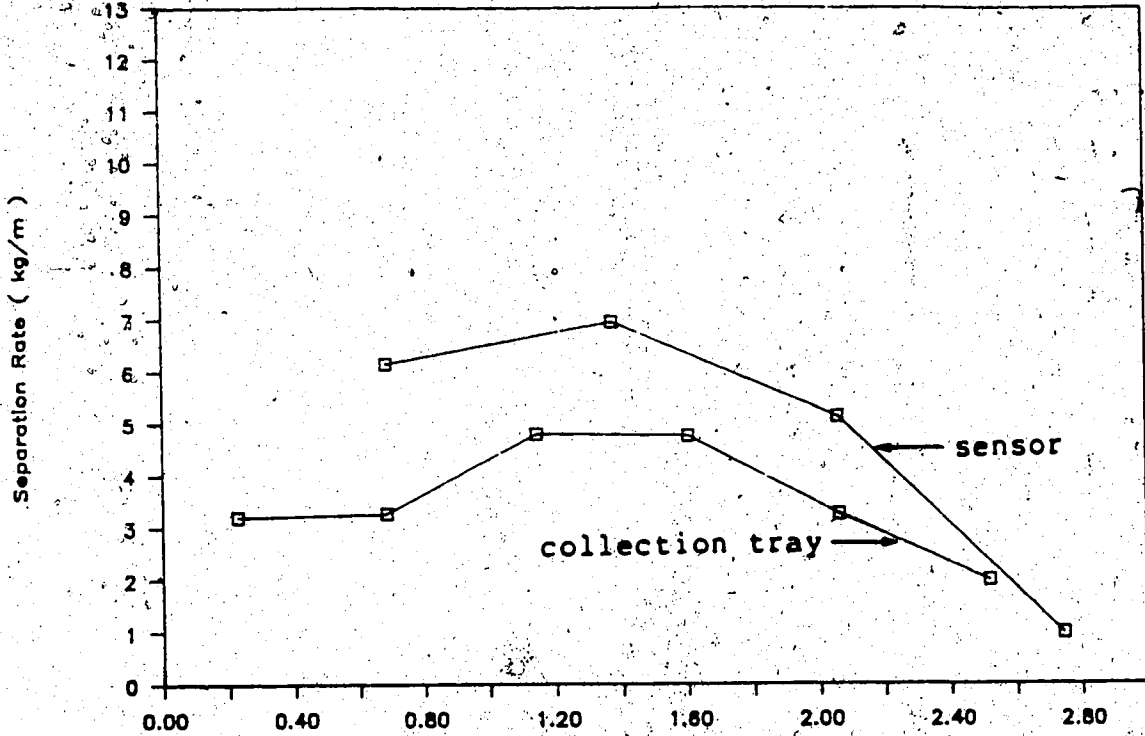


Figure 15.1 Laboratory Separation Curves. Run #1

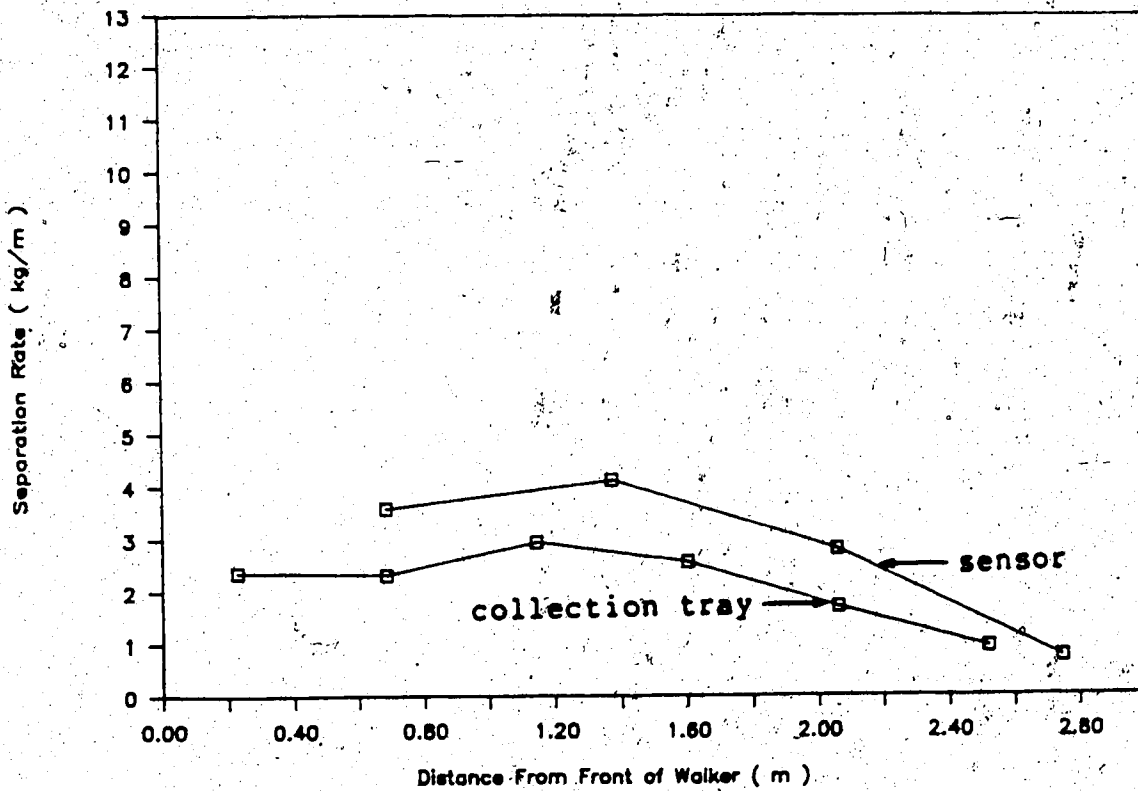


Figure 15.2 Laboratory Separation Curves. Run #2

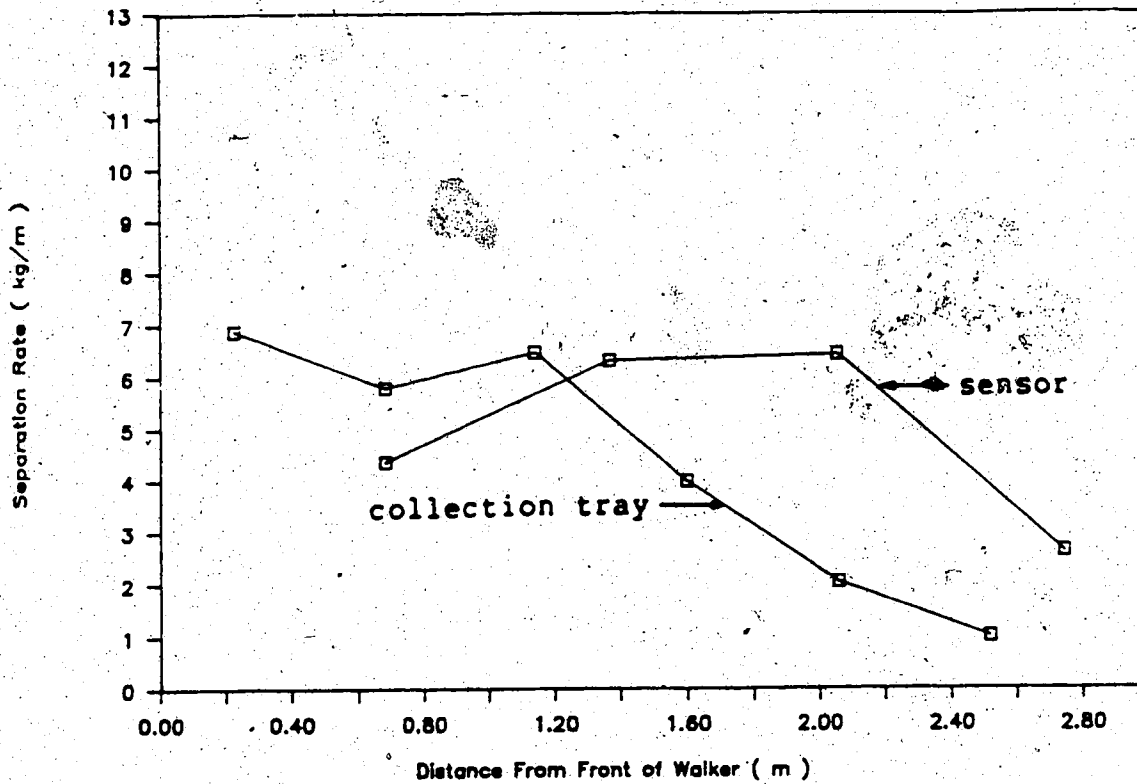


Figure 15.3 Laboratory Separation Curves. Run #3

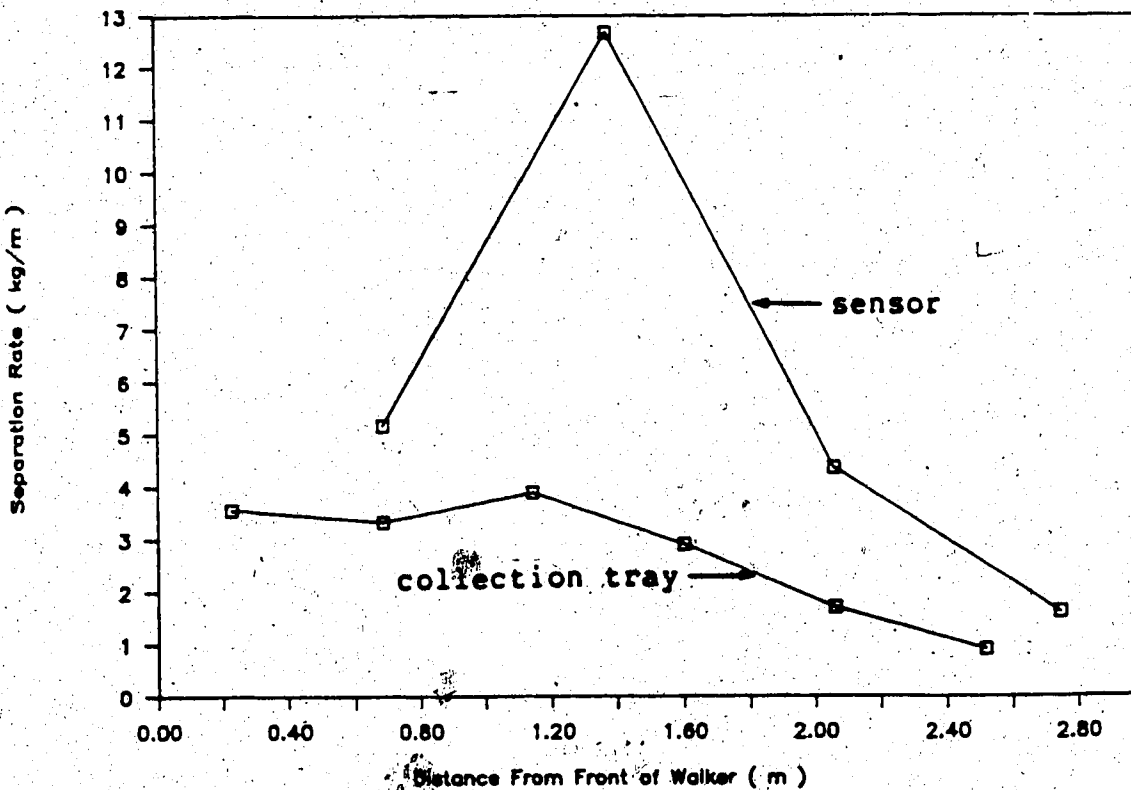


Figure 15.4 Laboratory Separation Curves. Run #4

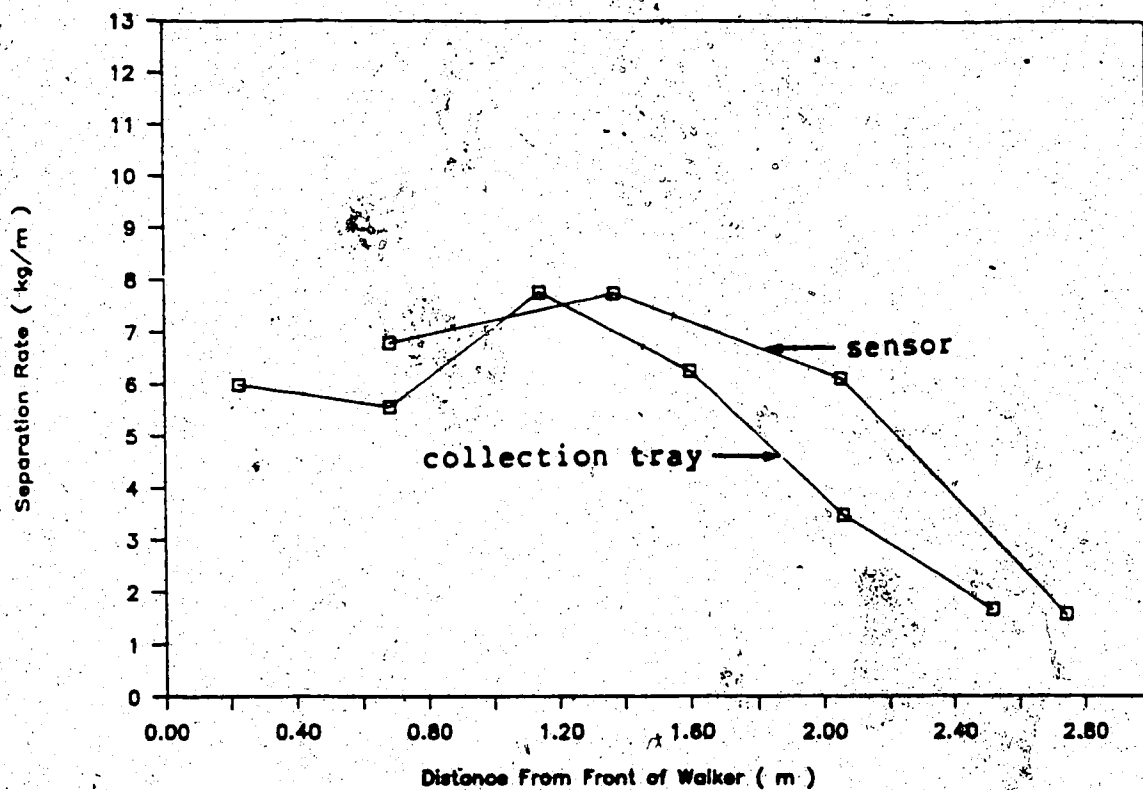


Figure 15.5 Laboratory Separation Curves. Run #5

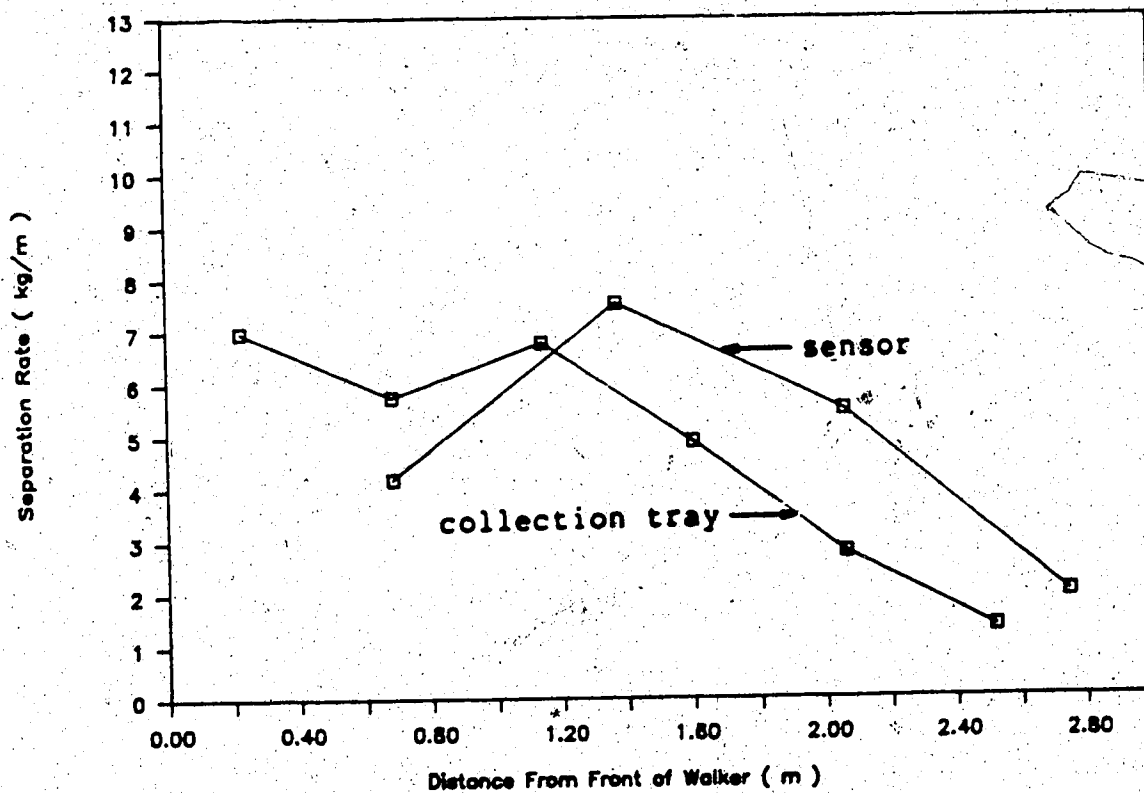


Figure 15.6 Laboratory Separation Curves. Run #6

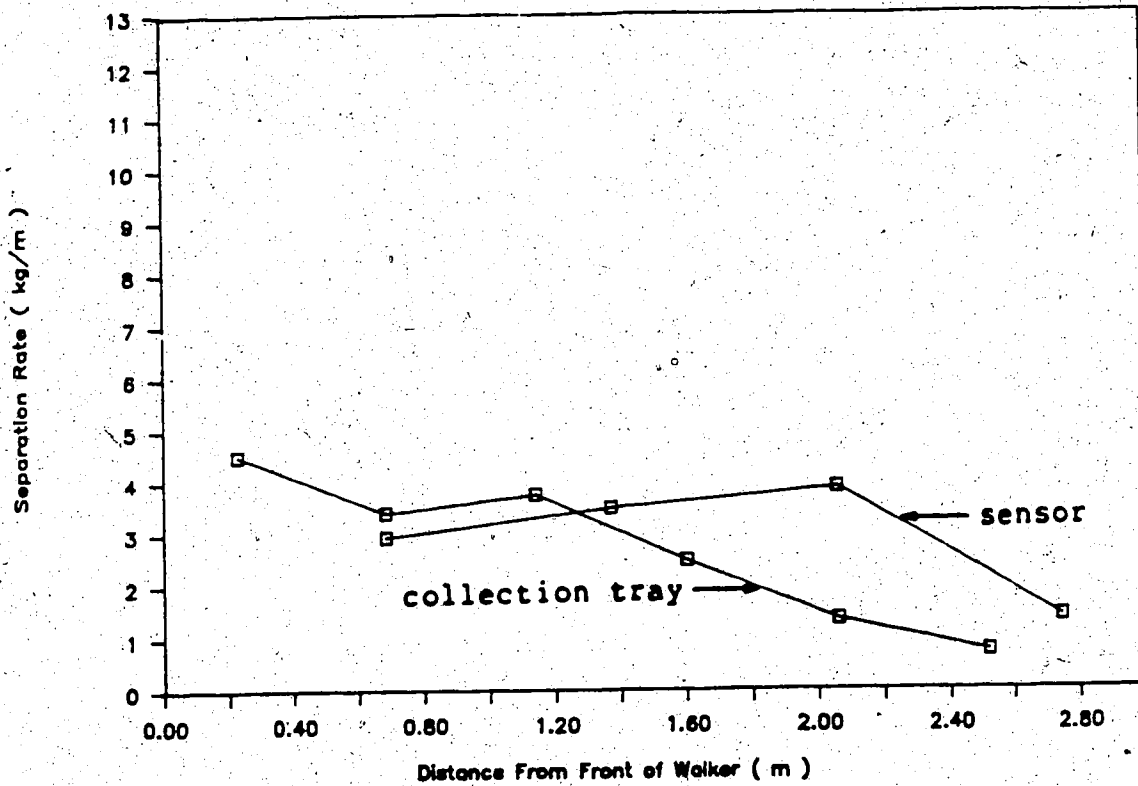


Figure 15.7 Laboratory Separation Curves. Run #7

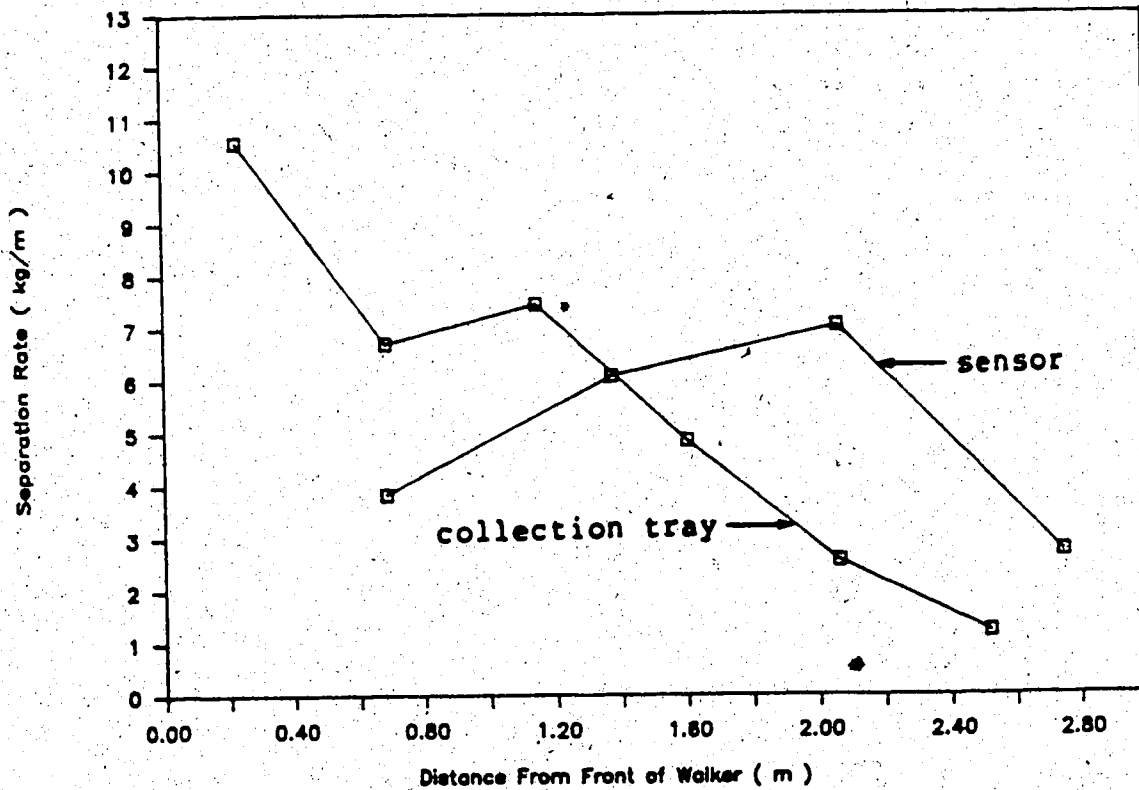


Figure 15.8 Laboratory Separation Curves. Run #8

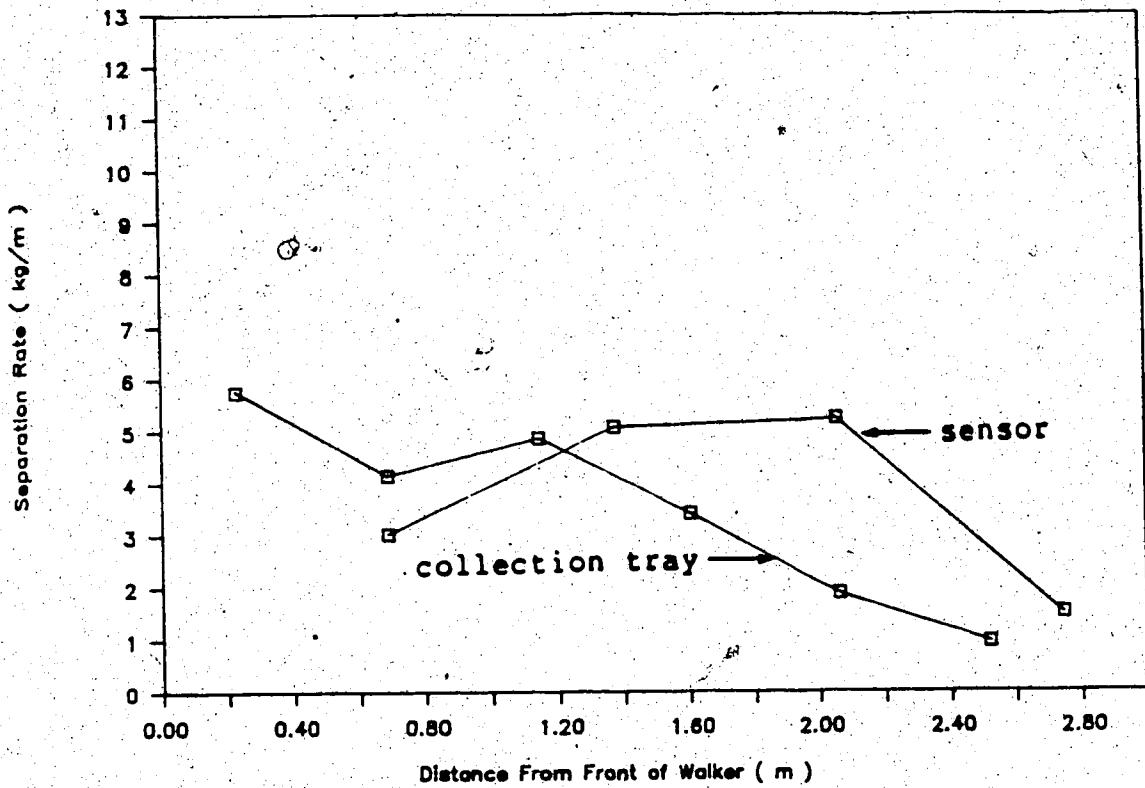


Figure 15.9 Laboratory Separation Curves. Run #9

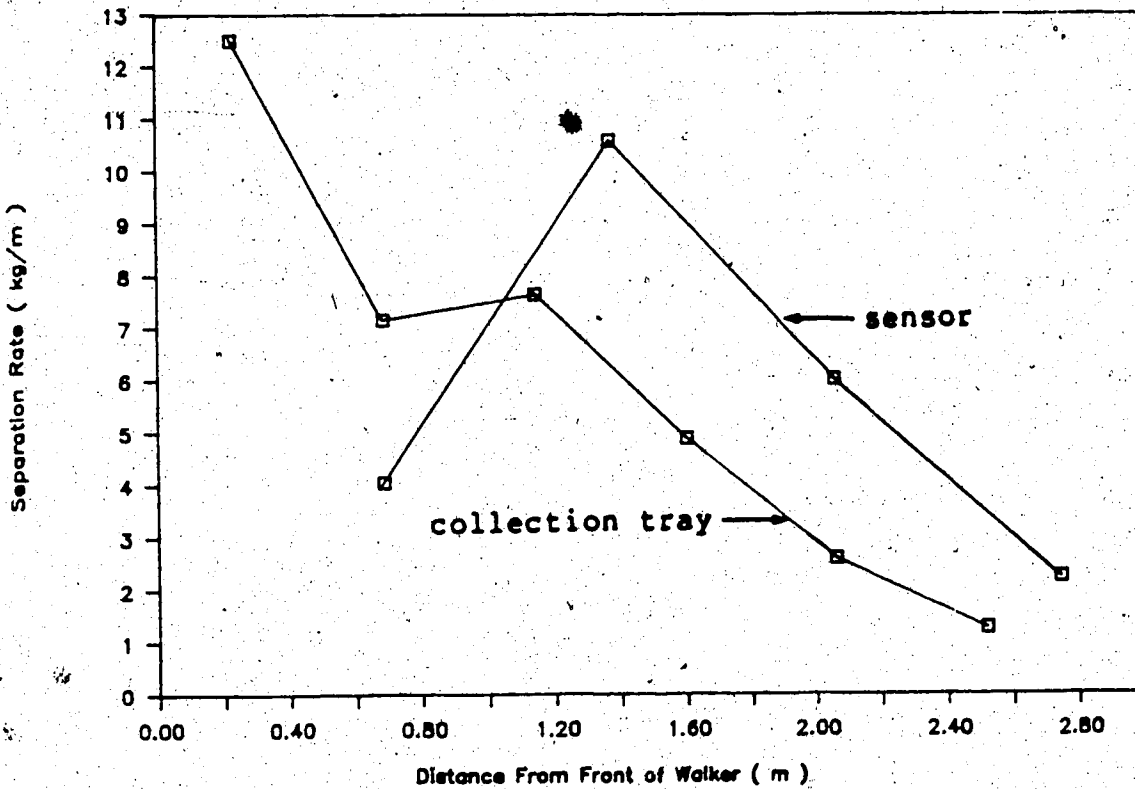


Figure 15.10 Laboratory Separation Curves. Run #10

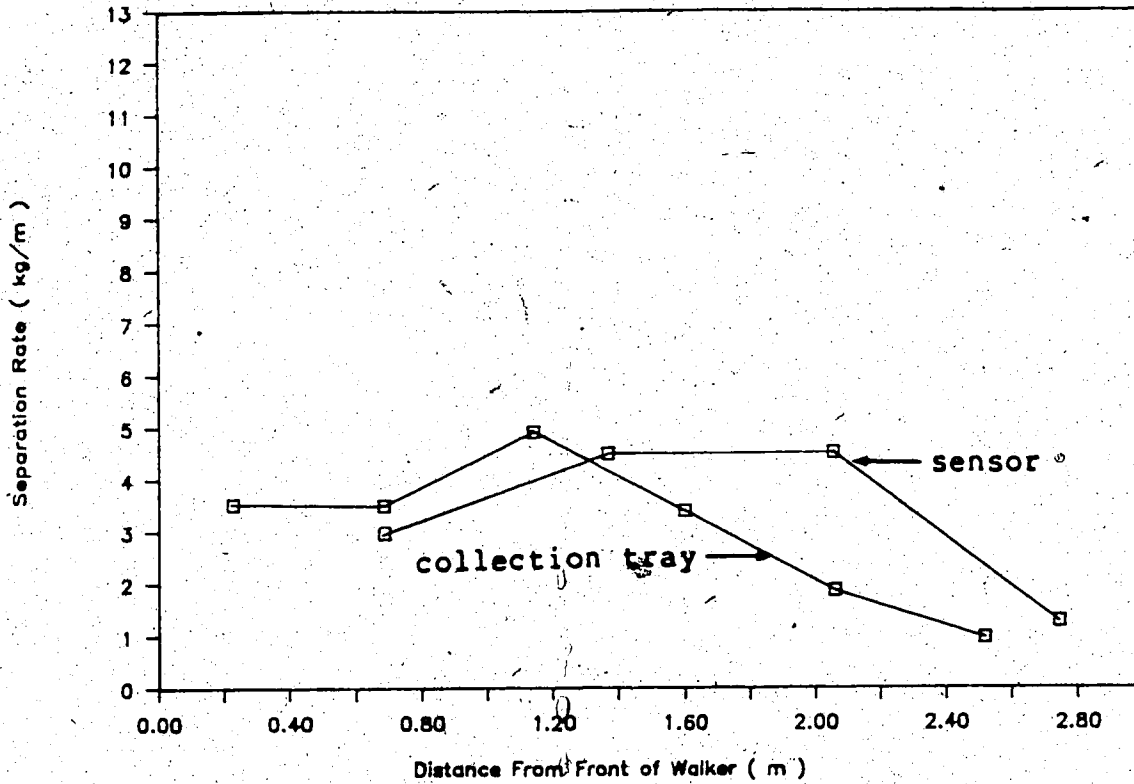


Figure 15.11 Laboratory Separation Curves. Run #11

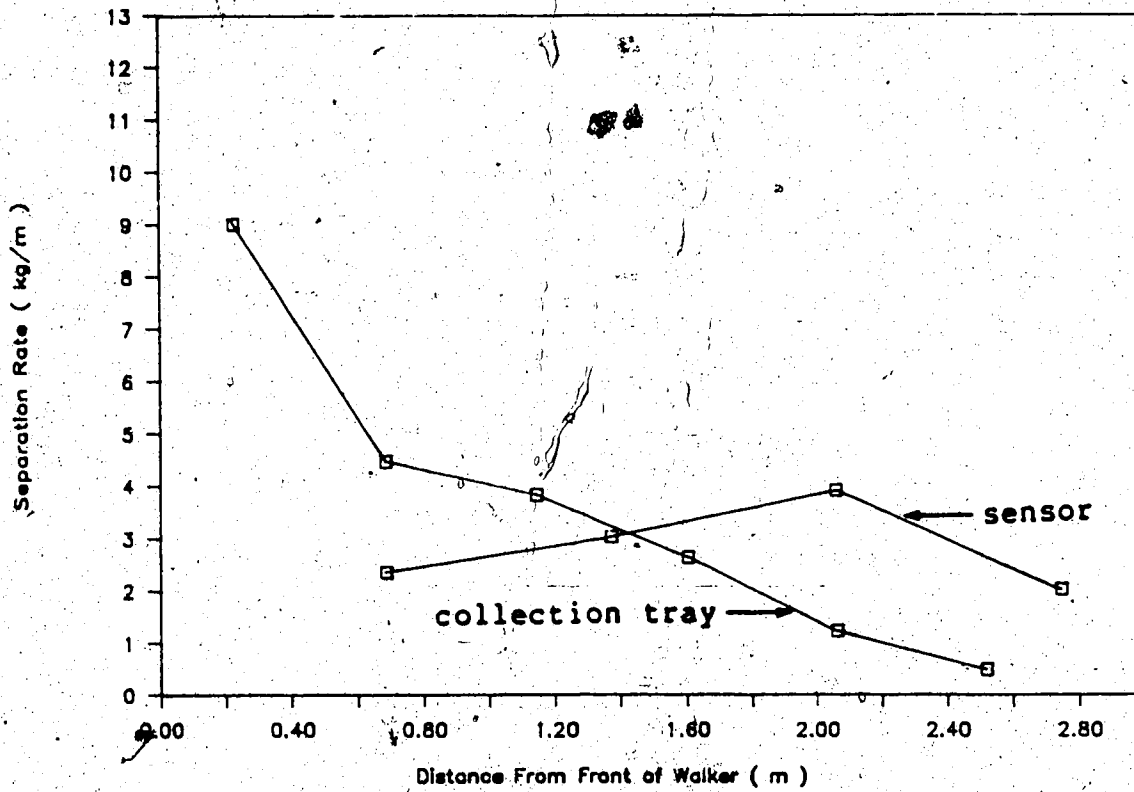


Figure 15.12 Laboratory Separation Curves. Run #12

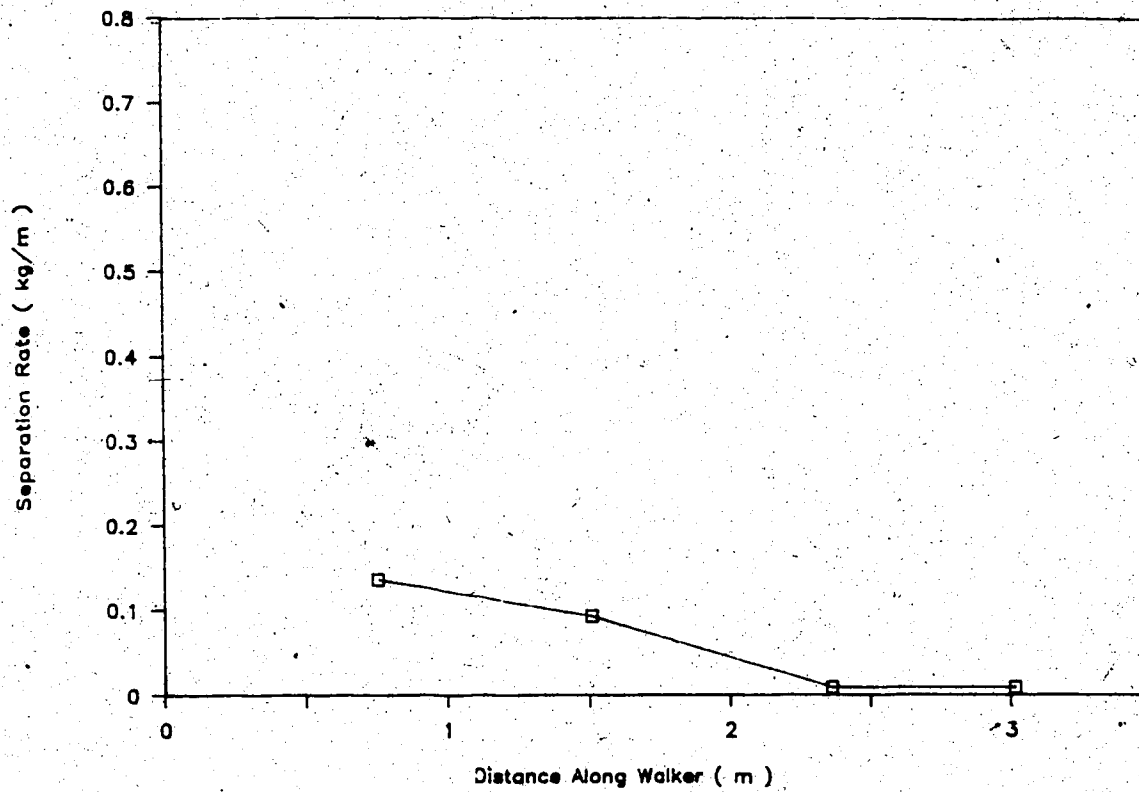


Figure 15.13 Field Separation Curve. Run #2

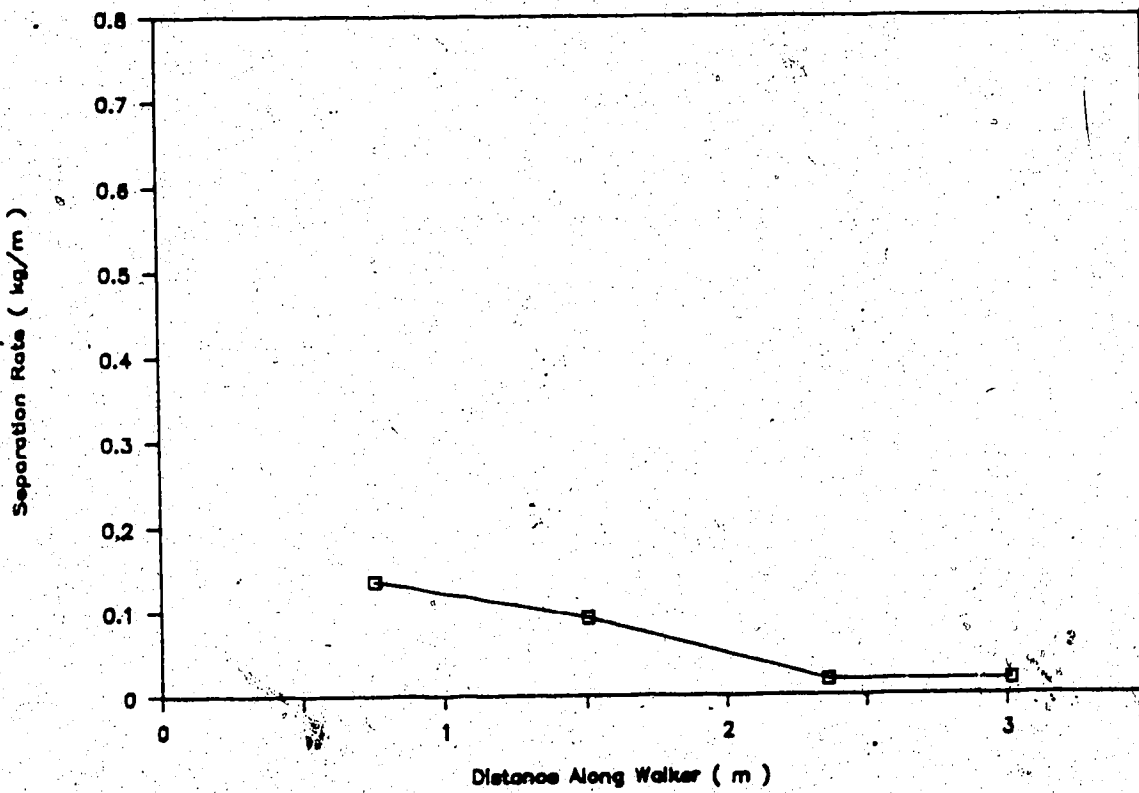


Figure 15.14 Field Separation Curve. Run #3



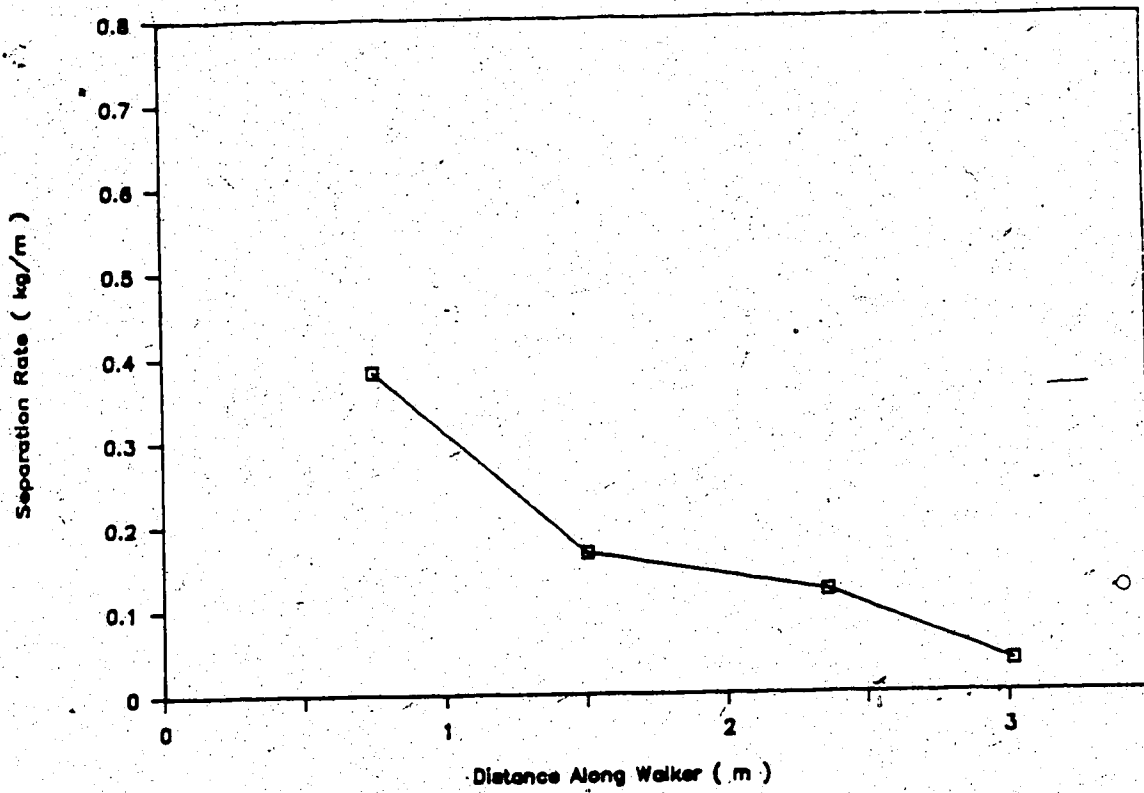


Figure 15.15 Field Separation Curve. Run #4

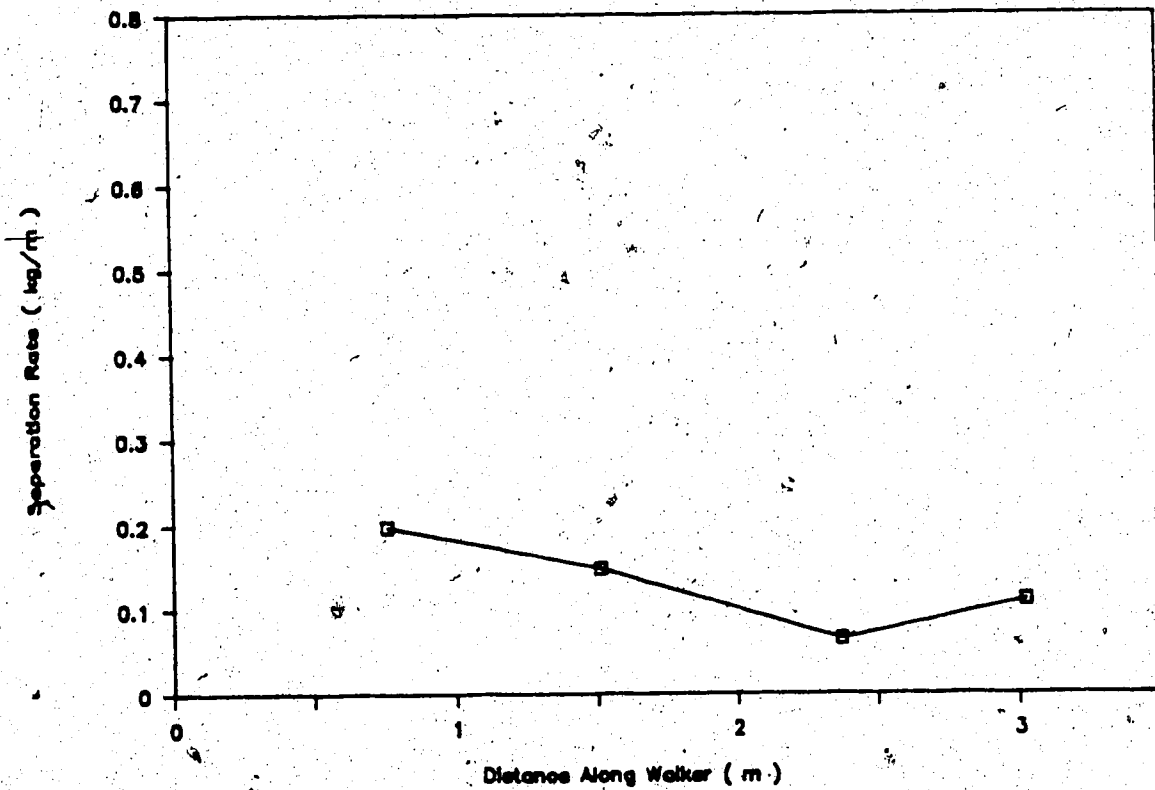


Figure 15.16 Field Separation Curve. Run #5

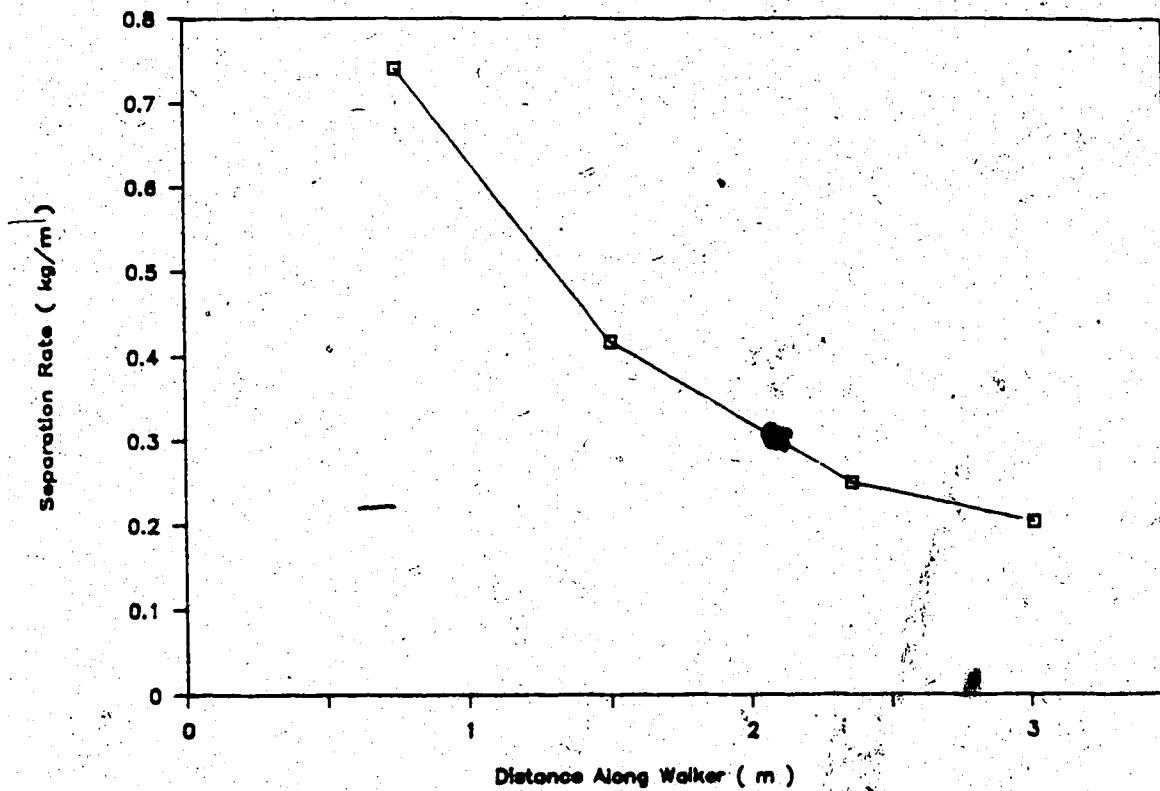


Figure 15.17 Field Separation Curve. Run #6

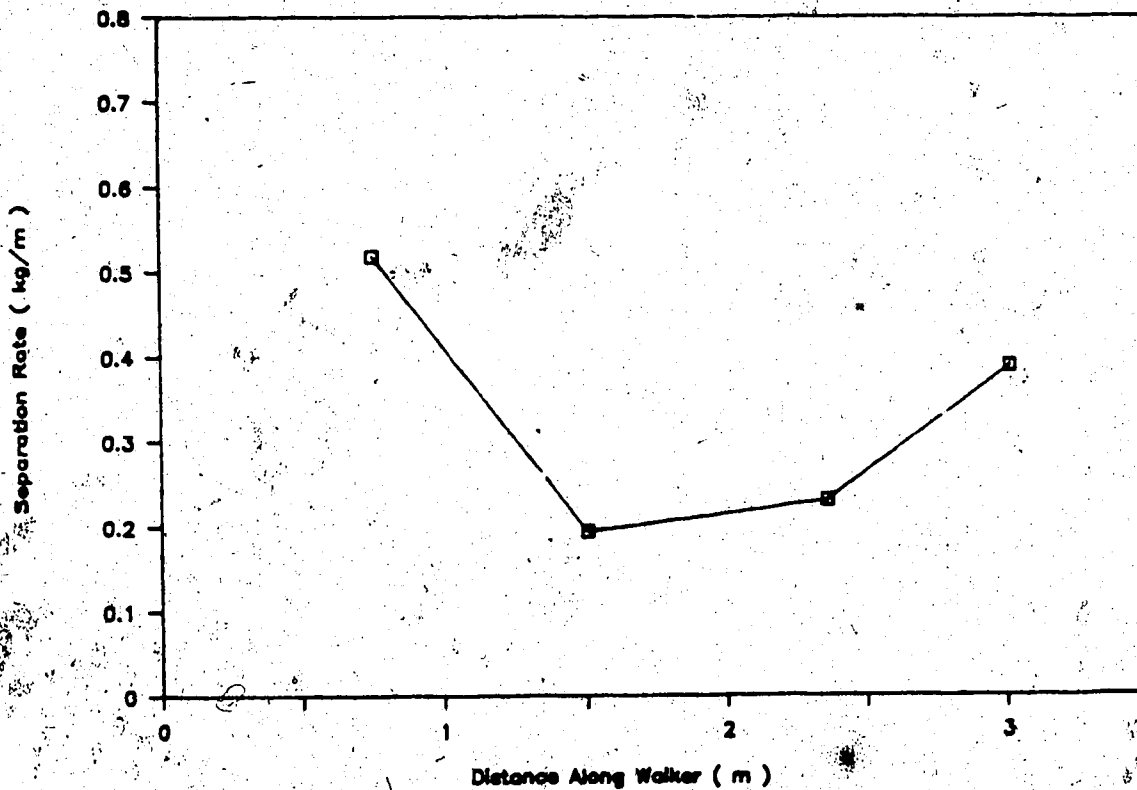


Figure 15.18 Field Separation Curve. Run #7

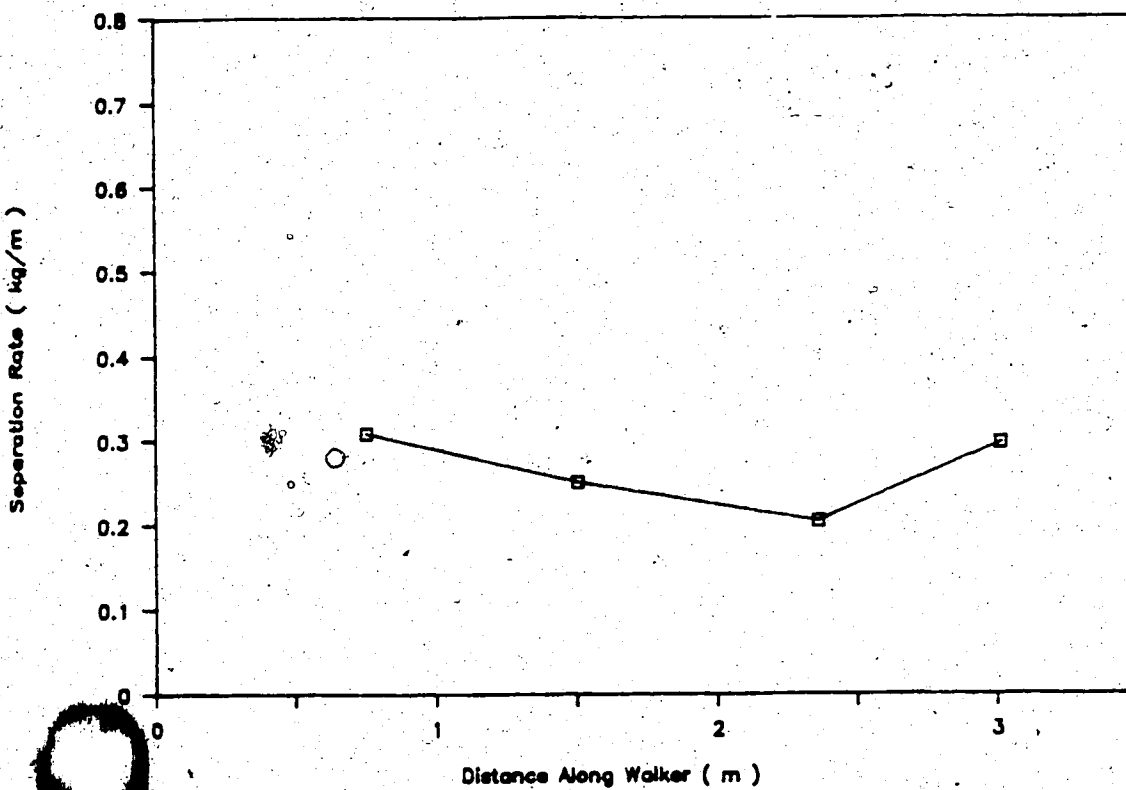


Figure 15.19 Field Separation Curve. Run #8

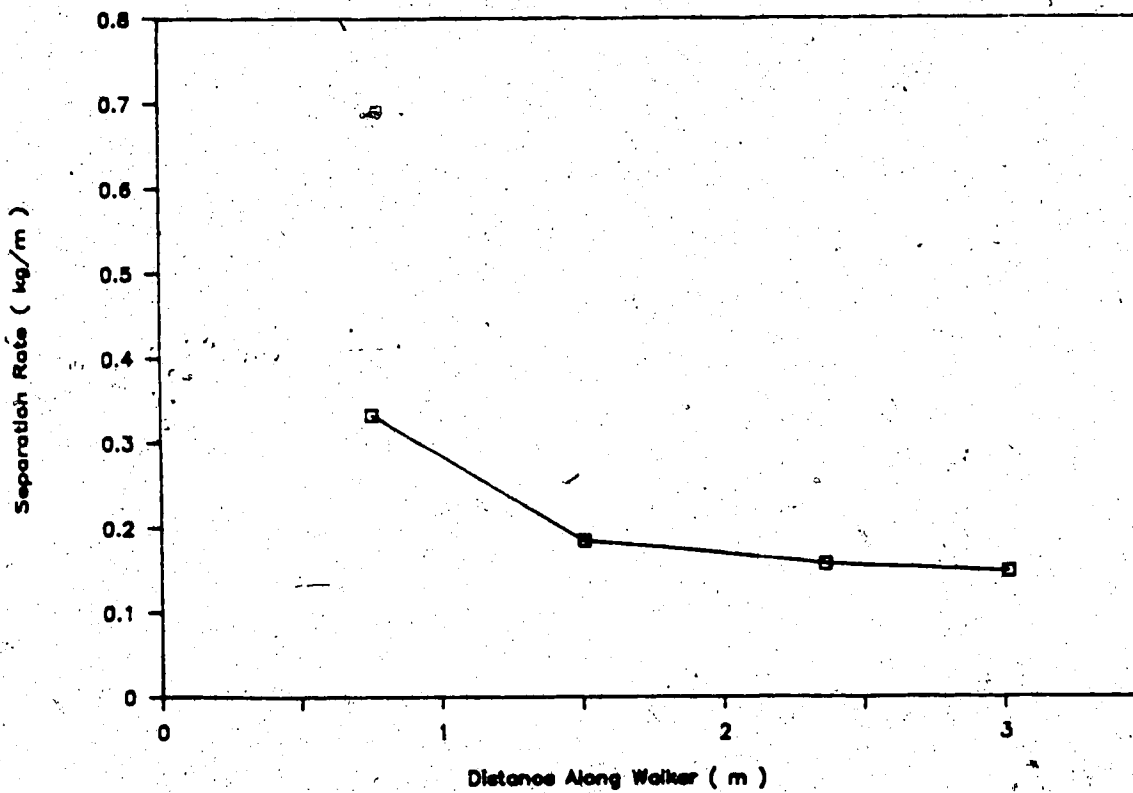


Figure 15.20 Field Separation Curve. Run #9

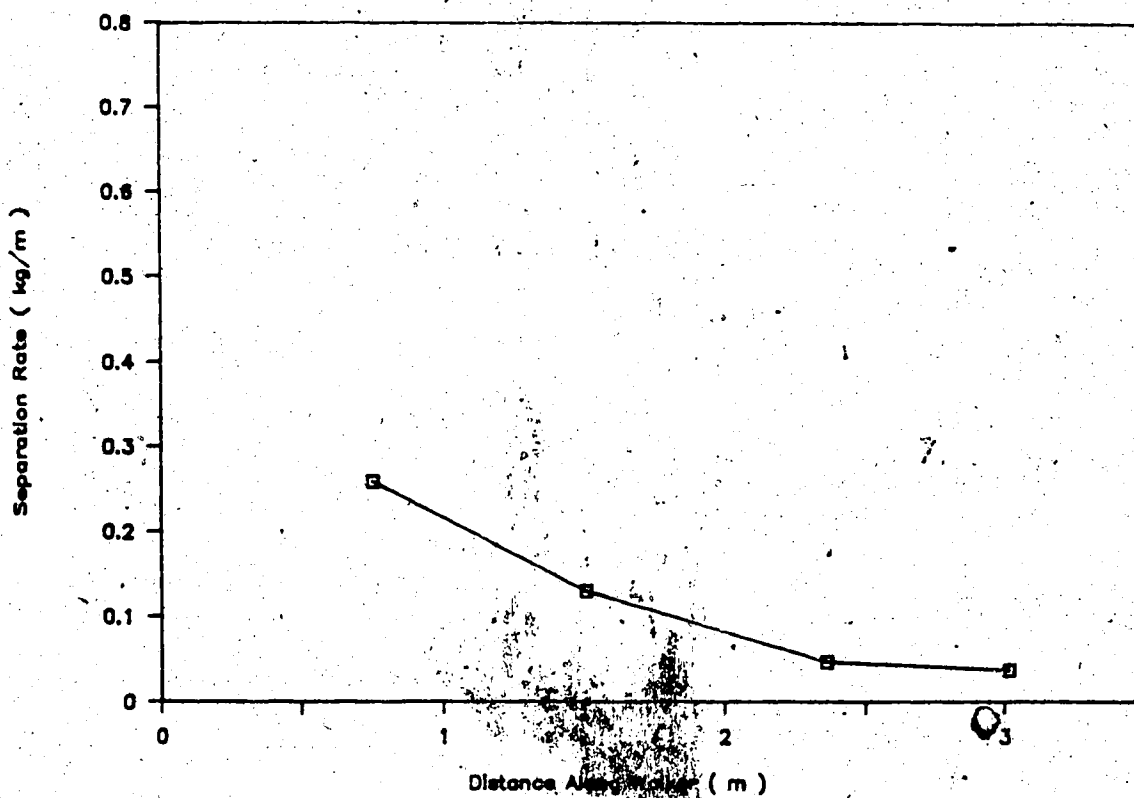


Figure 15.21 Field Separation Curve. Run #10

## 16. APPENDIX V DIGITIZATION OF FUNDAMENTAL SENSOR SIGNAL

Progress was made digitizing sensor signals from discrete impacts using the microprocessor system. Refer to Appendix I, Figure 12.2 for the circuit diagram and to Figure 16.1 for the block diagram of the digital signal processing system described below. Since the initial sensor signal is normally of very low amplitude, and the piezoelectric crystal has little ability to source current, pre-digitization amplification was necessary. A difference amplifier (1/2 - 1458 dual operational amplifier) was employed with high gain producing a full scale 'slamming' effect of the amplifier at, or near, maximum sensor output. The resulting signal was an amplification of the difference in potential across the piezoelectric crystal as the signal occurred. A potentiometer in a voltage divider circuit configuration provided baseline positioning of the amplified signal and placed the response in the range of 0.0 to +4.5 volts. Plate 16.1 shows a photograph of a typical amplified sensor signal for a barley kernel impact. The major aspects of the signal characteristics, such as frequencies, duration of signal, and impact-type-dependant amplitude variations were maintained after the amplification. No part of the pre-amplification altered the signal characteristics other than for magnitude and positioning to make the signal compatible with the remainder of the digitization circuitry.

Converting the voltage signal into a digital representation was accomplished by a

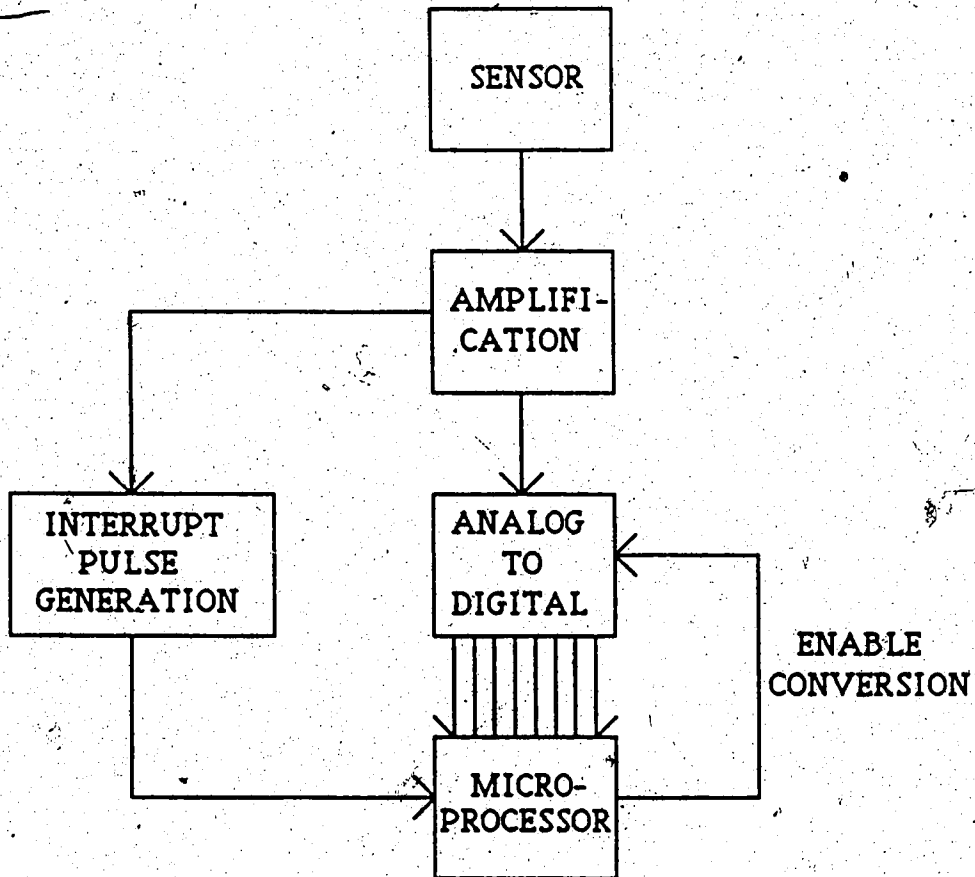


Figure 16.1 Digital Signal Processing Block Diagram.

microprocessor-controlled analog-to-digital (A/D) converter (AD7574, Analog Devices Inc., Norwood, MA.). The A/D converter was an eight-bit, successive approximation, high speed, microprocessor compatible device. An adjustable reference voltage from 0.0 to -6.0 volts was implemented to utilize the full scale representation of  $80_{16}$  ( $128_{10}$ ), at +4.5 volts. The resolution was 35.4 millivolts/bit. Choice of suitable resistors and capacitors in the timing network (Figure 12.2) yielded a conversion time of about twelve microseconds.

The microprocessor controlled the occurrence of conversions by 'asking' for a converted voltage representation at a constant rate. The 'asking' was performed everytime the microprocessor attempted to read any memory location in the range  $0000_{16}$  to  $7FFF_{16}$ . Address line 15 is low for this range and no other, therefore the line could be used to trigger the RD\* line of the analog to digital converter. All other functions of the microprocessor were performed at memory locations where the address line 15 was high, thus no conflict existed. The data lines of the converter were tied directly into the data lines of the microprocessor through appropriate buffers. The data lines were read by the microprocessor and data placed in memory at every conversion. A program loop was executed continuously, recording the digital voltage from the sensor signal as quickly as the conversions were taking place. Maximum storage for data was 768 points, each with eight bits. The

trace duration was about 6.4 milliseconds, which was slightly less than the complete duration of a typical grain impact.

The above sequence of data retrieval was initiated by an interrupt caused by the first rising edge of the sensor signal. A NAND gate (1/4 - 74LS00 quad NAND) was used to convert the first rising signal of the sensor into a negative pulse on the interrupt pin of the microprocessor. The first edge was exclusively responsible for the interrupt since interrupts were disabled in software after the first one occurred. Refer to Appendix II, section 13.2, for program listings and descriptions.

The data thus obtained were transferred to an IBM personal computer. The data were plotted using LOTUS 123 software (LOTUS Development Corporation, 1985, Cambridge, MA). A typical grain impact, captured by the digital signal processing system, is shown in Figure 4.1. The similarity between Plate 16.1 and Figure 16.1 shows that the actual signal was indeed captured by the system. With a more powerful and faster microprocessor system, software could be developed that would discriminate between grain and non-grain impacts.



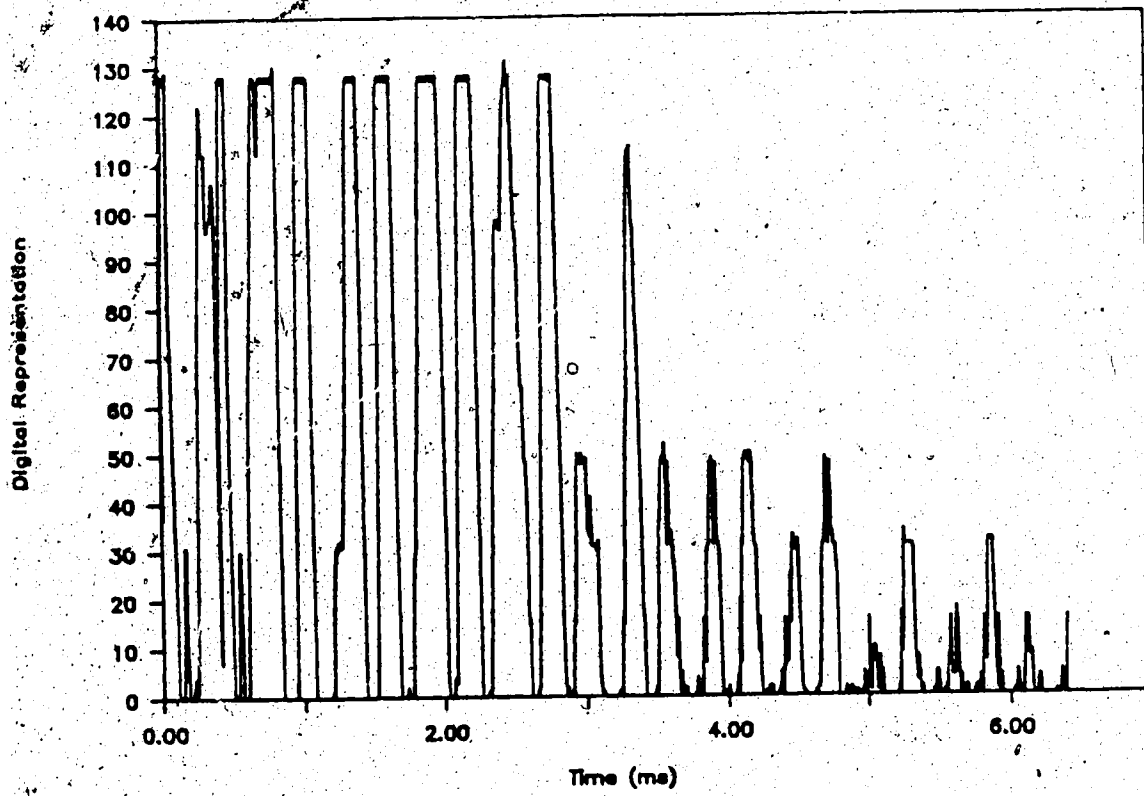


Figure 16.2 Digitized Barley Impact Signal.

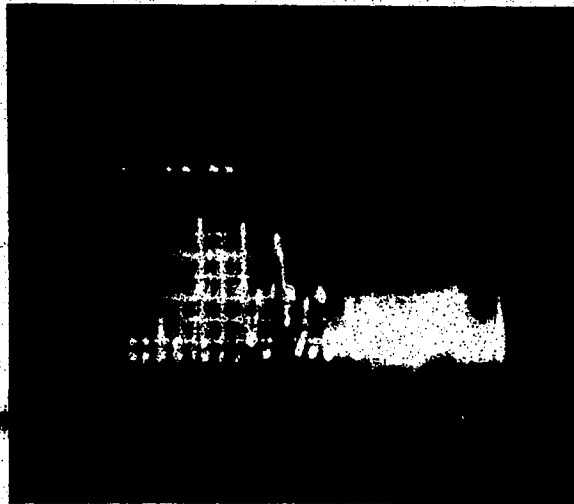


Plate 16.1 Amplified Barley Impact Signal (Amplitude=4.5V,  
Time base=1ms/div)